12-2021

Palmer amaranth [Amaranthus palmeri (S.) Wats.] resistance to S-metolachlor in the Mid-southern US and S-metolachlor dissipation in soil

Koffi Badou Jeremie Kouame
University of Arkansas, Fayetteville

Citation

Kouame, K. (2021). Palmer amaranth [Amaranthus palmeri (S.) Wats.] resistance to S-metolachlor in the Mid-southern US and S-metolachlor dissipation in soil. *Graduate Theses and Dissertations* Retrieved from https://scholarworks.uark.edu/etd/4275

Palmer amaranth [*Amaranthus palmeri* (S.) Wats.] resistance to *S*-metolachlor in the Mid-southern US and *S*-metolachlor dissipation in soil

A dissertation submitted in partial fulfillment
of the requirements for the degree of
Doctor of Philosophy in Crop, Soil, and Environmental Sciences

by

Koffi Badou Jeremie Kouame
Institut National Polytechnique Felix Houphouet-Boigny
Bachelor of Science in Agronomy, 2002
University of Nebraska-Lincoln
Master of Science in Agronomy and Horticulture, 2018

December 2021
University of Arkansas

This dissertation is approved for recommendation to the Graduate Council.

Nilda R. Burgos, Ph.D. Dissertation Co-Director	Mary C. Savin, Ph.D. Dissertation Co-Director
Vibha Srivastava, Ph.D. Committee member	Thomas R. Butts, Ph.D. Committee member
Matthew Bertucci, Ph.D. Committee member	

Abstract

Palmer amaranth [*Amaranthus palmeri* (S.) Wats.] presents both a high genetic diversity and propensity to evolve resistance to herbicides of several sites-of-action which have made it one of the worst weeds in US agriculture. In Arkansas, Palmer amaranth is resistant to herbicides of seven sites-of-action, which are 5-enolpyruvylshikimate-3-phosphate synthase (*EPSPS*) inhibitor, acetolactate synthase inhibitors, microtubule inhibitors, protoporphyrinogen oxidase inhibitors, very long chain fatty acid inhibitors, glutamine synthetase inhibitors, and hydroxyphenylpyruvate dioxygenase inhibitors. Sustainable management requires a better understanding of its biology and that of herbicide environmental fate. This research had five objectives: 1) characterize the current status of Palmer amaranth resistance to *S*-metolachlor in the Mid-southern US and evaluate alternative control methods for its proactive control, 2) investigate the influence of inter-annual and within-season multiple applications of the herbicide on its dissipation, 3) investigate the dynamics of *S*-metolachlor dissipation in soil samples collected throughout the growing season, 4) understand the influence of multiple mathematical equations on predictions of dissipation endpoints, and 5) investigate differences in threshold values for the initiation of stomatal closure between herbicide- susceptible and resistant accessions. A general herbicide resistance screening was conducted using seeds collected in Arkansas, Tennessee and Mississippi complemented by dose-response studies of parent populations and F_1 progenies. A greenhouse experiment was conducted to evaluate the differences in drought tolerance between *S*-metolachlor resistant- and susceptible accessions, and between glyphosate- resistant and susceptible plants differing by the number of *EPSPS* gene copy number. The influence of multiple annual applications on the dissipation half-life of *S*-metolachlor was evaluated using paired, commercial fields differing by the number of herbicide applications received within the previous six years across five Arkansas counties. The effect of frequency and timing of within-season applications of the herbicide on its dissipation was also evaluated. Five mathematical equations were evaluated for their performance at predicting *S*-metolachlor dissipation endpoints. Resistance to *S*-metolachlor was detected in four Arkansas counties and one Mississippi county. Parent populations and F_1 lines required up to 7- and 9.2-times more *S*-metolachlor, respectively, to reduce seedling emergence 50%. The half-life of *S*-metolachlor was longer for fields with high-use compared to fields with low-use history. A sequential application of *S*-metolachlor slowed *S*-metolachlor dissipation compared to the control. *S*-metolachlor dissipation was faster earlier compared to later during the growing season. Model selection and goodness of fit showed that the biphasic Gustafson and Holden and first-order double-exponential decay models better supported data compared to the single first order (SFO) model. The SFO under-predicted *S*-metolachlor residues during the later stages of the dissipation process. The threshold value for the initiation of stomatal closure was greater for the *S*-metolachlor- resistant than the susceptible accession. Glyphosate- resistant and susceptible plants, differing by the number of *EPSPS* gene copy number, did not show differences in their threshold values for the initiation of stomatal closure. Dissipation is not increased from use, but resistance is occurring and resistance in plant has consequences for plant function under stress conditions. Continued research into plant mechanisms and consequences of increasing resistance needs investigation.

Acknowledgements

I am grateful to Jesus Christ who made this milestone possible. He made amazing promises in His Word and this accomplishment is a proof of his faithfulness to his promises. I am thankful to my advisors Dr. Mary C. Savin and Dr. Nilda Roma-Burgos for their support, guidance, insightful comments and edits on my writing. I would like to extend my gratefulness to my committee members Drs. Vibha Srivastava, Tommy Butts and Matthew Bertucci for their guidance, and helpful comments and edits on my writing. I am also grateful to Dr. Cammy D. Willett, my advisor at the beginning of this program for her help and support at the start of my program. I am grateful to the University of Arkansas Fayetteville and the Crop, Soil and Environmental Sciences Department for all the support I received during my program. I would like to extend my gratitude to my Masters advisor Dr. John Lindquist for his guidance at the start of my graduate studies in the United States. Thank you to my fellow graduate students, both current and past, for their friendship and help with my research as well as our graduate school experiences. I want to thank all the people who have contributed to this research and provided input, guidance, and support Erin Grantz, Gulab Rangani, Fidel Gonzales, and the many others who have been along for this long ride. Finally, I want to thank my friends and family, back home, who have supported me during my graduate career.

Dedication

This achievement is dedicated to my lovely family that supported me during all the times of graduate studies. First, to Ange Patricia Kouame, my adorable wife. Without your prayers, help and faith this would not be possible. You are a true blessing. Second, Colombe Symphonie Kouame, our sweetheart and smart daughter for her understanding and patience.

Table of contents

List of tables

List of figures

Introduction

Palmer amaranth [*Amaranthus palmeri* S. (Wats.)] is one of the most troublesome weeds in many cropping systems not only in the Mid-southern US but also nation-wide (Riar et al., 2013a, 2013b, 2013c). Crop yield reduction from Palmer amaranth reveals yield losses of 79% in soybean [*Glycine max* (L.) Merr.] (Bensch et al., 2003) and 91% in corn (*Zea mays* L.) (Massinga et al., 2001). The significant loss induced by Palmer amaranth to many crops is due to various undesirable traits accumulated by this species (Ward et al., 2013).

Palmer amaranth shows plasticity and can grow under a wide range of conditions. Native of the Sonoran desert region (Ehleringer, 1983), it is now present in many states across a broad geographic range including Minnesota, North Dakota and Wisconsin. Its plasticity is highlighted by its ability to adapt to cultural practices and increase weediness. For example, under high nitrogen-fertilization conditions it can increase its nutrient-use efficiency (Bravo et al., 2018). It can also adapt to drought conditions and keep stomates open through osmotic adjustment under water stress conditions (Ehleringer, 1983). Palmer amaranth is a dioecious species; thus, the plant is an obligate out-crosser, which increases its genetic diversity and plasticity (Ward et al., 2013). Additionally, it is a prolific seed producer with a female plant capable of producing up to 600,000 seeds that can replenish the soil seedbank in a single generation (Ward et al., 2013), and it has a prolonged germination (Bensch et al., 2003; Ward et al., 2013).

Palmer amaranth is a fast growing weed for which different growth rates have been reported by previous researchers. For example, in Kansas height increase of 1.8 to 2.1 mm/growing degree day (GDD) was reported in two years (Horak and Loughin, 2000). Under non-limiting moisture and nutrient conditions, height increase rates reported in North and South Carolina reached 4.2 mm/GDD (Norsworthy et al., 2008b). As a result, growth can reach heights of 2 to 3 m (Horak and Loughin, 2000). Therefore, it can become very competitive with row crops for photosynthetically active radiation (PAR) interception as it positions its leaves above crop canopy with the consequences of reducing light quantity and altering light quality available to the crop. The competitive ability of a weed is greatly impacted by its growth rate as the one that rapidly grows tall, spreads laterally and shows a greater ground cover will outcompete other species (Zimdahl, 2004).

The C_4 photosynthetic pathway of Palmer amaranth gives it a higher carbon dioxide assimilation rate in comparison to many C_3 crops such as soybean, rice (*Oryza sativa* L.) and cotton. C_4 species have a greater maximum assimilation rate (A_{max}) granting them the ability to keep assimilating CO_2 under light conditions that are saturating for C_3 species. For example, Palmer amaranth attained photosynthetic rates of 81 µmol m^{-2} s^{-1} at 42ºC with 90% of peak photosynthetic rate between 36 and 46 ºC (Ehleringer, 1983). The carboxylation and oxygenation of ribulose-1,5-bisphosphate (RuBP) are two competing reactions catalyzed by Ribulose-1,5-bisphosphate carboxylase/oxygenase (Rubisco). Photosynthesis in C_4 plants such as Palmer amaranth, overcomes the low affinity of Rubisco for CO_2, leading to the inhibition of the oxygenation reaction, therefore, to the reduction of photorespiration rates (von Caemmerer, 2000). In fact, the coordinated functioning of C_4 leaf mesophyll and bundle-sheath cells and the CO_2 concentrating mechanism that characterize this C_4 photosynthetic pathway allow Rubisco, located in the bundle-sheath cells, to operate at high CO_2 partial pressures. PEP carboxylase, located in the leaf mesophyll cell, initially fix CO_2 into C_4 acids, which are decarboxylated in the bundle sheath to supply CO_2 to Rubisco (Ghannoum, 2009; von Caemmerer, 2000; von Caemmerer et al., 2017).

Finally, Palmer amaranth possesses a high potential to evolve resistance to herbicides of different chemical families and different sites-of-action. It is resistant to glyphosate (Culpepper et al., 2006; Norsworthy et al., 2008a), acetolactate synthase (ALS)-inhibiting herbicides (Burgos et al., 2001; Gaeddert et al., 1997; Horak and Peterson, 1995), dinitroanilines (Gossett et al., 1992), 4-hydroxyphenylpyruvate dioxygenase (HPPD) inhibitors (Jhala et al., 2014; Nakka et al., 2017b), photosystem II-inhibiting herbicides (Nakka et al., 2017a), glufosinate (Heap, 2021), and protoporphyrinogen oxidase (PPO) inhibitors (Salas et al., 2016; Salas-Perez et al., 2017; Varanasi et al., 2018a; Varanasi et al., 2018b). To date, according to Heap (2021), Palmer has evolved single herbicide resistance, resistance to multiple herbicides of the same chemical family, cross resistance and multiple resistance. Palmer amaranth resistance to various herbicides has been reported in 29 different states of the US and six different countries worldwide (Argentina, Brazil, Israel, Mexico, Spain, and the United States).

Palmer amaranth resistance to herbicides is via both target-site resistance (TSR) and non-target-site resistance (NTSR) mechanisms (Burgos et al., 2001; Burgos et al., 2018; Salas et al., 2016; Salas-Perez et al., 2017; Sales-Perez et al., 2018; Singh et al., 2018; Singh et al., 2019). Palmer amaranth has evolved resistance to glyphosate via amplification of the gene that encodes the target enzyme 5-enolpyruvylshikimate-3-phosphate synthase (*EPSPS*) (Chahal et al., 2017; Gaines et al., 2010; Kupper et al., 2017; Patterson et al., 2018). Also, Palmer amaranth has evolved resistance to glyphosate via a target-site mutation of proline 106 to serine (Kaundun et al., 2019). Similarly, resistance to ALS inhibitors is via both TSR and NTSR mechanisms (Nakka et al., 2017c). For example, previous research has documented a change of amino acid at position 574 and 653, from tryptophan to leucine and from serine to asparagine, respectively ($W_{574}L$, $S_{653}N$) (Berger et al., 2016; Kupper et al., 2017; Molin et al., 2018; Singh et al., 2019).

The mutation $S_{653}N$ is reported to confer resistance to imidazolinones and the pyrimidinylthio-benzoates; the mutation $W_{574}L$, on the other hand, confers resistance to triazolopyrimidines, sulfonylureas, imidazolinones, and pyrimidinylthio-benzoates (including pyrithiobac-sodium) (McNaughton et al., 2005; Patzoldt and Tranel, 2007; Whaley et al., 2006; Yu et al., 2012).

Previous researchers suspected the occurrence of NTSR mechanism in ALS-resistant accessions (Kupper et al., 2017). Palmer amaranth resistance to PPO inhibitors was reported to be due to the presence of the ΔG210 codon deletion (Salas et al., 2016; Salas-Perez et al., 2017) and to the R128G or R128M mutation (Salas et al., 2016; Salas-Perez et al., 2017; Varanasi et al., 2018a; Varanasi et al., 2018b). Additionally, the amino acid substitution of glycine to alanine in the catalytic domain of PPO2 at position 399 provoked a reduced affinity for several PPO-inhibiting herbicides in Palmer amaranth (Rangani et al., 2019); however, NTSR to PPO due to P450s and GSTs has been reported in Palmer amaranth (Varanasi et al., 2018a). Palmer amaranth resistance to atrazine is a metabolic resistance due to glutathione *S*-transferases (Chahal et al., 2019; Nakka et al., 2017a). NTSR is reported to be the cause of Palmer amaranth resistance to HPPD-inhibitors (Nakka et al., 2017b) and authors hypothesized that P450s are involved in the detoxification process.

In this context of herbicide resistance evolution, very long chain fatty acid (VLCFA)-inhibiting herbicides have been used widely because of their residual activity and effective weed control. These herbicides are selective for crops in which they are detoxified. Metolachlor [2-chloro-N-(2-ethyl-6-methylphenyl)-N-(2-methoxy-1-methylethyl)acetamide] is a VLCFA-inhibiting herbicide composed of two *R*-isomers and two *S*-isomers in equal proportions with herbicidal activity mainly from the *S*-isomer pair (O'Connell et al., 1998). *S*-metolachlor was developed in 1997 to allow commercial production of the enantiomerically-enriched form with more than 80% *S*-isomer and to reduce the use rate while maintaining biological performance (O'Connell et al., 1998). Used as preplant incorporated (PPI) or preemergence (PRE), it is effective on yellow nutsedge (*Cyperus esculentus* L.), annual grasses, and small-seeded broadleaf species, including Palmer amaranth.

Consequently, it has been a viable option for managing glyphosate-, microtubule-, ALS-, and PPO-resistant Palmer amaranth in Arkansas. Unfortunately, Palmer amaranth resistance to *S*-metolachlor was recently reported in Arkansas (Brabham et al., 2019), limiting options available to growers. To limit the spread of *S*-metolachlor resistance evolution, the key questions for this research are (i) How widespread is *S*-metolachlor resistance in the Mid-southern US? (ii) How does the use-history of the herbicide impact its dissipation in the soil? and ultimately (iii) How does this degradation rate impact Palmer amaranth resistance evolution? In addition to these important questions, it is also crucial to understand the impact of herbicide resistance evolution on physiological responses of Palmer amaranth to limited resources.

Water is a requirement for plants transpiration (Kropff and van Laar, 1993) and transpiration rate is controlled by stomatal closure. In response to water stress, plants send chemical signals, such as abscisic acid, to leaves (Saradadevi et al., 2017) and the increase of the concentration of abscisic acid around the guard cells triggers long-term depolarization of guard cells that leads to stomatal closure (Taiz et al., 2015). The knowledge of the threshold value for the initiation of stomatal closure can provide insight into the physiological responses of different ecotypes to drought (Sinclair 2012). Understanding how various Palmer amaranth ecotypes with different resistance profiles respond to abiotic stresses, particularly to drought, informs us about the fitness traits of resistant populations, which could help with adjustments of weed management tactics.

Therefore, the objectives of this research were to 1) characterize the current status of Palmer amaranth resistance to *S*-metolachlor in the Mid-southern United States and evaluate alternative herbicides for proactive control of this weed, 2) investigate the influence of inter-annual multiple applications of the herbicide on its dissipation in the soil, 3) investigate *S*-metolachlor dissipation in soil samples collected at various times during a single growing season, 4) understand the influence of multiple mathematical equations on the predictions of the dissipation endpoints of *S*-metolachlor, and 5) evaluate differential response of herbicide-resistant and -susceptible Palmer amaranth to drought.

References

Bensch C, Horak M, Peterson D (2003) Interference of redroot pigweed (*Amaranthus retroflexus*), Palmer amaranth (*A. palmeri*), and common waterhemp (*A. rudis*) in soybean. Weed Science 51: 37-43.

Berger S, Madeira PT, Ferrell J, Gettys L, Morichetti S, Cantero JJ, Nunez C (2016) Palmer Amaranth (*Amaranthus palmeri*) Identification and Documentation of ALS-Resistance in Argentina. Weed Science 64: 312-320.

Brabham C, Norsworthy JK, Houston M, Varanasi V, Barber T (2019) Confirmation of *S*-metolachlor resistance in Palmer amaranth (*Amaranthus palmeri*). Weed Technology 33: 720-726.

Bravo W, Leon R, Ferrell J, Mulvaney M, Wood C (2018) Evolutionary Adaptations of Palmer amaranth (*Amaranthus palmeri*) to nitrogen fertilization and crop rotation history affect morphology and nutrient-use efficiency. Weed Science 66: 180-189.

Burgos NR, Kuk Y, Talbert R (2001) *Amaranthus palmeri* resistance and differential tolerance of *Amaranthus palmeri* and *Amaranthus hybridus* to ALS-inhibitor herbicides. Pest Management Science 57: 449-457.

Burgos NR, Rouse C, Salas-Perez R, Noorai R, Lawton-Rauh A, Fan LJ, Qiu J, Saski C (2018) Cytochrome P450s and multiple resistance in *Amaranthus palmeri* and *Echinochloa colona*. Abstracts of Papers of the American Chemical Society 256.

Chahal P, Jugulam M, Jhala A (2019) Mechanism of atrazine resistance in atrazine- and HPPD inhibitor-resistant Palmer amaranth (*Amaranthus palmeri* S. Wats.) from Nebraska. Canadian Journal of Plant Science 99: 815-823.

Chahal P, Varanasi V, Jugulam M, Jhala A (2017) Glyphosate-Resistant Palmer Amaranth (*Amaranthus palmeri*) in Nebraska: Confirmation, *EPSPS* Gene Amplification, and Response to POST Corn and Soybean Herbicides. Weed Technology 31: 80-93.

Culpepper AS, Grey TL, Vencill WK, Kichler JM, Webster TM, Brown SM, York AC, Davis JW, Hanna WW (2006) Glyphosate-resistant Palmer amaranth (*Amaranthus palmeri*) confirmed in Georgia. Weed Science 54: 620-626.

Ehleringer J (1983) Ecophysiology of *Amaranthus palmeri*: A Sonoran desert summer annual. Oecologia 57: 107-112.

Gaeddert J, Peterson D, Horak M (1997) Control and cross-resistance of an acetolactate synthase inhibitor-resistant palmer amaranth (Amaranthus palmeri) biotype. Weed Technology 11: 132-137.

Gaines TA, Zhang WL, Wang DF, Bukun B, Chisholm ST, Shaner DL, Nissen SJ, Patzoldt WL, Tranel PJ, Culpepper AS, Grey TL, Webster TM, Vencill WK, Sammons RD, Jiang JM, Preston C, Leach JE, Westra P (2010) Gene amplification confers glyphosate resistance in *Amaranthus palmeri*. Proceedings of the National Academy of Sciences of the United States of America 107: 1029-1034.

Ghannoum O (2009) C-4 photosynthesis and water stress. Annals of Botany 103: 635-644.

Gossett B, Murdock E, Toler J (1992) Resistance of Palmer amaranth (*Amaranthus palmeri*) to the Dinitroaniline herbicides. Weed Technology 6: 587-591.

Heap I (2021) The International Herbicide-Resistant Weed Database. Available at www.weedscience.org. Accessed Friday, January 29, 2021, 2021.

Horak M, Loughin T (2000) Growth analysis of four *Amaranthus* species. Weed Sci. 48: 347-355.

Horak M, Peterson D (1995) Biotypes of palmer amaranth (*Amaranthus palmeri*) and common waterhemp (*Amaranthus rudis*) are resistant to imazethapyr and thifensulfuron. Weed Technol. 9: 192-195.

Jhala A, Sandell L, Rana N, Kruger G, Knezevic S (2014) Confirmation and control of triazine and 4-Hydroxyphenylpyruvate dioxygenase-inhibiting herbicide-resistant Palmer amaranth (*Amaranthus palmeri*) in Nebraska. Weed Technol. 28: 28-38.

Kaundun, SS., Jackson, LV., Hutchings, SJ., Galloway, J., Marchegiani, E., Howell, A., Carlin, R., Mcindoe, E., Tuesca, D., Moreno, R. 2019. Evolution of Target-Site Resistance to glyphosate in an *Amaranthus palmeri* population from Argentina and its expression at different plant growth temperatures. PLANTS-BASEL 8.

Klingaman T, Oliver L (1994) Palmer amaranth (*Amaranthus palmeri*) interference in soybeans (*Glycine max*). Weed Sci. 42: 523-527.

Kropff M, van Laar H (1993) Modelling crop-weeds interactions: CAB International.

Kupper A, Borgato EA, Patterson EL, Netto AG, Nicolai M, de Carvalho SJP, Nissen SJ, Gaines TA, Christoffoleti PJ (2017) Multiple resistance to glyphosate and acetolactate synthase inhibitors in Palmer amaranth (*Amaranthus palmeri*) identified in Brazil. Weed Sci. 65: 317-326.

Massinga R, Currie R, Horak M, Boyer J (2001) Interference of Palmer amaranth in corn. Weed Sci. 49: 202-208.

McNaughton K, Letarte J, Lee E, Tardif F (2005) Mutations in ALS confer herbicide resistance in redroot pigweed (*Amaranthus retroflexus*) and Powell amaranth (*Amaranthus powellii*). Weed Sci. 53: 17-22.

Molin WT, Wright AA, VanGessel MJ, McCloskey WB, Jugulam M, Hoagland RE (2018) Survey of the genomic landscape surrounding the 5-enolpyruvylshikimate-3-phosphate synthase (*EPSPS*) gene in glyphosate-resistant *Amaranthus palmeri* from geographically distant populations in the USA. Pest Management Science 74: 1109-1117.

Nakka S, Godar A, Thompson C, Peterson D, Jugulam M (2017a) Rapid detoxification via glutathione *S*-transferase (GST) conjugation confers a high level of atrazine resistance in Palmer amaranth (*Amaranthus palmeri*). Pest Management Science 73: 2236-2243.

Nakka S, Godar AS, Wani PS, Thompson CR, Peterson DE, Roelofs J, Jugulam M (2017b) Physiological and molecular characterization of hydroxyphenylpyruvate dioxygenase (HPPD)-inhibitor resistance in Palmer amaranth (*Amaranthus palmeri* S. Wats.). Frontiers in Plant Sci. 8.

Nakka S, Thompson C, Peterson D, Jugulam M (2017c) Target site-based and non-target site based resistance to ALS inhibitors in Palmer amaranth (*Amaranthus palmeri*). Weed Sci. 65: 681-689.

Norsworthy JK, Griffith G, Scott R, Smith K, Oliver L (2008a) Confirmation and control of glyphosate-resistant Palmer amaranth (*Amaranthus palmeri*) in Arkansas. Weed Technol. 22: 108-113.

Norsworthy JK, Oliveira MJ, Jha P, Malik M, Buckelew JK, Jennings KM, Monks DW (2008b) Palmer amaranth and large crabgrass growth with plasticulture-grown bell pepper. Weed Technol. 22: 296-302.

O'Connell P, Harms C, Allen J (1998) Metolachlor, *S*-metolachlor and their role within sustainable weed-management. Crop Protection 17: 207-212.

Patterson E, Pettinga D, Ravet K, Neve P, Gaines T (2018) Glyphosate Resistance and *EPSPS* Gene Duplication: Convergent Evolution in Multiple Plant Species. Journal of Heredity 109: 117-125.

Patzoldt W, Tranel P (2007) Multiple ALS mutations confer herbicide resistance in waterhemp (*Amaranthus tuberculatus*). Weed Sci. 55: 421-428.

Rangani G, Salas-Perez RA, Aponte RA, Knapp M, Craig IR, Mietzner T, Langaro AC, Noguera MM, Porri A, Roma-Burgos N (2019) A Novel single-site mutation in the catalytic domain of protoporphyrinogen oxidase IX (PPO) confers resistance to PPO-inhibiting herbicides. Frontiers in Plant Science 10.

Riar D, Norsworthy JK, Steckel L, Stephenson D, Bond J (2013a) consultant perspectives on weed management needs in midsouthern United States cotton: A follow-up survey. Weed Technol. 27: 778-787.

Riar DS, Norsworthy JK, Steckel LE, Stephenson DO, Eubank TW, Bond J, Scott RC (2013b) Adoption of best management practices for herbicide-resistant weeds in midsouthern United States Cotton, Rice, and Soybean. Weed Technol. 27: 788-797.

Riar DS, Norsworthy JK, Steckel LE, Stephenson DO, Eubank TW, Scott RC (2013c) Assessment of weed management practices and problem weeds in the midsouth United States-soybean: A consultant's perspective. Weed Technol. 27: 612-622.

Salas RA, Burgos NR, Tranel PJ, Singh S, Glasgow L, Scott RC, Nichols RL (2016) Resistance to PPO-inhibiting herbicide inPalmer amaranth from Arkansas. Pest Management Science 72: 864-869.

Salas-Perez RA, Burgos NR, Rangani G, Singh S, Refatti JP, Piveta L, Tranel PJ, Mauromoustakos A, Scott RC (2017) Frequency of Gly-210 deletion mutation among protoporphyrinogen oxidase inhibitor-resistant Palmer amaranth *Amaranthus palmeri*) populations. Weed Sci. 65: 718-731.

Sales-Perez RA, Saski CA, Noorai RE, Srivastava SK, Lawton-Rauh AL, Nichols RL, Roma-Burgos N (2018) RNA-Seq transcriptome analysis of *Amaranthus palmeri* with differential tolerance to glufosinate herbicide. Plos One 13.

Saradadevi R, Palta JA, Siddique KH (2017) ABA-mediated stomatal response in regulating water use during the development of terminal drought in wheat. Front. Plant Sci. 8, 1251. https://doi.org/10.3389/fpls.2017.01251.

Sinclair TR (2012) Is transpiration efficiency a viable plant trait in breeding for crop improvement? Functional Plant Biology 39: 359-365.

Singh S, Singh V, Lawton-Rauh A, Bagavathiannan M, Roma-Burgos N (2018) *EPSPS* gene amplification primarily confers glyphosate resistance among Arkansas Palmer amaranth (*Amaranthus palmeri*) Populations. Weed Sci. 66: 293-300.

Singh S, Singh V, Salas-Perez RA, Bagavathiannan MV, Lawton-Rauh A, Roma-Burgos N (2019) Target-site mutation accumulation among ALS inhibitor-resistant Palmer amaranth. Pest Management Science 75: 1131-1139.

Taiz L, Zeiger E, Møller I, Murphy A (2015) Plant physiology and development. 6th ed. University of California, Los Angeles: Sinauer Associates. Pp. 761.

Varanasi VK, Brabham C, Norsworthy JK (2018a) Confirmation and characterization of non-target site resistance to fomesafen in Palmer amaranth (*Amaranthus palmeri*). Weed Sci. 66: 702-709.

Varanasi VK, Brabham C, Norsworthy JK, Nie H, Young BG, Houston M, Barber T, Scott RC (2018b) A statewide survey of PPO-inhibitor resistance and the prevalent target-site mechanisms in palmer amaranth (*Amaranthus palmeri*) Accessions from Arkansas. Weed Sci. 66: 149-158.

von Caemmerer S (2000) Biochemical models of leaf photosynthesis Collingwood VIC 3066, Australia. CSIRO PUBLISHING.

von Caemmerer S, Ghannoum O, Furbank R (2017) C-4 photosynthesis: 50 years of discovery and innovation. Journal of Experimental Botany 68: 97-102.

Ward S, Webster T, Steckel L (2013) Palmer Amaranth (*Amaranthus palmeri*): A Review. Weed Technol. 27: 12-27.

Whaley C, Wilson H, Westwood J (2006) ALS resistance in several smooth pigweed (*Amaranthus hybridus*) biotypes. Weed Sci. 54: 828-832.

Yu Q, Han H, Li M, Purba E, Walsh MJ, Powles SB (2012) Resistance evaluation for herbicide resistance-endowing acetolactate synthase (ALS) gene mutations using Raphanus raphanistrum populations homozygous for specific ALS mutations. Weed Research 52: 178-186.

Zimdahl R (2004) Weed-crop competition: A review. Pages 219. 2121 State Avenue, Ames, Iowa 50014, USA: Blackwell Publishing Professional.

Literature review

Herbicide resistance evolution

To date, weed resistance evolution is a worldwide problem as many weeds have evolved resistance to major herbicide chemical families (Heap, 2021). It is a key factor compromising the objective of providing sufficient food to the world population in the future. Intensive use of herbicides has led to a strong and widespread selection pressure on weeds that has provoked herbicide resistance (Gaines et al., 2020). Worldwide, 521 species (272 Dicots and 249 Monocots) have evolved resistance to different herbicides (Heap, 2021). At the same time, no new herbicide mode of action has been introduced to the market since the 1980s (Westwood et al., 2018). Herbicide action is through (1) penetration in the plant and translocation to the site of action; (2) accumulation of the herbicide at the site of action; and (3) binding of the herbicide to its target protein, which results in the disruption of a vital metabolic pathway (Delye, 2013). Mechanisms of weed resistance to herbicides have been extensively studied and categorized as either Target Site Resistance (TSR) or Non-Target Site Resistance (NTSR).

Target site resistance

Target site resistance mechanisms affect the binding of herbicides either at or near catalytic domains or in regions affecting access to them, and they involve mutations in genes encoding the protein targets of herbicides (Gaines et al., 2020). For example, various point mutations in *Arabidopsis* sp. conferred resistance to acetolactate synthase (ALS)-inhibiting herbicides (Guttieri et al., 1996). Most of the time TSR mutations are synonymous with single nucleotide polymorphism (SNPs); they can also be due to polymorphisms in more than one codon or entire codon deletions (Gaines et al., 2020). Cases of TSR to photosystem II (PSII)-, protoporphyrinogen oxidase (PPO)-, acetyl-CoA carboxylase (ACCase)-, ALS-, microtubule-, 5-enolpyruvylshikimate-3-phosphate synthase (*EPSPS*)-inhibiting herbicides are reported in the literature.

Many cases of resistance to PSII-inhibiting herbicides are due to a Ser264 to Gly mutation in the D1 protein (Devine and Shukla, 2000), a Ser264 to Thr mutation (Masabni and Zandstra, 1999). A mutation in the vicinity of Ser264 (Phe265, Phe255, and His215) can play a role in resistance evolution. The TSR mechanisms associated with PPO-inhibiting herbicides include the presence of the ΔG210 codon deletion (Salas et al., 2016; Salas-Perez et al., 2017), the R128G or R128M mutation (Salas et al., 2016; Salas-Perez et al., 2017; Varanasi et al., 2018a; Varanasi et al., 2018b). They also involve the amino acid substitution of glycine to alanine in the catalytic domain of PPO2 at position 399 (Rangani et al., 2019).

Monocots and dicots present different forms of the ACCase in charge of catalyzing the first committed step in fatty acid biosynthesis. Plastids of dicots contain the prokaryotic form of the enzyme that is insensitive while monocots contain the sensitive eukaryotic form of ACCase in plastids. Two distinct ACCase genes code for the cytosolic and plastidic forms of the ACCase enzyme. Cases of resistance to ACCase-inhibiting-herbicides are due to an alteration in the target enzyme that reduces its sensitivity to herbicide inhibition (Devine and Shukla, 2000). Various altered forms of ACCase have been associated with different levels of resistance. The target of the aryloxyphenoxypropionate and cyclohexanedione is the plastid form and the alteration of this form causes resistance in weeds (Evenson et al., 1997). Target site resistance to ALS-inhibiting herbicides has been reported to be due to point mutations mainly occurring at the Pro197 position, including one based on a double mutation (Boutsalis et al., 1999). Other mutations reported include Trp_{573} to Leu and Ser_{653} to Asn (Sathasivan et al., 1991). Target site resistance to herbicides that inhibit cell division was reported to be due to a Thr_{239} to Ile mutation in an α-tubulin and a Met_{268} to Thr (Anthony et al., 1999; Anthony et al., 1998; Yamamoto et al., 1998). Target site resistance to glyphosate has been reported to be due to a Pro_{106} to Ser mutation in *EPSPS* gene and also a Thr102 to Ile substitution which strongly decreased the affinity of *EPSPS* to glyphosate (Fonseca et al., 2020). Moreover, increased gene expression leading to increased amounts of protein target can be involved in TSR mechanism (Gaines et al., 2010; Singh et al., 2018). Finally, reduced herbicide binding to auxin-binding proteins has been invoked in the mechanism of resistance in *Sinapis arvensis* (Webb and Hall, 1995).

Non-target site resistance (NTSR)

Mechanisms contributing to NTSR are complex and generally involve genes that are members of large gene families (Gaines et al., 2020). This second type of resistance can be caused by reduced absorption or translocation, increased sequestration or metabolic degradation of the herbicide. The NTSR is a major concern as it can confer resistance to multiple modes of action, including herbicides not commercialized (Petit et al., 2010). The NTSR in *Lolium rigidum* conferred resistance to up to sixteen herbicides of nine different modes of action (Burnet et al., 1994). Four gene families are generally involved in metabolism-based herbicide resistance: cytochrome P450 mono-oxygenases (P450s), glutathione-*S*-transferases (GSTs), glycosyltransferases (GTs) and ABC transporters (Yuan et al., 2007). They are multifunctional enzymes that have a protection role against different biotic and abiotic stresses including xenobiotics and oxidative stress (Lee et al., 2011).

GSTs are multifunctional enzymes encoded by large gene families, which have a protection role against different biotic and abiotic stresses including xenobiotics and oxidative stress (Lee et al., 2011; Montellano, 2005). Xenobiotics detoxification generally occurs in four phases namely oxidation, conjugation, transport and further compartmentation. GSTs, mediating the second phase, detoxify herbicides through glutathione (GSH) conjugation (Busi et al., 2018). The levels of GSH and the activity of GST enzymes determine herbicide detoxification via GSH conjugation (Roberts, 2000). Five distinct classes of GSTs have been recognized in plants (Phi, Tau, Zeta, Theta and Lambda) based on active site residues in the proteins, gene organization and sequence identity (Frova, 2003; Lee et al., 2011).

The name of P450 proteins is due to the absorption band of their carbon-monoxide-bound form at 450 nm; they are one of the largest super families of enzyme proteins (Werck-Reichhart and Feyereisen, 2000). They are a super family of heme, membrane-bound proteins present at very low concentrations in living species that catalyze monooxygenation or hydroxylation reactions (Montellano, 2005). The P450s play a critical role for plants to protect themselves and survive attacks from pests, herbivores and from exposure to adverse climatic conditions (Montellano, 2005). They are involved in most biosynthetic pathways responsible for natural products synthesis (cyanogenic glucosides, glucosinolates, isoflavonoids, and alkaloids) (Bak et al., 1999; Mikkelsen et al., 2002; Stanjek et al., 1999; Tattersall et al., 2001; Wittstock and Halkier, 2002). Additionally, P450s catalyze key steps of metabolism of xenobiotics in plants (Corbin et al., 1992; Siminszky et al., 1995; Siminszky et al., 1999; Siminszky et al., 2003; Siminszky et al., 2000; Yao et al., 2016; Yasuor et al., 2009). The main reactions catalyzed by P450s are O-deakylation, N-dealkylation and aromatic hydroxylation. Because of their role in metabolic degradation of xenobiotics, they are one of the most important enzymes responsible for herbicide selectivity between crops and weeds. Overexpression of P450 genes in weeds has been shown to increase the appearance and evolution of NTSR of weeds to herbicides (Burnet et al., 1994; Burnet et al., 1993; Busi et al., 2017a; Busi et al., 2011; Guo et al., 2019; Han et al., 2014; Siminszky et al., 2000). Increasing crops' P450 activity with safeners improves crops' tolerance to herbicides while providing effective weed control (Busi et al., 2017b). At the same time, inhibition of P450 activity in metabolism-based herbicide-resistant weeds reverses resistance and provides better weed control (Busi et al., 2017a; Christopher et al., 1994; Oliveira et al., 2018).

In many grasses, metabolic resistance has been documented to ACCase-inhibiting herbicides (Busi et al., 2011; Delye et al., 2011; Huan et al., 2011; Iwakami et al., 2019; Zhao et al., 2019a). Most cases reported enhanced metabolism due to the activity of P450s; however, GSTs are also reported in metabolism of ACCase-inhibiting herbicides (Huan et al., 2011; Matzrafi et al., 2017). Similarly, enhanced metabolism has been documented in weeds that are resistant to ALS-inhibiting herbicides (Iwakami et al., 2014; Iwakami et al., 2019; Owen et al., 2012; Shergill et al., 2018) and is due to P450s (Iwakami et al., 2014; Iwakami et al., 2019; Zhao et al., 2019b), GSTs (Zhao et al., 2017) and ABC transporters (Liu et al., 2018). Likewise, metabolism has been characterized as responsible for herbicide resistance to auxin-type herbicides (Figueiredo et al., 2018; Shergill et al., 2018; Torra et al., 2017). Enhanced metabolism is the cause of weed resistance to PSII-inhibiting herbicides (Anderson and Gronwald, 1991; Chahal et al., 2019; Evans et al., 2017; Lu et al., 2019; Nakka et al., 2017a; Plaisance and Gronwald, 1999; Svyantek et al., 2016; Vennapusa et al., 2018). Furthermore, metabolic resistance in weeds has been documented for glyphosate (Gonzalez-Torralva et al., 2012; Pan et al., 2019), HPPD inhibitors (Hausman et al., 2011; Kaundun et al., 2017; Kupper et al., 2018; Nakka et al., 2017b; Oliveira et al., 2018), clomazone (Guo et al., 2019) and PPO inhibitors (Varanasi et al., 2018a). Finally, metabolism-based resistance has been reported in species resistant to VLCFA inhibitors (Brabham et al., 2019; Busi et al., 2012; Busi et al., 2018; Busi and Powles, 2013; Ducker et al., 2020; Ducker et al., 2019a; Ducker et al., 2019b; Rangani et al., 2021).

Palmer amaranth

To understand the state of research on *Amaranthus palmeri* and to summarize global research during the past 21 years, the Web of Science (https://webofknowledge.com) database from 2000 to 2021 was systematically searched on April 3, 2021 using the basic search with the topic ("Palmer amaranth" OR "*Amaranthus palmeri*" OR "*A. palmeri*"). The search was refined by excluding meeting abstracts, letters, corrections or editorial materials, record reviews, proceedings papers and early access. Sources included original articles, review articles and book chapters. The objective was to summarize research on *Amaranthus palmeri* across the globe during the past 21 years. Articles (689) from the Web of Science core collection were summarized using a bibliometric tool *bibliometrix* (Aria and Cuccurullo, 2017) within the R software environment (R Core Team, 2020). The productivity of the top twenty countries in the timespan of interest is described by Figure 2.1. The United States led research about Palmer amaranth with about 87% of articles published. Among these published articles, 92% are single country production (SCP) and 8% are multiple country production (MCP) (Figure 2. 1).

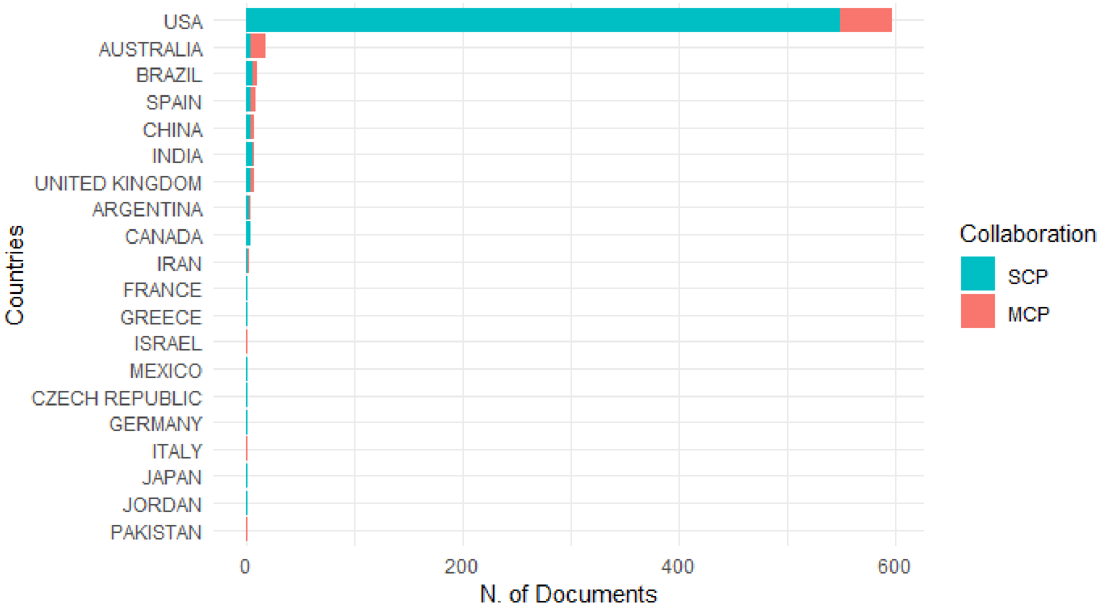

Figure 2. 1. Number of publications on *A. palmeri* on the Web of Science (https://webofknowledge.com) database from 2000 to 2021, systematically searched through the basic search with the topic ("Palmer amaranth" OR "*Amaranthus palmeri*" OR "*A. palmeri*"). The research was refined by excluding meeting abstracts, letters, corrections or editorial materials, record reviews, proceeding papers and early access. Only original articles, review articles and book chapters in the English language were included in the search (information collected on April 3, 2021).

These results indicate that Palmer amaranth is more of a problem in the United States compared to other countries. It is a “nightmare” for US producers in many cropping systems (Riar et al., 2013a, b, c). Palmer amaranth can drastically reduce yield in major cropping systems such as soybean [*Glycine max* (L.) Merr.] (Bensch et al., 2003b; Klingaman and Oliver, 1994) and corn (*Zea mays* L.) (Massinga et al., 2001). Palmer amaranth accumulates undesirable traits such as prolonged germination (Bensch et al., 2003a; Ward et al., 2013), plasticity (Bravo et al., 2018; Ehleringer, 1983), cross pollination (Ward et al., 2013), large number of seed production (Ward et al., 2013), and rapid growth (Horak and Loughin, 2000a; Norsworthy et al., 2008). Additionally, Palmer amaranth has evolved resistance to many herbicide modes of action in 29 different states (Heap, 2021). Palmer amaranth is resistant to glyphosate (Culpepper et al., 2006;

Norsworthy et al., 2008a), acetolactate synthase-inhibiting herbicides (Burgos et al., 2001; Gaeddert et al., 1997; Horak and Peterson, 1995), dinitroanilines (Gossett et al., 1992), 4-hydroxyphenylpyruvate dioxygenase (HPPD) inhibitors (Jhala et al., 2014; Nakka et al., 2017b), photosystem II-inhibiting herbicides (Nakka et al., 2017a), and protoporphyrinogen oxidase (PPO) inhibitors (Salas et al., 2016; Salas-Perez et al., 2017; Varanasi et al., 2018a; Varanasi et al., 2018b).

Outside of the US, only five countries (Argentina, Brazil, Israel, Mexico and Spain) have reported herbicide-resistant Palmer amaranth (Heap, 2021). *A. palmeri* has the ability to successfully hybridize with three other species: *A. spinosus*, *A. hybridus*, and *A. tuberculatus* (Gaines et al., 2012). Moreover, the ALS gene was transferred by a resistant male *A. rudis* to the hybrid obtained from the crossing with *A. palmeri* (Wetzel et al., 1999).

Metolachlor agricultural use and metabolism

Metolachlor [2-chloro-N-(2-ethyl-6-methylphenyl)-N-(2-methoxy-1-methylethyl) acetamide] is a very long chain fatty acid (VLCFA)-inhibiting herbicide. The racemic product of metolachlor is composed of two R-enantiomers and two S-enantiomers with *S*-metolachlor being more effective as a herbicide than rac-metolachlor (Zhan et al., 2006). *S*-metolachlor was developed in 1997 to allow both commercial production of enantiomerically-enriched form with more than 80% S-isomers and reduction of the use-rate, while maintaining its biological performance (O'Connell et al., 1998).

Very long chain fatty acids (VLCFAs) are fatty acids having a carbon (C) chain-length longer than C20 (Joubes et al., 2008; Naganuma et al., 2011; Sassa and Kihara, 2014). The determining activity of fatty acids formation, is the elongation process driven by multiple complexes of four enzymes (elongase system) (Trenkamp et al., 2004). They catalyze sequential condensation, ketoacyl reduction, dehydration and enoyl reduction steps (Figure 2. 2.) (Bach and Faure, 2010; Busi, 2014). The starting reaction, the condensation, is catalyzed by the condensing enzyme 3-ketoacyl-CoA synthase (KCS) FAE$_1$ (Boger, 2003; Busi, 2014; Millar and Kunst, 1997) (Figure 2. 2). In plants, VLCFAs are important components of lipids such as triacylglycerols (accumulated in seeds), some sphingolipids and phospholipids existing in various cell membranes and cuticular waxes on plant aerial surfaces (Trenkamp et al., 2004). Sphingolipids and phospholipids are required for cell division, polarity and differentiation (Lechelt-Kunze et al., 2003). In the epidermal tissues of young seedlings, suberin (roots) and insoluble wax-impregnated cutin (leaves) are an important barrier to the environment (PostBeittenmiller, 1996). A disruption of VLCFA levels in plants can lead to marked phenotypic consequences (growth inhibition, embryo mortality) (Du Granrut and Cacas, 2016). The target of chloroacetamide herbicides is the FAE1 within the elongase enzymatic complex bound to the endoplasmic reticulum (Boger, 2003; Busi, 2014; Millar and Kunst, 1997).

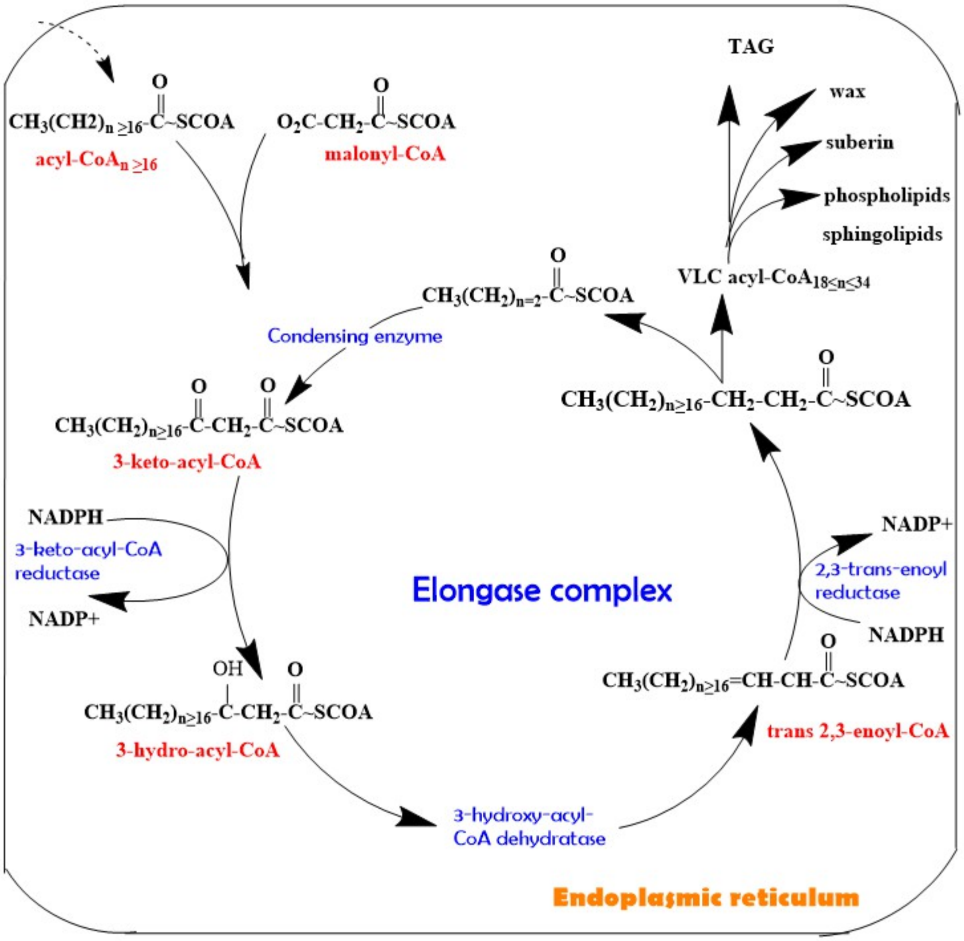

Figure 2. 2. VLCFA elongation cycle adapted from Bach and Faure (2010)

Plant uptake and metabolism

Uptake of soil applied herbicides can be made possible either by the growth of seedlings that bring roots into contact with the herbicide, or by mass flow, moving the herbicide molecule dissolved in the soil solution or by diffusion that move molecules from zones of high concentration to areas of lower concentration. Chloroacetamide herbicides are selective for crops in which they are detoxified. For these herbicides (acetochlor, alachlor, butachlor, metazachlor, pretilachlor, propachlor, thenylchlor and metolachlor), detoxification is mainly due to a glutathione-mediated nucleophilic displacement of the chlorine atom to form an initial glutathione (GSH) or homoglutathione conjugate, which may change from one crop species to the next (Roberts, 2000) (Figure 2.3). GSH (γ-glutamylcysteinylglycine) is a tripeptide composed of the three amino acids glutamate, cysteine and glycine (Berg et al., 2015). A further degradation of the initial conjugates produces different sulfur-containing metabolites such as cysteine and thiolactic acid derivatives. Based on the crop species, chloroacetamides herbicides can also be detoxified via reductive dichlorination, O-dealkylation, N-side-chain dealkylation, and arylalkyl substituent hydroxylation and subsequent glycosidation (Roberts, 2000). Tolerance of several species to chloroacetamide herbicides was reported to be positively correlated with GSH levels and the rate of GSH conjugation (Breaux et al., 1987); an induction of GSH and GST levels with dichloroacetamide safeners provoked an increase in plant resistance to chloroacetamide herbicides (Breaux, 1987; Breaux et al., 1987). On the contrary, a decrease in GSH levels in corn seedlings induced an increase in metolachlor phytotoxicity (Farago et al., 1993).

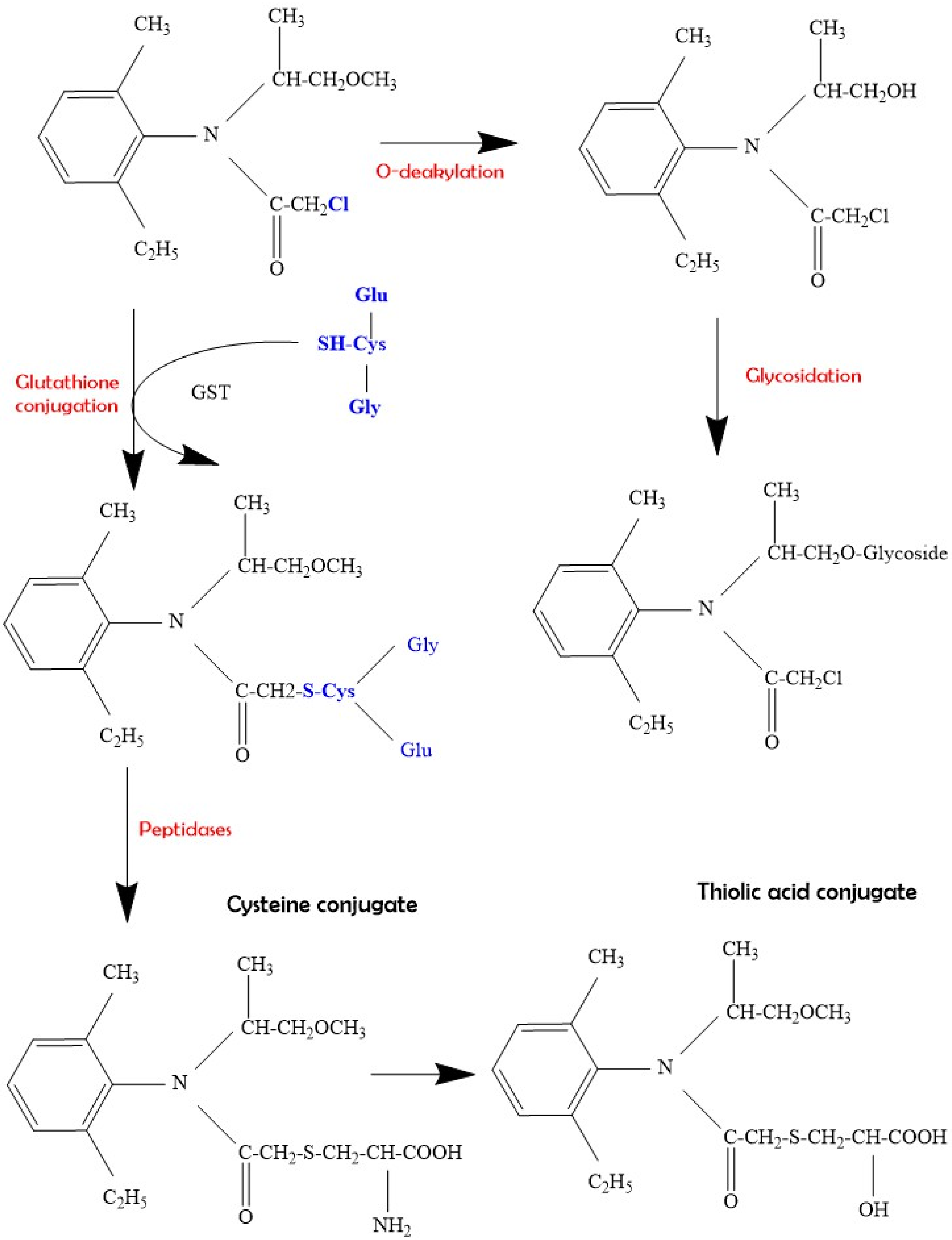

Figure 2. 3. Pathways for metolachlor metabolism in plants. Adapted from Roberts (2000)

Metolachlor environmental fate and transport

Microbial degradation

A major breakdown pathway of metolachlor in the soil is by both aerobic and anaerobic microorganisms. Under sandy soil conditions, half-lives of 81 and 67 d were reported for anaerobic and aerobic microbes, respectively (Senseman, 2007). Other factors that affect microbial degradation rates of metolachlor include soil depth, organic carbon and dissolved oxygen concentrations, temperature and size of microbial populations (Barbash et al., 2004). Microbial transformation of chloroacetamide is a detoxification catalyzed by GSTs and it involves conjugation between glutathione and the chloroacetamide moiety of the herbicide. The general mechanism of this reaction is a nucleophilic attack by glutathione on the 2-chloro electrophilic group of the chloroacetamide herbicide (Aga et al., 1996; Field and Thurman, 1996; Stamper and Tuovinen, 1998). Glutathione- chloroacetamide conjugates are subsequently degraded by carboxypeptidases (Wolf et al., 1996), gamma-glutamyl transpeptidases, and cysteine beta-lyases (Stamper and Tuovinen, 1998; Zablotowicz et al., 1995). After subsequent degradation of the conjugate moiety and oxidation of the SH-group to sulfonic acid, this pathway may lead to the formation of metolachlor-ethane sulfonic acid (MESA) (Stamper and Tuovinen, 1998). Another metolachlor metabolite is metolachlor oxanilic acid (MOXA), produced by oxidation of glutathione-metolachlor conjugate (White et al., 2010).

Many microbes able to degrade metolachlor have been reported. The fungus *Penicillium oxalicum* has been reported to degrade almost 90% of metolachlor with addition of glucose and yeast extract within 384 h, and degradation products [MOXA, metolachlor-2-hydroxy (M2H), and metolachlor deschloro (MDES)] were obtained via hydrolytic and reductive dichlorination

(Chang et al., 2020). After 4 days of growth in culture, *Candida xestobii* could degrade 60% added metolachlor. It converted up to 25% of the compound into CO_2 after 10 days while *Bacillus simplex* degraded 30% metolachlor after 5 days of growth in minimal medium (Munoz et al., 2011). Previous research has also documented that metolachlor is co-metabolized by different microbes including *Actinomycetes* (Krause et al., 1985), *Penicillium oxalicum* strain MET-F-1 (Chang et al., 2020), *Chaetomium globosum* (McGahen and Tiedje, 1978),

Metolachlor adsorption

Pesticide molecules in the soil partition between the aqueous and solid phases (Kah et al., 2006). Herbicide retention affects herbicide behavior in soils (Si et al., 2009); consequently, it impacts herbicide fate, persistence, and biological activity (Westra et al., 2015). The amount of herbicide available for effective weed control, the extent of leaching, and redistribution can be predicted with a better understanding of the processes of adsorption and desorption (Si et al., 2009). Measures of pesticide sorption by soil define sorption coefficients [Kd (distribution coefficient) and Koc (soil organic carbon coefficient)] (Li et al., 2019; Si et al., 2009). The distribution coefficient, measured in a water/soil slurry, can be defined as the ratio of the amount of herbicide sorbed to the soil relative to the amount left in water. The soil organic carbon coefficient, on the other hand is the ratio of Kd and the fraction of organic carbon in the soil. Prediction of the risks of pesticide movement by water-eroded soil, runoff, and leaching are possible with the use of pesticide fate models (Eason et al., 2004; Farenhorst, 2006; Farenhorst et al., 2008; Stewart and Loague, 1999), in which sorption coefficients are reported to be among the most sensitive input parameters (Farenhorst et al., 2008).

Soil properties are among the key factors that influence soil herbicide sorption. Previous researchers reported the variability of sorption coefficients (Kd) within soil landscapes as a result of differences in soil organic carbon content or soil pH between slope positions (Farenhorst et al., 2003; Novak et al., 1997). Nonpolar herbicides' soil retention is mainly due to hydrophobic partitioning (Cheng and Mulla, 1999) and organic matter is most often the determining factor of sorption (Kah et al., 2006). In addition to binding to soil organic matter, ionic herbicides can sorb to clay, iron and aluminum hydroxides. In contrast to nonpolar herbicides, the adsorption is sensitive to soil pH (Kah et al., 2006). The dominant retention mechanisms for polar herbicides are ion exchange and hydrogen bonding (Cheng and Mulla, 1999). Because soil particles and organic matter contain negatively charged sites that provide surface area for adsorption of ionized particles, positively charged ions are tightly bound to soil while negatively charged ions are repelled. Anions ($H_2PO_4^-$) exchange and or bind to the cationic metals calcium, iron, or aluminum that are associated to the soil CEC (Ross and Lembi, 2009).

Metolachlor sorption to soil is affected by many factors including organic amendments. Addition of an organic waste from olive oil production induced a 6-fold increase of the distribution coefficient (Kd) values on a sandy soil and 5-fold increase on a soil with a higher clay content (Canero et al., 2015). *S*-metolachlor sorption is affected differently by the type of cover crop, with highest sorption on red clover, followed by turnip, rape, and oat (Cassigneul et al., 2015).

Metolachlor volatilization

Volatilization is one pathway by which metolachlor is lost. For example, temperatures greater than 30ºC were reported to increase metolachlor volatilization from water due to the dependency of Henry's law (Feigenbrugel et al., 2004; Lau et al., 1995). Metolachlor volatilization under field conditions is affected differently by broadcast and banded applications with 3-fold higher cumulative volatilization for the broadcast application (Prueger et al., 1999). Residue cover, spatial concentration on soil surface, and rainfall timing are factors that influence metolachlor volatilization (Prueger et al., 1999). A long-term study of metolachlor volatilization revealed an important effect of moisture with cumulative volatilization reaching 63% of the applied herbicide within 5 days of application (Prueger et al., 2017). Largest flux profile concentrations of the herbicide occurred immediately after application and then declined (Bedos et al., 2017; Prueger et al., 2005; Prueger et al., 1999). Up to 25% losses can occur within 120 h after application, 87% of which happened during the first 72 h (Prueger et al., 2005).

Surface soil moisture is a determinant factor of metolachlor volatility (Gish et al., 2009; Prueger et al., 2017); beyond five days of application metolachlor volatilization is either an important loss process (when soil surface is moist) or a negligible pathway (when soil surface was dry) (Prueger et al., 2017). Crop residues on the field changed soil water content; as a consequence, residues changed *S*-metolachlor degradation and volatilization dynamics (Bedos et al., 2017). A correlation between soil surface temperatures and metolachlor volatilization has been established when soils are moist but not when they are dry (Gish et al., 2009). Additionally, metolachlor volatilization has a diurnal trend with 43-86% losses during the day and 14-57% losses during the night (Prueger et al., 2005).

References

Aga D, Thurman E, Yockel M, Zimmerman L, Williams T (1996) Identification of a new sulfenic acid metabolite of metolachlor in soil. Environmental Science & Technology 30: 592-597.

Anderson MP, Gronwald JW (1991) Atrazine resistance in a velvetleaf (*Abutilon theophrasti*) biotype due to enhanced glutathione *S*-transferase activity. Plant Physiology 96: 104-109.

Anthony RG, Reichelt S, Hussey PJ (1999) Dinitroaniline herbicide-resistant transgenic tobacco plants generated by co-overexpression of a mutant alpha-tubulin and a beta-tubulin. Nature Biotechnology 17: 712-716.

Anthony RG, Waldin TR, Ray JA, Bright SWJ, Hussey PJ (1998) Herbicide resistance caused by spontaneous mutation of the cytoskeletal protein tubulin. Nature 393: 260-263.

Aria M, Cuccurullo C (2017) Bibliometrix: An R-tool for comprehensive science mapping analysis. Journal of Informetrics 11: 959-975.

Bach L, Faure JD (2010) Role of very-long-chain fatty acids in plant development, when chain length does matter. Comptes Rendus Biologies 333: 361-370.

Bak S, Olsen C, Petersen B, Moller B, Halkier B (1999) Metabolic engineering of p-hydroxybenzylglucosinolate in Arabidopsis by expression of the cyanogenic CYP79A1 from Sorghum bicolor. Plant Journal 20: 663-671.

Barbash JE (2004) The geochemistry of pesticides, *in* Lollar BS (ed.) Environmental geochemistry, in Holland, HD, and Turekian KK, (eds.), Treatise on geochemistry: Oxford, UK, Elsevier–Pergamon, v. 9, p. 541–577

Bedos C, Alletto L, Durand B, Fanucci O, Brut A, Bourdat-Deschamps M, Giuliano S, Loubet B, Ceschia E, Benoit P (2017) Observed volatilization fluxes of *S*-metolachlor and benoxacor applied on soil with and without crop residues. Environmental Science and Pollution Research 24: 3985-3996.

Bensch C, Horak M, Peterson D (2003a) Interference of redroot pigweed (*Amaranthus retroflexus*), Palmer amaranth (*A. palmeri*), and common waterhemp (*A. rudis*) in soybean. Weed Science 51: 37-43.

Bensch C, Horak M, Peterson D (2003b) Interference of redroot pigweed (*Amaranthus retroflexus*), Palmer amaranth (*A. palmeri*), and common waterhemp (*A. rudis*) in soybean. Weed Science 51: 37-43.

Berg J, Tymoczko J, Gatto GJ, Stryer L (2015) Biochemistry. Pages 1056. New York, NY 10010: Kate Ahr Parker.

Bernasconi P, Woodworth AR, Rosen BA, Subramanian MV, Siehl DL (1996) A naturally occurring point mutation confers broad range tolerance to herbicides that target acetolactate synthase (vol 270, pg 17381, 1995). Journal of Biological Chemistry 271: 13925-13925.

Boger P (2003) Mode of action for Chloroacetamides and functionally related compounds. Journal of Pesticide Science 28: 324-329.

Boutsalis P, Karotam J, Powles SB (1999) Molecular basis of resistance to acetolactate synthase-inhibiting herbicides in *Sisymbrium orientale* and *Brassica tournefortii*. Pesticide Science 55: 507-516.

Brabham C, Norsworthy JK, Houston M, Varanasi V, Barber T (2019) Confirmation of *S*-metolachlor resistance in Palmer amaranth (*Amaranthus palmeri*). Weed Technology 33: 720-726.

Bravo W, Leon R, Ferrell J, Mulvaney M, Wood C (2018) Evolutionary Adaptations of Palmer amaranth (*Amaranthus palmeri*) to nitrogen fertilization and crop rotation history affect morphology and nutrient-use efficiency. Weed Science 66: 180-189.

Breaux E (1987) Initial metabolism of acetochlor in tolerant and susceptible seedlings. Weed Science 35: 463-468.

Breaux E, Patanella J, Sanders E (1987) Chloroacetanilide herbicide selectivity: Analysis of glutathione and homoglutathione in tolerant, susceptible, and safened seedlings. Journal of Agricultural and Food Chemistry 35: 474-478.

Burgos NR, Kuk Y, Talbert R (2001) *Amaranthus palmeri* resistance and differential tolerance of *Amaranthus palmeri* and *Amaranthus hybridus* to ALS-inhibitor herbicides. Pest Management Science 57: 449-457.

Burnet M, Barr A, Powles S (1994a) Chloroacetamide resistance in rigid ryegrass (*Lolium rigidum*). Weed Science 42: 153-157.

Burnet M, Loveys B, Holtum J, Powles S (1993) A mechanism of chlorotoluron resistance in *Lolium rigidum*. Planta 190: 182-189.

Burnet MWM, Hart Q, Holtum JAM, Powles SB (1994b) Resistance to 9 herbicide classes in a population of rigid ryegrass (*Lolium rigidum*). Weed Science 42: 369-377.

Busi R (2014) Resistance to herbicides inhibiting the biosynthesis of very-long-chain fatty acids. Pest Management Science 70: 1378-1384.

Busi R, Gaines T, Powles S (2017a) Phorate can reverse P450 metabolism-based herbicide resistance in *Lolium rigidum*. Pest Management Science 73: 444-451.

Busi R, Gaines T, Walsh M, Powles S (2012). Understanding the potential for resistance evolution to the new herbicide pyroxasulfone: field selection at high doses versus recurrent selection at low doses. Weed Research 52: 489-499.

Busi R, Nguyen NK, Chauhan BS, Vidotto F, Tabacchi M, Powles SB (2017b). Can herbicide safeners allow selective control of weedy rice infesting rice crops? Pest Management Science 73: 71-77.

Busi R, Porri A, Gaines T, Powles S (2018) Pyroxasulfone resistance in *Lolium rigidum* is metabolism-based. Pesticide Biochemistry and Physiology 148: 74-80.

Busi R, Powles S (2013). Cross-resistance to prosulfocarb and triallate in pyroxasulfone-resistant *Lolium rigidum*. Pest Management Science 69: 1379-1384.

Busi R, Vila-Aiub M, Powles S (2011) Genetic control of a cytochrome P450 metabolism-based herbicide resistance mechanism in *Lolium rigidum*. Heredity 106: 817-824.

Canero AI, Cox L, Cabrera A, Cornejo J (2015) Different effects of a by-product from olive oil extraction on *S*-metolachlor and bentazone soil fate. Clean-Soil Air Water 43: 948-957.

Cassigneul A, Alletto L, Benoit P, Bergheaud V, Etievant V, Dumeny V, Le Gac A, Chuette D, Rumpel C, Justes E (2015) Nature and decomposition degree of cover crops influence pesticide sorption: Quantification and modelling. Chemosphere 119: 1007-1014.

Chahal P, Jugulam M, Jhala A (2019) Mechanism of atrazine resistance in atrazine- and HPPD inhibitor-resistant Palmer amaranth (*Amaranthus palmeri* S. Wats.) from Nebraska. Canadian Journal of Plant Science 99: 815-823.

Chang XP, Liang JF, Sun Y, Zhao LX, Zhou B, Li XJ, Li YT (2020) Isolation, degradation performance and field application of the metolachlor-degrading fungus *Penicillium oxalicum* MET-F-1. Applied Sciences-Basel 10: 13.

Cheng HH, Mulla DJ (1999) The Soil Environment, in Adriano DC, Bollag JM, Frankenberger WT, Sims RC (Eds.) Bioremediation of Contaminated Soils, Monograph 37, American Society of Agronomy, Crop Science Society of America, Soil Science Society of America, Madison (WI), Chapter 1, pp. 1-13.

Christopher J, Preston C, Powles S (1994) Malathion antagonizes metabolism-based chlorsulfuron resistance in *Lolium rigidum*. Pesticide Biochemistry and Physiology 49: 172-182.

Corbin F, Moreland D, Siminszky B (1992) Monooxygenase studies in plants - invivo and invitro metabolism of primisulfuron by corn and grain-sorghum. Abstracts of Papers of the American Chemical Society 204: 11-AGRO.

Culpepper AS, Grey TL, Vencill WK, Kichler JM, Webster TM, Brown SM, York AC, Davis JW, Hanna WW (2006) Glyphosate-resistant Palmer amaranth (*Amaranthus palmeri*) confirmed in Georgia. Weed Science 54: 620-626.

Delye C (2013) Unravelling the genetic bases of non-target-site-based resistance (NTSR) to herbicides: a major challenge for weed science in the forthcoming decade. Pest Management Science 69: 176-187.

Delye C, Gardin JAC, Boucansaud K, Chauvel B, Petit C (2011) Non-target-site-based resistance should be the centre of attention for herbicide resistance research: *Alopecurus myosuroides* as an illustration. Weed Research 51: 433-437.

Devine MD, Shukla A (2000) Altered target sites as a mechanism of herbicide resistance. Crop Protection 19: 881-889.

Du Granrut A, Cacas J (2016) How very-long-chain fatty acids could signal stressful conditions in plants? Frontiers in Plant Science 7.

Ducker R, Parcharidou E, Beffa R (2020) Flufenacet activity is affected by GST inhibitors in blackgrass (*Alopecurus myosuroides*) populations with reduced flufenacet sensitivity and higher expression levels of GSTs. Weed Science 68: 451-459.

Ducker R, Zollner P, Lummen P, Ries S, Collavo A, Beffa R (2019a) Glutathione transferase plays a major role in flufenacet resistance of ryegrass (*Lolium* spp.) field populations. Pest Management Science 75: 3084-3092.

Ducker R, Zollner P, Parcharidou E, Ries S, Lorentz L, Beffa R (2019b) Enhanced metabolism causes reduced flufenacet sensitivity in black-grass (*Alopecurus myosuroides* Huds.) field populations. Pest Management Science 75: 2996-3004.

Eason A, Tim U, Wang X (2004) Integrated modeling environment for statewide assessment of groundwater vulnerability from pesticide use in agriculture. Pest Management Science 60: 737-745.

Ehleringer J (1983) Ecophysiology of *Amaranthus palmeri*: A Sonoran desert summer annual. Oecologia 57: 107-112.

Evans AF, O'Brien SR, Ma R, Hager AG, Riggins CW, Lambert KN, Riechers DE (2017) Biochemical characterization of metabolism-based atrazine resistance in *Amaranthus tuberculatus* and identification of an expressed GST associated with resistance. Plant Biotechnology Journal 15: 1238-1249.

Evenson KJ, Gronwald JW, Wyse DL (1997) Isoforms of acetyl-coenzyme A carboxylase in *Lolium multiflorum*. Plant Physiology and Biochemistry 35: 265-272.

Farago S, Kreuz K, Brunold C (1993) Decreased glutathione levels enhance the susceptibility of maize seedlings to metolachlor. Pesticide Biochemistry and Physiology 47: 199-205.

Farenhorst A (2006) Importance of soil organic matter fractions in soil-landscape and regional assessments of pesticide sorption and leaching in soil. Soil Science Society of America Journal 70: 1005-1012.

Farenhorst A, Florinsky I, Monreal C, Muc D (2003) Evaluating the use of digital terrain modelling for quantifying the spatial variability of 2,4-D sorption by soil within agricultural landscapes. Canadian Journal of Soil Science 83: 557-564.

Farenhorst A, Papiernik SK, Saiyed I, Messing P, Stephens KD, Schumacher JA, Lobb DA, Li S, Lindstrom MJ, Schumacher TE (2008) Herbicide sorption coefficients in relation to soil properties and terrain attributes on a cultivated prairie. Journal of Environmental Quality 37: 1201-1208.

Feigenbrugel V, Le Calve S, Mirabel P (2004) Temperature dependence of Henry's law constants of metolachlor and diazinon. Chemosphere 57: 319-327.

Field J, Thurman E (1996) Glutathione conjugation and contaminant transformation. Environmental Science & Technology 30: 1413-1418.

Figueiredo MRA, Leibhart LJ, Reicher ZJ, Tranel PJ, Nissen SJ, Westra P, Bernards ML, Kruger GR, Gaines TA Jugulam M (2018) Metabolism of 2,4-dichlorophenoxyacetic acid contributes to resistance in a common waterhemp (*Amaranthus tuberculatus*) population. Pest Management Science 74: 2356-2362.

Fonseca ECM, da Costa KS, Lameira J, Alves CN, Lima AH (2020) Investigation of the target-site resistance of EPSP synthase mutants P106T and T102I/P106S against glyphosate. Rsc Advances 10: 44352-44360.

Frova C (2003) The plant glutathione transferase gene family: genomic structure, functions, expression and evolution. Physiologia Plantarum 119: 469-479.

Gaeddert J, Peterson D, Horak M (1997) Control and cross-resistance of an acetolactate synthase inhibitor-resistant Palmer amaranth (*Amaranthus palmeri*) biotype. Weed Technology 11: 132-137.

Gaines TA, Zhang WL, Wang DF, Bukun B, Chisholm ST, Shaner DL, Nissen SJ, Patzoldt WL, Tranel PJ, Culpepper AS, Grey TL, Webster TM, Vencill WK, Sammons RD, Jiang JM, Preston C, Leach JE, Westra P (2010) Gene amplification confers glyphosate resistance in *Amaranthus palmeri*. Proceedings of the National Academy of Sciences of the United States of America 107: 1029-1034.

Gaines TA, Duke SO, Morran S, Rigon CAG, Tranel PJ, Kupper A, Dayan FE (2020) Mechanisms of evolved herbicide resistance. Journal of Biological Chemistry 295: 10307-10330.

Gaines TA, Ward SM, Bukun B, Preston C, Leach JE, Westra P(2012) Interspecific hybridization transfers a previously unknown glyphosate resistance mechanism in *Amaranthus* species. Evolutionary Applications 5: 29-38.

Gish TJ, Prueger JH, Kustas WP, Daughtry CST, McKee LG, Russ A, Hatfield JL (2009) Soil moisture and metolachlor volatilization observations over three years. Journal of Environmental Quality 38: 1785-1795.

Gonzalez-Torralva F, Rojano-Delgado AM, de Castro MDL, Mulleder N, De Prado R (2012) Two non-target mechanisms are involved in glyphosate-resistant horseweed (*Conyza canadensis* L. Cronq.) biotypes. Journal of Plant Physiology 169: 1673-1679.

Gossett B, Murdock E, Toler J (1992) Resistance of Palmer amaranth (*Amaranthus palmeri*) to the Dinitroaniline herbicides. Weed Technology 6: 587-591.

Guo F, Iwakami S, Yamaguchi T, Uchino A, Sunohara Y, Matsumoto H (2019) Role of CYP81A cytochrome P450s in clomazone metabolism in *Echinochloa phyllopogon*. Plant Science 283: 321-328.

Guttieri MJ, Eberlein CV, MallorySmith CA, Thill DC (1996) Molecular genetics of target-site resistance to acetolactate synthase inhibiting herbicides. Molecular Genetics and Evolution of Pesticide Resistance 645: 10-16.

Han H, Yu Q, Vila-Aiub M, Powles S (2014) Genetic inheritance of cytochrome P450-mediated metabolic resistance to chlorsulfuron in a multiple herbicide resistant *Lolium rigidum* population. Crop Protection 65: 57-63.

Hausman NE, Singh S, Tranel PJ, Riechers DE, Kaundun SS, Polge ND, Thomas DA, Hager AG (2011) Resistance to HPPD-inhibiting herbicides in a population of waterhemp (*Amaranthus tuberculatus*) from Illinois, United States. Pest Management Science 67: 258-261.

Heap I (2021) The international herbicide-resistant weed database online. Available at www.weedscience.org. Accessed January 29, 2021.

Horak M, Loughin T (2000) Growth analysis of four *Amaranthus* species. Weed Science 48: 347-355.

Horak M, Peterson D (1995) Biotypes of palmer amaranth (*Amaranthus palmeri*) and common waterhemp (*Amaranthus rudis*) are resistant to imazethapyr and thifensulfuron. Weed Technology 9: 192-195.

Huan ZB, Zhang HJ, Hou Z, Zhang SY, Zhang Y, Liu WT, Bi YL, Wang JX (2011) Resistance level and metabolism of barnyardgrass (*Echinochloa crusgalli* (L.) Beauv.) populations to quizalofop-P-ethyl in Heilongjiang Province, China. Agricultural Sciences in China 10: 1914-1922.

Iwakami S, Endo M, Saika H, Okuno J, Nakamura N, Yokoyama M, Watanabe H, Toki S, Uchino A, Inamura T (2014) Cytochrome P450 CYP81A12 and CYP81A21 are associated with resistance to two acetolactate synthase inhibitors in *Echinochloa phyllopogon*. Plant Physiology 165: 618-629.

Iwakami S, Kamidate Y, Yamaguchi T, Ishizaka M, Endo M, Suda H, Nagai K, Sunohara Y, Toki S, Uchino A, Tominaga T, Matsumoto H (2019) CYP81A P450s are involved in concomitant cross-resistance to acetolactate synthase and acetyl-CoA carboxylase herbicides in *Echinochloa phyllopogon*. New Phytologist 221: 2112-2122.

Jhala A, Sandell L, Rana N, Kruger G, Knezevic S (2014) Confirmation and control of triazine and 4-Hydroxyphenylpyruvate dioxygenase-inhibiting herbicide-resistant Palmer amaranth (*Amaranthus palmeri*) in Nebraska. Weed Technology 28: 28-38.

Joubes J, Raffaele S, Bourdenx B, Garcia C, Laroche-Traineau J, Moreau P, Domergue F, Lessire R (2008) The VLCFA elongase gene family in *Arabidopsis thaliana*: phylogenetic analysis, 3D modelling and expression profiling. Plant Molecular Biology 67: 547-566.

Kah M, Brown C, Ware G (2006) Adsorption of ionisable pesticides in soils. Reviews of Environmental Contamination and Toxicology, Vol 188 188: 149-217.

Kaundun SS, Hutchings SJ, Dale RP, Howell A, Morris JA, Kramer VC, Shivrain VK, Mcindoe E (2017) Mechanism of resistance to mesotrione in an *Amaranthus tuberculatus* population from Nebraska, USA. Plos One 12.

Klingaman T, Oliver L (1994) Palmer amaranth (*Amaranthus palmeri*) interference in soybeans (*Glycine max*). Weed Science 42: 523-527.

Krause A, Hancock WG, Minard RD, Freyer AJ, Honeycutt RC, Lebaron HM, Paulson DL, Liu SY, Bollag JM (1985) Microbial transformation of the herbicide metolachlor by a soil actinomycete. Journal of Agricultural and Food Chemistry 33: 584-589.

Kupper A, Peter F, Zollner P, Lorentz L, Tranel PJ, Beffa R, Gaines TA (2018) Tembotrione detoxification in 4-hydroxyphenylpyruvate dioxygenase (HPPD) inhibitor-resistant Palmer amaranth (*Amaranthus palmeri* S. Wats.). Pest Management Science 74: 2325-2334.

Lau YL, Liu DLS, Pacepavicius GJ, Maguire RJ (1995) Volatilization of metolachlor from water. Journal of Environmental Science and Health Part B-Pesticides Food Contaminants and Agricultural Wastes 30: 605-620.

Lechelt-Kunze C, Meissner R, Drewes M, Tietjen K (2003) Flufenacet herbicide treatment phenocopies the fiddlehead mutant in *Arabidopsis thaliana*. Pest Management Science 59: 847-856.

Lee J, Jo H, Kong K (2011) A Plant-specific Tau class glutathione *S*-transferase from *Oryza sativa* having significant detoxification activity towards Chloroacetanilide herbicides. Bulletin of the Korean Chemical Society 32: 3756-3759.

Li X, Grey T, Price K, Vencill W, Webster T (2019) Adsorption, desorption and persistence of fomesafen in soil. Pest Management Science 75: 270-278.

Liu WT, Bai S, Zhao N, Jia SS, Li W, Zhang LL, Wang JX (2018) Non-target site-based resistance to tribenuron-methyl and essential involved genes in *Myosoton aquaticum* (L.). Bmc Plant Biology 18.

Lu H, Yu Q, Han H, Owen M, Powles S (2019) Metribuzin resistance in a wild radish (*Raphanus raphanistrum*) population via both psbA gene mutation and enhanced metabolism. Journal of Agricultural and Food Chemistry 67: 1353-1359.

Masabni J. G, Zandstra BH (1999) A serine-to-threonine mutation in linuron-resistant *Portulaca oleracea*. Weed Science 47: 393-400.

Massinga R, Currie R, Horak M, Boyer J (2001) Interference of Palmer amaranth in corn. Weed Science 49: 202-208.

Matzrafi M, Shaar-Moshe L, Rubin B, Peleg Z (2017) Unraveling the transcriptional basis of temperature-dependent pinoxaden resistance in *Brachypodium hybridum*. Frontiers in Plant Science 8: 1-11.

McGahen L, Tiedje J (1978) Metabolism of 2 new Acylanilide herbicides, Antor herbicide (H-22234) and Dual (metolachlor) by soil fungus *Chaetomium globosum*. Journal of Agricultural and Food Chemistry 26: 414-419.

Mikkelsen M, Petersen B, Olsen C, Halkier B (2002) Biosynthesis and metabolic engineering of glucosinolates. Amino Acids 22: 279-295.

Millar A, Kunst L (1997) Very-long-chain fatty acid biosynthesis is controlled through the expression and specificity of the condensing enzyme. Plant Journal 12: 121-131.

Montellano P (2005) Cytochrome P450: Structure, mechanism, and biochemistryNew York: Kluwer Academic/Plenum Publishers

Munoz A, Koskinen WC, Cox L, Sadowsky MJ (2011) Biodegradation and mineralization of metolachlor and alachlor by *Candida xestobii*. Journal of Agricultural and Food Chemistry 59: 619-627.

Naganuma T, Sato Y, Sassa T, Ohno Y, Kihara A (2011) Biochemical characterization of the very long-chain fatty acid elongase ELOVL7. Febs Letters 585: 3337-3341.

Nakka S, Godar A, Thompson C, Peterson D, Jugulam M (2017a) Rapid detoxification via glutathione *S*-transferase (GST) conjugation confers a high level of atrazine resistance in Palmer amaranth (*Amaranthus palmeri*). Pest Management Science 73: 2236-2243.

Nakka S, Godar AS, Wani PS, Thompson CR, Peterson DE, Roelofs J, Jugulam M (2017b) Physiological and molecular characterization of hydroxyphenylpyruvate dioxygenase (HPPD)-inhibitor resistance in Palmer amaranth (*Amaranthus palmeri* S. Wats.). Frontiers in Plant Sci. 8.

Norsworthy JK, Griffith G, Scott R, Smith K, Oliver L (2008a) Confirmation and control of glyphosate-resistant Palmer amaranth (*Amaranthus palmeri*) in Arkansas. Weed Technology 22: 108-113.

Norsworthy JK, Oliveira MJ, Jha P, Malik M, Buckelew JK, Jennings KM, Monks DW (2008b) Palmer amaranth and large crabgrass growth with plasticulture-grown bell pepper. Weed Technol. 22: 296-302.

Novak J, Moorman T, Cambardella C (1997) Atrazine sorption at the field scale in relation to soils and landscape position. Journal of Environmental Quality 26: 1271-1277.

O'Connell P, Harms C, Allen J (1998) Metolachlor, *S*-metolachlor and their role within sustainable weed-management. Crop Protection 17: 207-212.

Oliveira MC,Gaines TA, Dayan FE, Patterson EL, Jhala AJ, Knezevic SZ (2018) Reversing resistance to tembotrione in an *Amaranthus tuberculatus* (var. *rudis*) population from Nebraska, USA with cytochrome P450 inhibitors. Pest Management Science 74: 2296-2305.

Owen MJ, Goggin DE, Powles SB (2012) Non-target-site-based resistance to ALS-inhibiting herbicides in six *Bromus rigidus* populations from Western Australian cropping fields. Pest Management Science 68: 1077-1082.

Pan L, Yu Q, Han HP, Mao LF, Nyporko A, Fan LJ, Bai LY, Powles S (2019) Aldo-keto reductase metabolizes glyphosate and confers glyphosate resistance in *Echinochloa colona*(1). Plant Physiology 181: 1519-1534.

Petit C, Duhieu B, Boucansaud K, Delye C (2010) Complex genetic control of non-target-site-based resistance to herbicides inhibiting acetyl-coenzyme A carboxylase and acetolactate-synthase in *Alopecurus myosuroides* Huds. Plant Science 178: 501-509.

Plaisance KL, Gronwald JW (1999) Enhanced catalytic constant for glutathione *S*-transferase (atrazine) activity in an atrazine-resistant *Abutilon theophrasti* biotype. Pesticide Biochemistry and Physiology 63: 34-49.

PostBeittenmiller D (1996) Biochemistry and molecular biology of wax production in plants. Annual Review of Plant Physiology and Plant Molecular Biology 47: 405-430.

Prueger JH, Alfieri J, Gish TJ, Kustas WP, Daughtry CST, Hatfield JL, McKee LG (2017) Multi-year measurements of field-scale metolachlor volatilization. Water Air and Soil Pollution 228: 11.

Prueger JH, Gish TJ, McConnell LL, McKee LG, Hatfield JL, Kustas WP (2005) Solar radiation, relative humidity, and soil water effects on metolachlor volatilization. Environmental Science & Technology 39: 5219-5226.

Prueger JH, Hatfield JL, Sauer TJ (1999) Field-scale metolachlor volatilization flux estimates from broadcast and banded application methods in central Iowa. Journal of Environmental Quality 28: 75-81.

R Core Team R (2020) R: A language and environment for statistical computing. Vienna, Austria: R Core Team (2020).

Rangani G, Noguera M, Salas-Perez R, Benedetti L, Roma-Burgos N (2021) Mechanism of resistance to *S*-metolachlor in Palmer amaranth. Frontiers in Plant Science 12: 13.

Rangani G, Salas-Perez RA, Aponte RA, Knapp M, Craig IR, Mietzner T, Langaro AC, Noguera MM, Porri A, Roma-Burgos N (2019) A novel single-site mutation in the catalytic domain of protoporphyrinogen oxidase IX (PPO) confers resistance to PPO-inhibiting herbicides. Frontiers in Plant Science 10.

Riar D, Norsworthy J, Steckel L, Stephenson D, Bond J (2013a) Consultant perspectives on weed management needs in midsouthern united states cotton: A follow-up survey. Weed Technology 27: 778-787.

Riar DS, Norsworthy JK, Steckel LE, Stephenson DO, Eubank TW, Bond J, Scott RC (2013b) Adoption of best management practices for herbicide-resistant weeds in midsouthern United States cotton, rice, and soybean. Weed Technology 27: 788-797.

Riar DS, Norsworthy JK, Steckel LE, Stephenson DO, Eubank TW, Scott RC (2013c) Assessment of Weed Management Practices and Problem Weeds in the Midsouth United States-Soybean: A Consultant's Perspective. Weed Technology 27: 612-622.

Roberts T (2000) Metabolism of agrochemicals in plants. Pp. 300.

Ross M, Lembi C (2009) Applied weed science: including the ecology and management of invasive plants. 3rd ed.: Pearson. Pp. 576.

Salas RA, Burgos NR, Tranel PJ, Singh S, Glasgow L, Scott RC, Nichols RL (2016) Resistance to PPO-inhibiting herbicide inPalmer amaranth from Arkansas. Pest Management Science 72: 864-869.

Salas-Perez RA, Burgos NR, Rangani G, Singh S, Refatti JP, Piveta L, Tranel PJ, Mauromoustakos A, Scott RC (2017) Frequency of Gly-210 deletion mutation among protoporphyrinogen oxidase inhibitor-resistant Palmer amaranth *Amaranthus palmeri*) populations. Weed Sci. 65: 718-731.

Sassa T, Kihara A (2014) Metabolism of very long-chain fatty acids: genes and pathophysiology. Biomolecules & Therapeutics 22: 83-92.

Sathasivan K, Haughn GW, Murai N (1991) Molecular-basis of imidazolinone herbicide resistance in *Arabidopsis thaliana* var *columbia*. Plant Physiology 97: 1044-1050.

Senseman S (2007) Herbicide handbook. 9th ed. Lawrence, KS: Weed Science Society of America. Pp. 458.

Shergill LS, Bish MD, Jugulam M, Bradley KW (2018) Molecular and physiological characterization of six-way resistance in an *Amaranthus tuberculatus* var. *rudis* biotype from Missouri. Pest Management Science 74: 2688-2698.

Si Y, Takagi K, Iwasaki A, Zhou D (2009) Adsorption, desorption and dissipation of metolachlor in surface and subsurface soils. Pest Management Science 65: 956-962.

Siminszky B, Corbin F, Sheldon Y (1995) Nicosulfuron resistance and metabolism in terbufos-treated and naphthalic anhydride-treated corn. Weed Science 43: 163-168.

Siminszky B, Corbin F, Ward E, Fleischmann T, Dewey R (1999) Expression of a soybean cytochrome P450 monooxygenase cDNA in yeast and tobacco enhances the metabolism of phenylurea herbicides. Proceedings of the National Academy of Sciences of the United States of America 96: 1750-1755.

Siminszky B, Freytag A, Sheldon B, Dewey R (2003) Co-expression of a NADPH : P450 reductase enhances CYP71A10-dependent phenylurea metabolism in tobacco. Pesticide Biochemistry and Physiology 77: 35-43.

Siminszky B, Sheldon B, Corbin F, Dewey R (2000) A cytochrome P450 monooxygenase cDNA (CYP71A10) confers resistance to linuron in transgenic *Nicotiana tabacum*. Weed Science 48: 291-295.

Singh S, Singh V, Lawton-Rauh A, Bagavathiannan M, Roma-Burgos N (2018) *EPSPS* gene amplification primarily confers glyphosate resistance among Arkansas Palmer amaranth (*Amaranthus palmeri*) Populations. Weed Sci. 66: 293-300.

Stamper D, Tuovinen O (1998) Biodegradation of the acetanilide herbicides alachlor, metolachlor, and propachlor. Critical Reviews in Microbiology 24: 1-22.

Stanjek V, Pie, J, Boland W (1999) Synthesis of furanocoumarins: mevalonate-independent prenylation of umbelliferone in *Apium graveolens* (Apiaceae). Phytochemistry 50: 1141-1145.

Stewart I, Loague K (1999) A type transfer function approach for regional-scale pesticide leaching assessments. Journal of Environmental Quality 28: 378-387.

Svyantek AW, Aldahir P, Chen S, Flessner ML, McCullough PE, Sidhu SS, McElroy JS (2016) Target and nontarget resistance mechanisms induce annual bluegrass (*Poa annua*) resistance to atrazine, amicarbazone, and diuron. Weed Technology 30: 773-782.

Tattersall DB, Bak S, Jones PR, Olsen CE, Nielsen JK, Hansen ML, Hoj PB, Moller BL (2001) Resistance to an herbivore through engineered cyanogenic glucoside synthesis. Science 293: 1826-1828.

Torra J, Rojano-Delgado AM, Rey-Caballero J, Royo-Esnal A, Salas ML, De Prado R (2017) Enhanced 2,4-D metabolism in two resistant papaver rhoeas populations from Spain. Frontiers in Plant Science 8.

Trenkamp S, Martin W, Tietjen K (2004). Specific and differential inhibition of very-long-chain fatty acid elongases from *Arabidopsis thaliana* by different herbicides. Proceedings of the National Academy of Sciences of the United States of America 101: 11903-11908.

Varanasi VK, Brabham C, Norsworthy JK (2018a) Confirmation and characterization of non-target site resistance to fomesafen in Palmer amaranth (*Amaranthus palmeri*). Weed Sci. 66: 702-709.

Varanasi VK, Brabham C, Norsworthy JK, Nie H, Young BG, Houston M, Barber T, Scott RC (2018b) A statewide survey of PPO-inhibitor resistance and the prevalent target-site mechanisms in palmer amaranth (*Amaranthus palmeri*) Accessions from Arkansas. Weed Sci. 66: 149-158.

Vennapusa AR, Faleco F, Vieira B, Samuelson S, Kruger GR, Werle R, Jugulam M (2018) Prevalence and mechanism of atrazine resistance in waterhemp (*Amaranthus tuberculatus*) from Nebraska. Weed Science 66: 595-602.

Ward S, Webster T, Steckel L (2013) Palmer amaranth (*Amaranthus palmeri*): A review. Weed Technology 27: 12-27.

Webb SR, Hall JC (1995) Auxinic herbicide-resistant and herbicide-susceptible wild mustard (*Sinapis arvensis* L) Biotypes - effect of auxinic herbicides on seedling growth and auxin-binding activity. Pesticide Biochemistry and Physiology 52: 137-148.

Werck-Reichhart D, Feyereisen R (2000) Cytochromes P450: a success story. Genome Biology 1: reviews3003.1.

Westra E, Shaner D, Barbarick K, Khosla R (2015) Evaluation of sorption coefficients for pyroxasulfone, *S*-metolachlor, and dimethenamid-P. Air Soil and Water Research 8: 9-15.

Westwood JH, Charudattan R, Duke SO, Fennimore SA, Marrone P, Slaughter DC, Swanton C, Zollinger R (2018) Weed management in 2050: Perspectives on the future of Weed Science. Weed Science 66: 275-285.

Wetzel DK, Horak MJ, Skinner DZ (1999) Use of PCR-based molecular markers to identity weedy *Amaranthus* species. Weed Science 47: 518-523.

White P, Potter T, Culbreath A (2010) Fungicide dissipation and impact on metolachlor aerobic soil degradation and soil microbial dynamics. Science of the Total Environment 408: 1393-1402.

Wittstock U, Halkier B (2002) Glucosinolate research in the *Arabidopsis* era. Trends in Plant Science 7: 263-270.

Wolf A, Dietz K, Schroder P (1996) Degradation of glutathione *S*-conjugates by a carboxypeptidase in the plant vacuole. Febs Letters 384: 31-34.

Yamamoto E, Zeng LH, Baird WV (1998) Alpha-tubulin missense mutations correlate with antimicrotubule drug resistance in *Eleusine indica*. Plant Cell 10: 297-308.

Yao X, Wang Y, Yue X, Liu M, Liu K (2016) Generation of tribenuron-methyl herbicide-resistant OsCYP81A6-expressing rapeseed (*Brassica napus* L.) plants for hybrid seed production using chemical-induced male sterility. Plant Breeding 135: 349-354.

Yasuor H, Osuna MD, Ortiz A, Saldain NE, Eckert JW, Fischer AJ (2009) Mechanism of resistance to penoxsulam in late watergrass [*Echinochloa phyllopogon* (Stapf) Koss.]. Journal of Agricultural and Food Chemistry 57: 3653-3660.

Yuan JS, Tranel PJ, Stewart CN (2007) Non-target-site herbicide resistance: a family business. Trends in Plant Science 12: 6-13.

Zablotowicz R, Hoagland R, Locke M, Hickey W (1995) Glutathione *S*-transferase activity and metabolism of glutathione conjugates by rhizosphere bacteria. Applied and Environmental Microbiology 61: 1054-1060.

Zhan XM, Liu HJ, Miao YG, Liu WP (2006). A comparative study of rac- and *S*-metolachlor on some activities and metabolism of silkworm, *Bombyx mori* L. Pesticide Biochemistry and Physiology 85: 133-138.

Zhao N, Ge LA, Yan YY, Bai S, Wang DD, Liu WT, Wang JX (2019a) Trp-1999-Ser mutation of acetyl-CoA carboxylase and cytochrome P450s-involved metabolism confer resistance to fenoxaprop-P-ethyl in *Polypogon fugax*. Pest Management Science 75: 3175-3183.

Zhao N, Li W, Bai S, Guo WL, Yuan GH, Wang F, Liu WT, Wang JX (2017) Transcriptome profiling to identify genes involved in mesosulfuron-methyl resistance in *Alopecurus aequalis*. Frontiers in Plant Science 8.

Zhao N, Yan YY, Ge LA, Zhu BL, Liu WT, Wang JX (2019b) Target site mutations and cytochrome P450s confer resistance to fenoxaprop-P-ethyl and mesosulfuron-methyl in Alopecurus aequalis. Pest Management Science 75: 204-214.

Resistance of Palmer amaranth (*Amaranthus palmeri*) to *S*-metolachlor in the Mid-southern United States

Abstract

Palmer amaranth (*Amaranthus palmeri* S. Wats.) is one of the most problematic weeds in many cropping systems in the Mid-southern US because of its multiple weedy traits and its propensity to evolve resistance to many herbicides of different modes of action. In Arkansas, Palmer amaranth has evolved metabolic resistance to *S*-metolachlor, compromising the effectiveness of an important weed management tool. Greenhouse studies were conducted to evaluate the differential response of Palmer amaranth accessions from three states (Arkansas, Mississippi and Tennessee) to (1) assess the occurrence of resistance to *S*-metolachlor among Palmer amaranth populations, (2) evaluate the resistance level in selected accessions and their resistant progeny, (3) and determine the susceptibility of most highly-resistant accessions to other soil-applied herbicides. Seeds were collected from 168 crop fields between 2017 and 2019. One hundred seeds per accession were planted in silt loam soil without herbicide for >20 years and sprayed with the labelled rate of *S*-metolachlor (1120 g ai ha^{-1}). Six accessions (four from Arkansas and two from Mississippi) were classified resistant. The effective doses (LD_{50}) to control the parent accessions ranged between 73 and 443 g ai ha^{-1} and those of F_1 progeny of survivors were 73 to 577 g ai ha^{-1}. The resistant field populations required 2.2 to 7.0 times more herbicide to reduce seedling emergence 50% while the F1 of survivors needed up to 9.2 times more herbicide to reduce emergence 50%. The resistance level was generally greater among progenies of surviving plants than among resistant field populations.

Key words: herbicide resistance, preemergence herbicides, *Amaranthus palmeri* S. Wats, *S*-metolachlor

Introduction

Palmer amaranth is one of the most common, problematic, and economically detrimental weeds throughout the southern United States (Ward et al. 2013). It is one of the two most troublesome weeds in Arkansas, Louisiana, Mississippi, and Tennessee (Riar et al. 2013). In 2013, glyphosate-resistant Palmer amaranth infestations represented 16% of scouted areas in Louisiana, while it was present in 54% of scouted areas in Mississippi, Tennessee and Arkansas, and the average cost of hand-weeding Palmer amaranth was US\$59 ha^{-1} (Riar et al. 2013). Palmer amaranth emerges continuously from late spring to late summer as long as the soil temperature is favorable (Chahal et al. 2021; Keeley et al. 1987). The propensity of Palmer amaranth to evolve resistance to many herbicides has made it difficult to control. To date, it is resistant to glyphosate (Culpepper et al. 2006; Norsworthy et al. 2008), acetolactate synthase (ALS)-inhibiting herbicides (Burgos et al. 2001; Gaeddert et al. 1997; Horak and Peterson 1995), dinitroanilines (Gossett et al. 1992), 4-hydroxyphenylpyruvate dioxygenase (HPPD) inhibitors (Jhala et al. 2014; Nakka et al. 2017b), photosystem II-inhibiting herbicides (Nakka et al. 2017a), and protoporphyrinogen oxidase (PPO) inhibitors (Salas et al. 2016; Salas-Perez et al. 2017; Varanasi et al. 2018a; Varanasi et al. 2018b). Palmer amaranth (*Amaranthus palmeri* S. Wats.) has also evolved resistance to *S*-metolachlor in Arkansas (Brabham et al. 2019; Rangani et al. 2021).

S-metolachlor inhibits very long chain fatty acid (VLCFA) synthesis (Matthes et al. 1998). Very long chain fatty acids are important components of lipids such as triacylglycerols (accumulated in seeds), some sphingolipids and phospholipids found in cell membranes, and cuticular waxes on plant aerial surfaces (Trenkamp et al. 2004). Therefore, VLCFAs are major components of hydrophobic polymers that prevent desiccation at the leaf surface (Trenkamp et al. 2004). Sphingolipids and phospholipids are required for cell division, polarity and differentiation (Lechelt-Kunze et al. 2003). The VLCFA-inhibiting herbicides target the condensing enzyme 3-ketoacyl-CoA synthase (KCS) FAE1 within the elongase enzymatic complex bound to the endoplasmic reticulum (Boger 2003; Busi 2014; Millar and Kunst 1997). By provoking a disruption of VLCFA levels in plants, these herbicides can inhibit growth or cause embryo mortality (Du Granrut and Cacas 2016). The VLCFA-inhibiting herbicides have been used for more than 60 years (Busi 2014). Important VLCFA-inhibiting herbicides include pyroxasulfone, dimethenamid-P, acetochlor and *S*-metolachlor. The latter has been labeled for use in more than 70 crops (O'Connell et al. 1998). *S*-metolachlor effectively controls yellow nutsedge, annual grasses, and small-seeded broadleaf species including Palmer amaranth (Barber et al., 2021). Prior to *Amaranthus* species, only five grasses had evolved resistance to VLCFA-inhibiting herbicides despite their prevalent use (Busi 2014, Heap 2021) (Table 3. 1).

Herbicide resistance is a major concern in modern agriculture as it compromises producers’ efforts to sustainably manage productive systems. Weeds generally cause greater yield reductions than other pests; therefore, weed management is mandatory to crop production (Oerke 2006). The use of synthetic herbicides has permitted simple and effective management of weeds in many cropping systems (Busi et al. 2018). Unfortunately, the evolution of herbicide resistance in many weed species worldwide is reducing the effectiveness of chemical weed control (Beckie and Tardif 2012; Busi et al. 2018; Powles and Yu 2010; Roma-Burgos et al. 2019). Therefore, herbicide resistance, is a key factor that spurs the search for new herbicide targets and intervention technologies (Burgos 2015), and the promotion of best management practices (Burgos 2015; Norsworthy et al. 2012). The loss of crucial herbicides and the need for immediate answers to growers' needs require extensive research on weed resistance to herbicides to enable proactive management of herbicide-resistant weeds (Burgos et al. 2013).

For a comprehensive assessment of the resistance problem, other soil-applied herbicides need to be tested on populations deemed resistant to *S*-metolachlor. PPO-inhibiting herbicides, such as fomesafen, flumioxazin, saflufenacil and sulfentrazone, have been extensively used as alternative herbicides to manage weed resistance to other herbicide modes of action (Umphres et al. 2018). The PPO-inhibiting herbicides have been used for more than 60 years (Salas et al. 2016) and can be applied either preemergence (PRE) or postemergence (POST). Flumioxazin and fomesafen are effective on major weeds in field crop production (Askew et al. 1999; Askew et al. 2002; Clewis et al. 2007; Niekamp et al. 1999; Umphres et al. 2018). Flumioxazin can be applied with nonselective preplant burndown herbicides, PRE alone or tank-mixed with other PRE herbicides (Umphres et al. 2018). It is effective on glyphosate-resistant Palmer amaranth (Whitaker et al. 2010) or species resistant to ALS inhibitors or atrazine (Taylor-Lovell et al. 2002). Fomesafen, in combination with *S*-metolachlor or pendimethalin, can control glyphosate-resistant Palmer amaranth (Nandula et al., 2013). Photosystem II (PSII)-inhibiting herbicides are widely used for weed control in corn (*Zea mays* L.) and sorghum [(*Sorghum bicolor* (L.) Moench] production (Anonymous 2021). Many PSII-inhibiting herbicides have soil and foliar activity. Among the oldest PSII inhibitors with the broadest weed spectrum is atrazine (Anonymous 2021). Together, the VLCFA, PPO, and PSII inhibitors comprise the most important groups of herbicides used in several production systems.

The extent of Palmer amaranth resistance to *S*-metolachlor in the Mid-southern US has not been investigated. The response of *S*-metolachlor-resistant populations to other soil applied herbicides needs to be assessed to determine effective alternative chemical tools. The objectives of this research were to (i) evaluate the extent of Palmer amaranth resistance to *S*-metolachlor in the Mid-southern US, (ii) determine the resistance level of accessions classified as resistant, (iii) determine the change in resistance level from original populations to their progenies, and (iv) investigate alternative PRE herbicides for the control of resistant populations.

Materials and Methods

Palmer amaranth seed collection

Palmer amaranth seeds were collected in crop fields in 2017, 2018 and 2019 from Mid-southern US states Arkansas, Mississippi, and Tennessee (Figure 3. 1). In Arkansas, samples were collected from 61 crop fields (15 counties) in 2017 and 35 crop fields (14 counties) in 2018. In Mississippi, samples were collected from 54 fields (17 counties) in 2017. In Tennessee, a total of 18 fields (10 counties) were collected for the years 2018 and 2019. Samples were collected according to standard procedures (Burgos 2015). Samples were collected from fields reported by growers to university extension agents showing control failure with *S*-metolachlor. Palmer amaranth inflorescences were harvested from at least 10 female plants and bagged to make one composite sample per field. The inflorescences were air-dried, threshed, and the seeds cleaned. Seeds were stored at room temperature.

During fall 2019, county extension agents collected additional seeds from fields with accessions that were the most difficult to control after the fall 2018 seed collection. Accessions from these fields had high frequency of survivors in the resistance test (discussed further in Results and Discussion). The 2019 accessions were labeled 19CRI-D, 19PHI-C and 19WOO-B, respectively, and included in subsequent dose-response studies.

Herbicide resistance testing

A large-scale test for resistance was conducted in the greenhouse at the Milo J. Shult Agricultural Research & Extension Center, Fayetteville, AR, of the University of Arkansas System Division of Agriculture. Roxana silt loam field soil, with no herbicide use history, was collected from the Vegetable Research Station, University of Arkansas System Division of Agriculture in Kibler, AR. Soil was air-dried in a greenhouse and sieved. A sub-sample was submitted to the Fayetteville Agricultural Diagnostic Laboratory of the Arkansas Agricultural Experiment Station in Fayetteville, AR for soil analysis (Table 3. 2). Soil pH and electrical conductivity (EC) were measured in a 1:2 soil:water mixture (Sikora and Kissel 2014) and total nitrogen (N) was measured by thermal combustion analysis (Provin, 2014). Soil nutrients were analyzed using Mehlich-3 method (Zhang et al. 2014).

Palmer amaranth accessions were treated with the labelled rate of *S*-metolachlor (1120 g ai ha^{-1}) in three replicates. The experimental units (flats) were arranged in a completely randomized design and the resistance test was repeated in time. The experimental units were 12.2 by 9.5 by 5.7-cm^3 flats (Insert TO standard; Hummert International, Earth City, MO) filled with the same amount of soil. The day prior to planting and herbicide application, the soil-filled flats were saturated with tap water and allowed to drain to obtain uniform, water-holding capacity soil moisture. One hundred seeds were spread uniformly on the soil surface of each tray and were subsequently covered with a thin layer of soil. The assay had two treatments per accession (treated and nontreated control). *S*-metolachlor (Dual II Magnum; Syngenta Crop Protection, LLC, Greensboro, NC, USA) was applied at the field-labelled rate of 1120 g ai ha^{-1} using a spray chamber equipped with Teejet 1100067 nozzles (Spraying Systems Inc., Wheaton, IL) calibrated to deliver 187 L ha^{-1} at a pressure of 276 kPa. *S*-metolachlor was activated shortly after spraying the herbicide by misting approximately 0.8 cm of water over the surface. Plants were misted overhead twice a day for the first week after which plants were sub-irrigated for the remainder of the study. Survivors of the labelled rate from the first resistance test (conducted during fall 2018) were grown, isolated within cages by accession, and allowed to interbreed for seed production to evaluate progression of herbicide resistance from parents to progenies.

S-metolachlor dose-response bioassays

Accessions with the least susceptibility to *S*-metolachlor in initial tests were subjected to a follow-up dose-response study. In 2019 and 2020 dose-response studies were conducted using nine rates of *S*-metolachlor (0, 0.125x, 0.25x, 0.5x, 0.75x, 1x, 1.5x, 2x, 2.5x) for the putative resistant accessions with the 1x rate being 1120 g ai ha^{-1}. A susceptible standard (SS) was used as reference with eight rates of *S*-metolachlor (0, 0.03125x, 0.125x, 0.25x, 0.5x, 0.75x, 1x, 1.5x). Overall, seven parent accessions were used: five from Arkansas (17PRA-A, 17RAN-A, 18CRI-D, 18PHI-C, and 18WOO-B) and two from Mississippi (17TUN-A and 17TUN-D). The planting medium, seeding rate, herbicide application volume, watering, and plant maintenance were as described in the herbicide resistance testing section.

Survivors of the 1x rate from 18PHI-C and 18WOO-B were grown, isolated within cages by accession, and allowed to interbreed for seed production. The respective offspring were referred to as "18PHI-C-F$_1$" and "18WOO-B-F$_1$". Survivors from accession 18CRI-D, were also cultured, but did not produce enough seeds for a dose-response study. Samples collected from 19CRI-D, 19PHI-C and 19WOO-B were included in the dose-response assay with the corresponding accessions collected from the same fields in 2018, and their respective progenies after having survived *S*-metolachlor treatment. The intent was to compare resistance levels between the 2018 and 2019 populations from the same fields and compare resistance levels between field-collected parents in 2018 and the progeny of plants surviving herbicide treatment in the greenhouse. Similar dose response rate structures as the first year were utilized. The experimental design, plant establishment and herbicide application details were as described in the resistance testing section. The assays were repeated in time.

Response of S-metolachlor-resistant accessions to other soil-applied herbicides

The response of the four accessions most resistant to *S*-metolachlor from dose-response assays (18CRI-D, 18WOO-B, 17TUN-A and 17TUN-D) and one SS to five alternative residual herbicides across three modes-of-action (Table 3. 3) was evaluated. These accessions (one hundred seeds per accession) were treated with dimethenamid-P, pyroxasulfone, flumioxazin, fomesafen, and atrazine. Herbicides were applied at their respective field-use rates (Table 3. 3). Each accession had a nontreated control. The experimental units were arranged in a completely randomized design with three treatment replicates and was experimentally-repeated in two separate greenhouses. Plant establishment and herbicide application details were as described earlier.

Data collection and analysis

All bioassays were evaluated 21 d after treatment (DAT). In each case, live plants were counted and the data were converted to percent survival based on the number of live plants in the respective nontreated control. For the responses of *S*-metolachlor-resistant accessions to other applied herbicides bioassay, survival rates were also evaluated 14 DAT. Dose-response data were pooled across replicated runs for each experiment. Palmer amaranth percent survival in response to increasing rates of *S*-metolachlor, for parents and F_1 progenies, were analyzed using a non-linear regression equation. A 3-parameter log-logistic model (equation 3. 1) was used to relate Palmer amaranth percent survival to *S*-metolachlor rates using non-linear least squares regression (nls) in R version 4.0.0 (R Core Team, 2020).

$$Y = \frac{d}{1+\exp[b(\log(x)-loge)]} \qquad [3.\ 1]$$

where Y is Palmer amaranth percent survival, d is the upper asymptotic value of Y, b is the slope of the curve, e is the rate of the herbicide required to reduce seedling emergence 50% (LD_{50}), and x is the *S*-metolachlor dose.

For the resistance profiling bioassay, Palmer amaranth percent control were subjected to ANOVA using the GLIMMIX procedure in SAS 9.4 (SAS Institute Inc., Cary, NC, USA) assuming a beta distribution (Gbur et al., 2012. Greenhouses were considered random effects while herbicides and accessions were considered fixed effects. Treatment means were separated at P≤0.05 using a Tukey HSD adjustment.

Results and Discussion

Differential responses to S-metolachlor of Palmer amaranth from the Mid-southern US

This research included 168 accessions (57-, 32- and 11% from Arkansas, Mississippi and Tennessee, respectively) and covered 23-, 16-, and 10 counties, respectively in each state. Out of 61 accessions from Arkansas in 2017, 3.3% were controlled less than 90%, 10% were controlled between 90 and 95%, and 87% were controlled 95% or higher (Figure 3. 2). Among 35 accessions collected in Arkansas in 2018, 23% were controlled less than 90%, 17% were controlled between 90 and 95% and 60% were controlled 95% or higher. Of the 54 accessions from Mississippi in 2017, 4% were controlled less than 90%; the rest were controlled 90% or higher. No accession from Tennessee was controlled less than 90%. Of the 18 accessions evaluated, 6% were controlled between 90 and 95% and 94% were controlled at least 95%.

It is commonly understood that weed populations would have differential tolerance to herbicides as influenced by background genetic variation within and among populations. The labeled rates of herbicides are set to ensure that the most tolerant individuals, or populations of target species, are controlled 100% as consistently as possible across environments. In crop production, weed control at ≥90% is considered excellent. Differential tolerance to labeled rate of herbicides has been documented among older, susceptible Palmer amaranth populations from Arkansas, for example, with respect to fomesafen (Salas et al. 2016), glufosinate (Sales-Perez et al. 2018), and mesotrione (Singh et al. 2018), and ALS-inhibiting herbicides (Bond et al. 2006; Burgos et al. 2001), from Kansas with respect to glyphosate, 2,4-D, atrazine, and mesotrione (Kumar et al. 2020). According to Singh et al. (2018), 34% Palmer amaranth surveyed in Arkansas survived mesotrione applications with injury ranging from 61% to 90%.

When a population starts having an increasing number of individuals surviving the labeled rate, this is an indication of evolving resistance, as was observed with Palmer amaranth populations resistant to PPO-inhibiting herbicides (Salas et al. 2016). The fact that a number of recent populations showed less than 90% control with the labeled rate of *S*-metolachlor indicates possible evolving resistance in those populations. The occurrence of resistance to *S*-metolachlor has already been confirmed in a few populations (Brabham et al. 2019; Rangani et al. 2021). The current survey indicated additional populations might have also evolved resistance to *S*-metolachlor.

Resistance level to S-metolachlor

The resistance level to *S*-metolachlor was evaluated for accessions that were controlled less than 88% during the general screening. In total, seven accessions were used for the dose-response studies with two accessions from Arkansas in 2017 (17PRA-A and 17RAN-A), three accessions from Arkansas in 2018 (18CRI-D, 18PHI-C, and 18WOO-B), and two accessions from Mississippi in 2017 (17TUN-A and 17TUN-D). The LD_{50} values (e) ranged between 73 and 443 g ai ha^{-1} for field populations of all seven accessions evaluated. The SS required 63 ± 16 g ai ha^{-1} while resistant accessions required 443±36, 289 ± 12, 156 ± 16, 140 ± 11, 73 ± 21, 313 ± 54, and 242 ± 32 g ai ha^{-1} to reduce seedling emergence 50% for 18WOO-B, 18CRI-D, 17PRA-A, 17RAN-A, 18PHI-C, 17TUN-A, and 17TUN-D, respectively (Tables 3. 4; Figure 3. 3). The levels of resistance of 18WOO-B, 18CRI-D, 17RAN-A, 17PRA-A, 18PHI-C, 17TUN-A, and 17TUN-D to *S*-metolachlor were 7.0-, 4.6-, 2.2-, 2.5-, 5.0-, and 3.8- fold, respectively. Accession 18PHI-C was deemed susceptible while the other populations with elevated frequency of survivors were resistant to *S*-metolachlor. This survey confirmed resistance to *S*-metolachlor in four Arkansas counties (Randolf, Prairie, Crittenden, Woodruff) and one county in Mississippi (Tunica). Brabham et al. (2019) had also reported two resistant populations from Marion and Crawfordsville (Crittenden county) while Rangani et al. (2021) reported resistant populations in Crittenden, Woodruff and Mississippi counties in 2014 and 2015. Resistant accessions reported by Brabham et al. (2019) required 156 and 133 g ha^{-1} of *S*-metolachlor to attain 50% control and were 9.8 and 8.3 times less responsive to *S*-metolachlor than the susceptible standards. According to Rangani et al. (2021) LD_{50} values of resistant accessions were between 88 and 785 g ai ha^{-1}, which equated to resistance levels between 3- to 29-fold. Results from this research documented, for the first time, *S*-metolachlor resistance in accessions collected from two crop fields collected in Tunica County in Mississippi. The dose-response studies produced survivors at a 2x rate of *S*-metolachlor. Should these types of individuals be allowed to produce seeds in the field, owing to insufficient supplemental control measures, complete failure of the herbicide would be expected in a few years.

Resistance progression in the progenies

Progenies of surviving plants had the greatest levels of resistance to *S*-metolachlor application in the dose-response studies. Accessions 19CRI-D and 19WOO-B required 327±47 and 520±64 g ai ha^{-1} to reduce seedling emergence 50%. Based on LD_{50} values, these populations were 5 and 8 times less sensitive to *S*-metolachlor compared to the SS (Figure 3. 4). Accession 19PHI-C required 73±19 g ai ha^{-1} to reduce seedling emergence 50% and was as sensitive as SS. The F_1 progenies, 18PHI-C-F_1 and 18WOO-B-F_1, were 2.1 and 9.2 times less sensitive to *S*-metolachlor compared to the SS, requiring 130±15 and 577±52 g ai ha^{-1}, respectively, to reduce seedling emergence 50%.

Resistance to VLCFA-inhibiting herbicides evolved more slowly compared to herbicides that target other sites of action (Heap 2021), despite the extensive use of VLCFA-inhibiting herbicides in numerous crops and millions of hectares for decades. Several hypotheses may explain the slower evolution of resistance of weeds to VLCFA-inhibiting herbicides, including the infrequent target-site mutations in the condensing enzyme (Boger et al. 2000; Busi 2014); the requirement of highly improbable simultaneous changes in several different targets to deliver resistance to VLCFA-inhibiting herbicides due to the interaction of these herbicides with multiple targets (Busi 2014; Tanetani et al. 2009; Trenkamp et al. 2004); and the low proportion of survivors of these herbicides that grow to maturity and produce seeds because postemergence applications of herbicides with different modes of action are typically utilized (Busi 2014). However, the occurrence of resistance has been increasing in recent years with five grasses [Wimmera ryegrass (*Lolium rigidum* Gaud.) (Busi et al. 2018), Italian ryegrass (*L. multiflorum* Lam.) (Ducker et al. 2019a), slender meadow foxtail (*Alopecurus myosuroides* Huds.) (Ducker et al. 2019b), barnyardgrass [*Echinochloa crus-galli* (L.) P. Beauv.] (Juliano et al. 2010), and wild oat (*Avena fatua* L.) (Heap 2021)], wild radish (*Raphanus raphanistrum* L.) (Heap 2021) and two *Amaranthus* species {waterhemp [*A. tuberculatus* (Moq.) Sauer], Palmer amaranth (*A. palmeri* S. Wats.)} that have also evolved resistance to VLCFA-inhibiting herbicides (Brabham et al. 2019; Rangani et al. 2021; Strom et al. 2020).

Efficacy of other soil-applied herbicides on Palmer amaranth resistant to S-metolachlor

Four S-metolachlor-resistant accessions (18CRI-D, 18WOO-B, 17TUN-A and 17TUN-D) were evaluated. The three-way greenhouse-by-accession-by-herbicide interaction was not significant at 14 and 21 ($P > 0.05$) DAT. The two-way greenhouse-by-accession, greenhouse-by-herbicide, and accession-by-herbicide interactions were not significant at 14 and 21 DAT ($P > 0.05$) (Table 3. 5). At full labelled rates, all soil-applied herbicides tested provided excellent control of *S*-metolachlor-resistant Palmer amaranth (≥ 90%) (Table 3. 6).

These results are consistent with previous research. All five herbicides are viable options for the control of *S*-metolachlor resistant Palmer amaranth from the Mid-southern US. Brabham et al. (2019) reported a decrease in sensitivity of *S*-metolachlor-resistant accessions to dimethenamid-P, but accessions were either completely killed or severely stunted upon a 1/4× rate application of dimethenamid-P. *S*-metolachlor-resistant accessions in their study did not show cross-resistance to other VLCFA-inhibiting herbicides acetochlor, dimethenamid-P, or pyroxasulfone. In a larger survey of Palmer amaranth populations, atrazine remains an effective option for most Palmer amaranth accessions from Arkansas (Gonzalez-Torralva et al. 2020), likely aided by the small acreage of corn and sorghum produced in the state. Increasing the frequency of corn and grain sorghum in crop rotations would be a good strategy for delaying *S*-metolachlor resistance evolution in the Mid-southern US. Umphres (2018) reported more than 90% control of Palmer amaranth by flumioxazin in a greenhouse study in Tennessee.

Because Palmer amaranth resistance evolution to *S*-metolachlor is recent in the Mid-southern US, adoption of best management practices is critical for slowing the spread of resistance evolution. Adopting an integrated weed management program that involves the use of cultural and mechanical methods (Norsworthy et al., 2012), herbicide tank-mixtures, sequential herbicide applications (PRE followed by POST), and rotation of herbicides and crop traits will be beneficial for controlling *S*-metolachlor resistant Palmer amaranth accessions. For example, growing corn or sorghum in rotation with soybean [*Glycine max* (L.) Merr.]/cotton (*Gossypium hirsutum* L.) will allow the use of atrazine, which continues to control *S*-metolachlor Palmer amaranth accessions from the Mid-south. Because *S*-metolachlor resistance reported in the Arkansas is metabolism-based (Rangani et al. 2021), the addition of GST-inhibitors may help reverse resistance in these accessions; thus, it could be a potential strategy to delay *S*-metolachlor resistance in Palmer amaranth accessions. However, future research is needed to validate this prospective theory.

Conclusion

This research has documented decreased sensitivity to *S*-metolachlor of Palmer amaranth accessions from four counties of Arkansas and one county of Mississippi. Palmer amaranth accessions from the Mid-south showed a differential response to *S*-metolachlor, which could not provide a complete control of resistant accessions. This decreased sensitivity will increase management problems growers must confront. The majority of the accessions from the Mid-south are susceptible to *S*-metolachlor currently, and the resistant accessions exhibit different levels of resistance. Recurrent selection with the same herbicide increased the level and frequency of resistant plants from parents to progenies. All the soil-applied herbicides tested in this study provided ≥ 90% control of *S*-metolachlor-resistant accessions, demonstrating viability as options for the management of resistant Palmer amaranth accessions in the Mid-southern US.

Acknowledgements

Support for this research was provided by Arkansas soybean producers through check-off funds administered by the Arkansas Soybean Promotion Board and the Southern Integrated Pest Management Center. The authors thank the University of Arkansas System Division of Agriculture for all other personnel support and facilities. The following County Extension Agents assisted in contacting growers, finding fields to sample, and in some cases collected seed samples: Stanley Baker, Ray Benson, Robert Goodson, Brett Gordon, Cody Griffin, Steven Kelley, Kevin Lawson, Russell Parker, Keith Perkins, Phil Sims, Jesse Taylor, and Jan Yingling. The authors also thank Matthew Janorschke, Diego Belapart, Nelson Diehl Kruse, Pâmela Carvalho-Moore and Isabel Schlegel Werle for their help in planting and spraying the plants.

References

Anonymous (2021) Atrazine label. http://www.cdms.net/LDat/ld280001.pdf. Accessed July 10, 2021. P 13

Askew SD, Wilcut JW, Cranmer JR (1999) Weed management in peanut (*Arachis hypogaea*) with flumioxazin preemergence. Weed Technol. 13: 594-598.

Askew SD, Wilcut JW, Cranmer JR (2002) Cotton (*Gossypium hirsutum*) and weed response to flumioxazin applied preplant and postemergence directed. Weed Technol. 16: 184-190.

Baldwin F, Boyd J, Smith K (2000) Recommended chemicals for weed and brush control (MP-44). Little Rock, AR: University of Arkansas cooperative Extension Service, Fayetteville, AR. Publication #MP44-12M-1-00RV.

Barber LT, Butts TR, Boyd JW, Cunningham K, Selden G, Norsworthy JK, Burgos N, Bertucci MB (2021) Recommended chemicals for weed and brush control (MP-44). Little Rock, AR: University of Arkansas cooperative Extension Service, Fayetteville, AR. Publication #MP44-12M-1-00RV

Beckie HJ, Tardif FJ (2012) Herbicide cross resistance in weeds. Crop Prot. 35: 15-28.

Boger P (2003) Mode of action for Chloroacetamides and functionally related compounds. Journal of Pesticide Science 28: 324-329.

Boger P, Matthes B, Schmalfuss J (2000) Towards the primary target of chloroacetamides - new findings pave the way. Pest. Manage. Sci.56: 497-508.

Bond JA, Oliver LR, Stephenson DO (2006) Response of palmer amaranth (*Amaranthus palmeri*) accessions to glyphosate, fomesafen, and pyrithiobac. Weed Technol. 20: 885-892.

Brabham C, Norsworthy JK, Houston M, Varanasi V, Barber T (2019) Confirmation of *S*-metolachlor resistance in Palmer amaranth (*Amaranthus palmeri*). Weed Technol. 33: 720-726.

Brunton DJ, Boutsalis P, Gil G, Preston C (2018) Resistance to multiple pre herbicides in a field-evolved rigid ryegrass (*Lolium rigidum*) population. Weed Sci. 66: 581-585.

Brunton DJ, Boutsalis P, Gill G, Preston C (2019) Resistance to very-long-chain fatty-acid (VLCFA)-inhibiting herbicides in multiple field-selected rigid ryegrass (*Lolium rigidum*) populations. Weed Sci. 67: 267-272.

Burgos NR (2015) Whole-plant and seed bioassays for resistance confirmation. Weed Sci. 63: 152-165.

Burgos NR, Kuk Y, Talbert R (2001) *Amaranthus palmeri* resistance and differential tolerance of *Amaranthus palmeri* and *Amaranthus hybridus* to ALS-inhibitor herbicides. Pest. Manage. Sci.57: 449-457.

Burgos NR, Tranel PJ, Streibig JC, Davis VM, Shaner D, Norsworthy JK, Ritz C (2013) Review: Confirmation of resistance to herbicides and evaluation of resistance levels. Weed Sci. 61: 4-20.

Busi R (2014) Resistance to herbicides inhibiting the biosynthesis of very-long-chain fatty acids. Pest. Manage. Sci.70: 1378-1384.

Busi R, Gaines T, Vila-Aiub M, Powles S (2014) Inheritance of evolved resistance to a novel herbicide (pyroxasulfone). Plant Sci. 217: 127-134.

Busi R, Porri A, Gaines T, Powles S (2018) Pyroxasulfone resistance in *Lolium rigidum* is metabolism-based. Pesticide Biochemistry and Physiology 148: 74-80.

Busi R, Powles S (2013) Cross-resistance to prosulfocarb and triallate in pyroxasulfone-resistant *Lolium rigidum*. Pest. Manage. Sci.69: 1379-1384.

Busi R, Powles S (2016) Cross-resistance to prosulfocarb plus *S*-metolachlor and pyroxasulfone selected by either herbicide in *Lolium rigidum*. Pest. Manage. Sci.72: 1664-1672.

Butts T, Barber L, Norsworthy JK (2019) Distribution and management of herbicide-resistant Palmer amaranth in Arkansas. University of Arkansas System Division of agriculture, Research & extension. FSA2188. https://www.uaex.uada.edu/publications/PDF/FSA2188.pdf

Clewis SB, Everman WJ, Jordan DL, Wilcut JW (2007) Weed management in North Carolina peanuts (*Arachis hypogaea*) with *S*-metolachlor, diclosulam, flumioxazin, and sulfentrazone systems. Weed Technol. 21: 629-635.

Culpepper AS, Grey TL, Vencill WK, Kichler JM, Webster TM, Brown SM, York AC, Davis JW, Hanna WW (2006) Glyphosate-resistant Palmer amaranth (*Amaranthus palmeri*) confirmed in Georgia. Weed Sci. 54: 620-626.

Ducker R, Parcharidou E, Beffa R (2020) Flufenacet activity is affected by GST inhibitors in blackgrass (*Alopecurus myosuroides*) populations with reduced flufenacet sensitivity and higher expression levels of GSTs. Weed Sci. 68: 451-459.

Ducker R, Zollner P, Lummen P, Ries S, Collavo A, Beffa R (2019a). Glutathione transferase plays a major role in flufenacet resistance of ryegrass (*Lolium* spp.) field populations. Pest. Manage. Sci.75: 3084-3092.

Ducker R, Zollner P, Parcharidou E, Ries S, Lorentz L, Beffa R (2019b) Enhanced metabolism causes reduced flufenacet sensitivity in black-grass (*Alopecurus myosuroides* Huds.) field populations. Pest. Manage. Sci.75: 2996-3004.

Gaeddert J, Peterson D, Horak M (1997) Control and cross-resistance of an acetolactate synthase inhibitor-resistant palmer amaranth (*Amaranthus palmeri*) biotype. Weed Technol. 11: 132-137.

Gbur EE, Stroup WW, McCarter KS, Durham S, Young LJ, Christman M, West M, Kramer M (2012) Analysis of Generalized Linear Mixed Models in the Agricultural and Natural Resources Sciences. Madison, WI: American Society of Agronomy, Soil Science Society of America, Crop Science Society of America. 298 p.

Gonzalez-Torralva F, Norsworthy JK, Piveta LB, Varanasi VK, Barber T, Brabham C (2020) Susceptibility of Arkansas Palmer amaranth accessions to common herbicide sites of action. Weed Technol. 34: 770-775.

Gossett B, Murdock E, Toler J (1992) Resistance of Palmer amaranth (*Amaranthus palmeri*) to the Dinitroaniline herbicides. Weed Technol. 6: 587-591.

Heap I (2021) The International Herbicide-Resistant Weed Database. Available at www.weedscience.org. Accessed Tuesday, November 16, 2021.

Horak M, Peterson D (1995) Biotypes of Palmer amaranth (*Amaranthus palmeri*) and common waterhemp (*Amaranthus rudis*) are resistant to imazethapyr and thifensulfuron. Weed Technol. 9: 192-195.

Jhala A, Sandell L, Rana N, Kruger G, Knezevic S (2014) Confirmation and control of triazine and 4-hydroxyphenylpyruvate dioxygenase-inhibiting herbicide-resistant palmer amaranth (*Amaranthus palmeri*) in Nebraska. Weed Technol. 28: 28-38.

Juliano LM, Casimero MC, Llewellyn R (2010) Multiple herbicide resistance in barnyardgrass (*Echinochloa crus-galli*) in direct-seeded rice in the Philippines. International Journal of Pest Management 56: 299-307.

Kumar V, Liu R, Stahlman PW (2020) Differential sensitivity of Kansas Palmer amaranth populations to multiple herbicides. Agronomy Journal 112: 2152-2163.

Millar A, Kunst L (1997) Very-long-chain fatty acid biosynthesis is controlled through the expression and specificity of the condensing enzyme. Plant Journal 12: 121-131.

Nakka S, Godar A, Thompson C, Peterson D, Jugulam M (2017a). Rapid detoxification via glutathione *S*-transferase (GST) conjugation confers a high level of atrazine resistance in Palmer amaranth (*Amaranthus palmeri*). Pest. Manage. Sci.73: 2236-2243.

Nakka S, Godar AS, Wani PS, Thompson CR, Peterson DE, Roelofs J, Jugulam M (2017b) Physiological and Molecular Characterization of Hydroxyphenylpyruvate Dioxygenase (HPPD)-inhibitor Resistance in Palmer Amaranth (*Amaranthus palmeri* S. Wats.). Front. Plant Sci. 8.

Nandula VK, Ray JD, Ribeiro DN, Pa, Z, Reddy KN (2013) Glyphosate resistance in tall waterhemp (*Amaranthus tuberculatus*) from Mississippi is due to both altered target-site and nontarget-site mechanisms. Weed Sci. 61: 374-383.

Niekamp JW, Johnson WG, Smeda RJ (1999) Broadleaf weed control with sulfentrazone and flumioxazin in no-tillage soybean (*Glycine max*). Weed Technol. 13: 233-238.

Norsworthy JK, Griffith G, Scott R, Smith K, Oliver L (2008) Confirmation and control of glyphosate-resistant Palmer amaranth (*Amaranthus palmeri*) in Arkansas. Weed Technol. 22: 108-113.

Norsworthy JK, Ward SM, Shaw DR, Llewellyn RS, Nichols RL, Webster TM, Bradley KW, Frisvold G, Powles SB, Burgos NR, Witt WW, Barrett M (2012) Reducing the risks of herbicide resistance: best management practices and recommendations. Weed Sci. 60: 31-62.

O'Connell P, Harms C, Allen J (1998) Metolachlor, *S*-metolachlor and their role within sustainable weed-management. Crop Prot. 17: 207-212.

Oerke EC (2006) Crop losses to pests. Journal of Agricultural Science 144: 31-43.

Powles SB, Yu Q (2010) Evolution in action: plants resistant to herbicides. Annual Review of Plant Biology, Vol 61 61: 317-347.

Provin T (2014) Total carbon and nitrogen and organic carbon via thermal combustion analysis. *In*: Sikora FJ, Moore KP (Eds.), Soil test methods from the southeastern United States. Southern Coop. Ser. Bull. 419: 149-154.

R Core Team R (2020) R: A language and environment for statistical computing. Vienna, Austria: R Core Team (2020).

Rangani G, Noguera M, Salas-Perez R, Benedetti L, Roma-Burgos N (2021) Mechanism of resistance to *S*-metolachlor in Palmer amaranth. Front. Plant Sci. 12: 13.

Ransom CV (2013) Common and chemical names of herbicides approved by the Weed Science Society of America. Weed Sci. 61: 601-608.

Riar DS, Norsworthy JK, Steckel LE, Stephenson DO, Eubank TW, Scott RC (2013) Assessment of weed management practices and problem weeds in the Midsouth United States-soybean: A consultant's perspective. Weed Technol. 27: 612-622.

Roma-Burgos N, Heap IM, Rouse CE, Lawton-Rauh AL (2019). Evolution of herbicide-resistant weeds. Pages 92 - 132 *in*: Korres NE, NR Burgos, SO Duke (eds), Chapter 6. CRC Press, Taylor & Francis Group https://www.crcpress.com/Weed-control-sustainability-hazards-and-risks-in-cropping-systems-worldwide/Korres-Burgos-Duke/p/book/9781498787468

Salas RA, Burgos NR, Tranel PJ, Singh S, Glasgow L, Scott RC, Nichols RL (2016) Resistance to PPO-inhibiting herbicide in Palmer amaranth from Arkansas. Pest. Manage. Sci.72: 864-869.

Salas-Perez RA, Burgos NR, Rangani G, Singh S, Refatti JP, Piveta L, Tranel PJ, Mauromoustakos A, Scott RC (2017) Frequency of Gly-210 deletion mutation among protoporphyrinogen oxidase inhibitor-resistant Palmer Amaranth (*Amaranthus palmeri*) populations. Weed Sci. 65: 718-731.

Senseman S (2007) Herbicide handbook. 9th ed. Lawrence, KS: Weed Sci. Society of America. Pp. 458.

Singh S, Roma-Burgos N, Singh V, Alcober EAL, Salas-Perez R, Shivrain V (2018) Differential response of Arkansas Palmer Amaranth (*Amaranthus palmeri*) to glyphosate and mesotrione. Weed Technol. 32: 579-585.

Sikora FJ, Kissel DE (2014) Soil pH. *In*: Sikora FJ, KP Moore (Eds), Soil test methods from the southeastern United States. Southern Coop. Ser. Bull. 419. p.48-53.

Strom SA, Hager AG, Seiter NJ, Davis AS, Riechers DE (2020) Metabolic resistance to *S*-metolachlor in two waterhemp (*Amaranthus tuberculatus*) populations from Illinois, USA. Pest. Manage. Sci.76: 3139-3148.

Tanetani Y, Kaku K, Kawai K, Fujioka T, Shimizu T (2009) Action mechanism of a novel herbicide, pyroxasulfone. Pesticide Biochemistry and Physiology 95: 47-55.

Taylor-Lovell S, Wax LM, Bollero G (2002) Preemergence flumioxazin and pendimethalin and postemergence herbicide systems for soybean (*Glycine max*). Weed Technol. 16: 502-511.

Trenkamp S, Martin W, Tietjen K (2004) Specific and differential inhibition of very-long-chain fatty acid elongases from *Arabidopsis thaliana* by different herbicides. Proceedings of the National Academy of Sciences of the United States of America 101: 11903-11908.

Umphres AM, Steckel LE, Mueller TC (2018) Control of protoporphyrinogen oxidase inhibiting herbicide resistant and susceptible Palmer Amaranth (*Amaranthus palmeri*) with soil-applied protoporphyrinogen oxidase-inhibiting herbicides. Weed Technol. 32: 95-100.

Varanasi V, Brabham C, Norsworthy JK (2018a) Confirmation and characterization of non-target site resistance to fomesafen in Palmer amaranth (*Amaranthus palmeri*). Weed Sci. 66: 702-709.

Varanasi VK, Brabham C, Norsworthy JK, Nie H, Young BG, Houston M, Barber T, Scott RC (2018b). A statewide survey of PPO-inhibitor resistance and the prevalent target-site mechanisms in Palmer amaranth (*Amaranthus palmeri*) accessions from Arkansas. Weed Sci. 66: 149-158.

Ward S, Webster T, Steckel L (2013) Palmer Amaranth (*Amaranthus palmeri*): A review. Weed Technol. 27: 12-27.

Whitaker JR, York AC, Jordan DL, Culpepper S (2010) Palmer Amaranth (*Amaranthus palmeri*) control in soybean with glyphosate and conventional herbicide systems. Weed Technol. 24: 403-410.

Zhang H, Hardy DH, Mylavarapu R, Wang J (2014) Mehlich-3. *In*: Sikora FJ, Moore KP (Eds). Soil test methods from the southeastern United States. Southern Coop. Ser. Bull. 419. p. 101-110.

Tables and Figures

Table 3. 1**.** Weed species that evolved resistance to very long chain fatty acid-inhibiting herbicides globally, between 1982 and 2020[a].

Species	**Herbicide**	**Country**	**Reference**
Lolium rigidum Gaud	pyroxasulfone	Australia	Brunton et al. 2018; Busi et al. 2014 and 2018; Busi and Powles 2013 and 2016
Lolium rigidum Gaud.	*S*-metolachlor, metazachlor, pyroxasulfone	Australia	Brunton et al. 2019
Lolium multiflorum Lam.	flufenacet	France, United Kingdom, Australia, United States of America	Ducker et al. 2019a
Alopecurus myosuroides Huds.	flufenacet	France, United Kingdom, Germany	Ducker et al. 2019b, Ducker et al. 20120
Echinochloa crus-galli (L.) Beauv.	butachlor	Philippines, China, Thailand	Juliano et al. 2010; Heap 2021
Avena fatua L.	pyroxasulfone	Canada	Heap 2021
Amaranthus tuberculatus (Moq.) Sauer	*S*-metolachlor	United States	Strom et al. 2020
Amaranthus palmeri (S.) Wats.	*S*-metolachlor	United States	Brabham et al. 2019
Raphanus raphanistrum L.	pyroxasulfone	Australia	Heap 2021

[a]Timespan of resistance recorded by Heap (2021).

Table 3. 2**.** Chemical and physical characteristics of soil used for the greenhouse experiments conducted in 2018 to 2020 at the Milo J. Shult Agricultural Research & Extension Center, University of Arkansas, Fayetteville, USA[a].

				Mehlich-3 extractable soil nutrients[b]													
pH[c]	EC[c]	Total N[d]	Total C	P	K	Ca	Mg	S	Na	Fe	Mn	Zn	Cu	B	Sand	Silt	Clay
	μmhos/cm	%	%	mg kg^{-1}											%	%	%
7.3	112	0.04	0.4	111	164	1308	237	5.0	17.1	232.8	103	3.39	1.59	0.42	18.8	68.2	12.9

[a] Roxana silt loam soil from the Vegetable Research Station of the University of Arkansas, Kibler

[b] Extracted using Mehlich-3 method.

[c] Soil pH and EC measured in a 1:2 soil: water mixture.

[d] Measured by thermal combustion analysis.

Table 3. 3. Herbicides used in resistance testing of Palmer amaranth from the Mid-southern US (Arkansas, Mississippi, Tennessee), in the greenhouse at the Milo J. Shult Agricultural Research & Extension Center, University of Arkansas, Fayetteville) .

Herbicide	Product and manufacturer	Family	MOA	Chemical name[a]	Labelled rate
					g ai ha^{-1}
S-metolachlor	Dual II Magnum, Syngenta Crop Protection, LLC, Greensboro, NC, USA	Chloroacetamide	very long chain fatty acid inhibitor	2-chloro-N-(2-ethyl-6-methylphenyl)-N-(2-methoxy-1-methylethyl)acetamide	1120
Pyroxasulfone	Zidua SC; BASF Corporation, Research Triangle Park, NC	Pyrazole	very long chain fatty acid inhibitor	3-[[[5-(difluoromethoxy)-1-methyl-3-(trifluoromethyl)-1H-pyrazol-4-yl]methyl]sulfonyl]-4,5-dihydro-5,5-dimethylisoxazole	120
Dimethenamid-P	Outlook; BASF Corporation, Research Triangle Park, NC	Chloroacetamide	Very Long Chain Fatty acid inhibitor	(RS) 2-chloro-N-(2,4-dimethyl-3-thienyl)-N-(2-methoxy-1-methylethyl)acetamide	631
Atrazine	Aatrex 4L, Syngenta Crop Protection, LLC, Greensboro, NC, USA	Triazine	Photosystem II inhibitor	6-chloro-N-ethyl-N9-(1-methylethyl)-1,3,5-triazine-2,4-diamine	2240
Fomesafen	Flexstar, Syngenta Crop Protection, LLC, Greensboro, NC	Diphenylether	Protoporphyrinogen Oxidase inhibitor	5-[2-chloro-4-(trifluoromethyl)phenoxy]-N-(methylsulfonyl)-2-nitrobenzamide	280
Flumioxazin	Valor SX, Valent U.S.A. Corporation, Walnut Creek, CA	N-phenylphthalimide	Protoporphyrinogen Oxidase inhibitor	2-[7-fluoro-3,4-dihydro-3-oxo-4-(2-propynyl)-2H-1,4-benzoxazin-6-yl]-4,5,6,7-tetrahydro-1H-isoindole-1,3(2H)-dione	70

[a] Chemical names used from Ransom (2013).

Table 3. 4. Resistance levels of Palmer amaranth populations to *S*-metolachlor in greenhouse experiments conducted at the Milo J. Shult Agricultural Research & Extension Center, University of Arkansas, Fayetteville, USA.

Populations	LD_{50}[a]	R/S[b]
	g ai ha^{-1}	
18WOO-B	443(36)	7.0
19WOO-B	520(64)	8.3
18WOO-B-F_1	577(52)	9.2
18CRI-D	289(12)	4.6
19CRI-D	327(47)	5.2
17TUN-A	313(54)	5.0
17TUN-D	242(32)	3.8
17PRA-A	156(16)	2.5
17RAN-A	140(11)	2.2
18PHI-C	73(21)	1.2
19PHI-C	73(19)	1.2
18PHI-C-F_1	130(15)	2.1
SS	63(16)	1.0

[a] LD_{50}, *S*-metolachlor rate that reduced seedling emergence by 50%. Values in parenthesis are standard errors of the mean.

[b] R/S, resistance index, ratio between the LD_{50} value of the *S*-metolachlor-resistant accessions and the LD_{50} value of the susceptible accession.

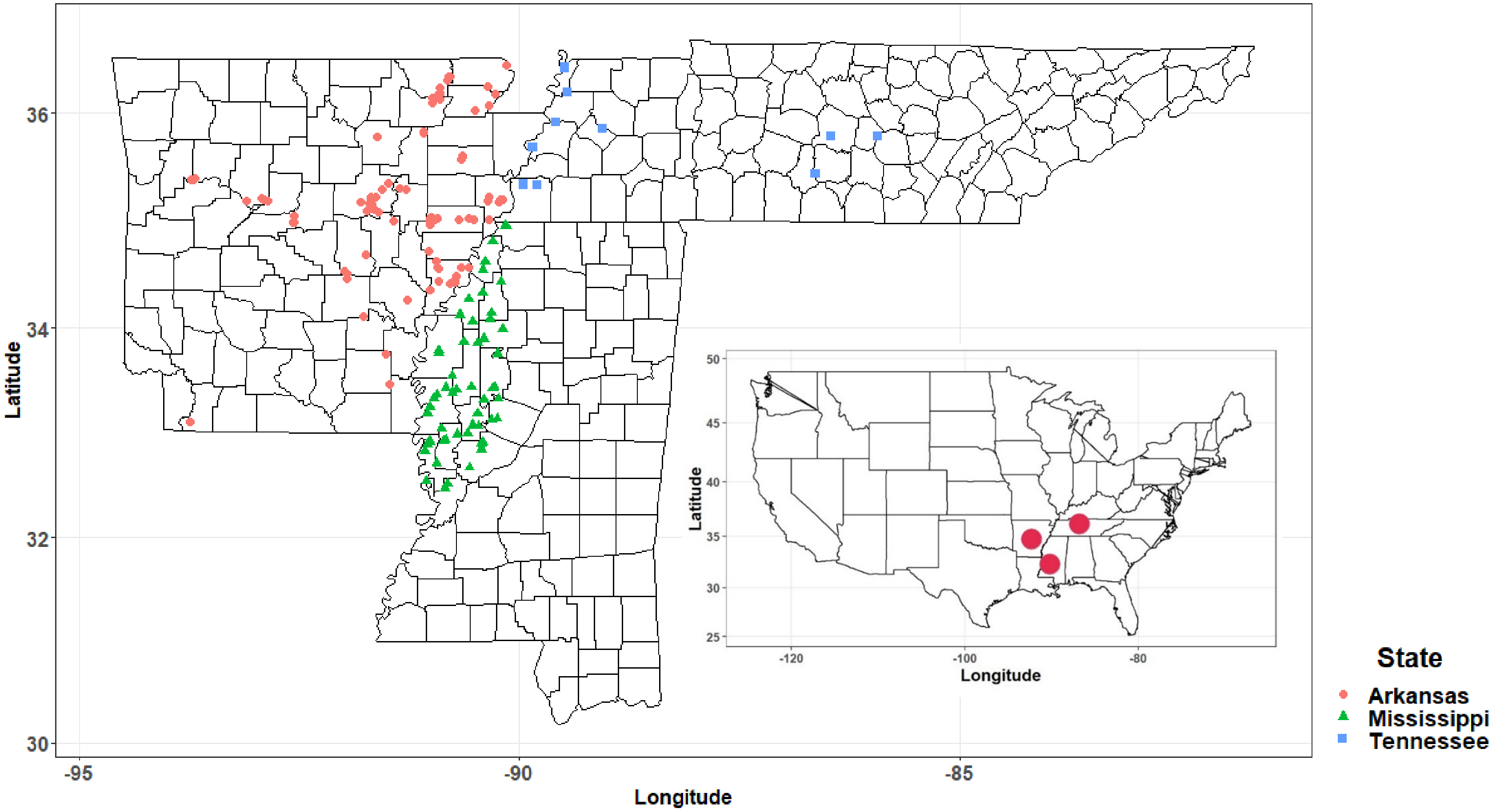

Figure 3. 1. Maps of Arkansas, Mississippi and Tennessee where Palmer amaranth accessions were collected for greenhouse experiments conducted at the Milo J. Shult Agricultural Research & Extension Center (University of Arkansas, Fayetteville) to evaluate the extent of Palmer amaranth resistance to *S*-metolachlor in the Mid-southern US and the profile of resistance of resistant accessions.

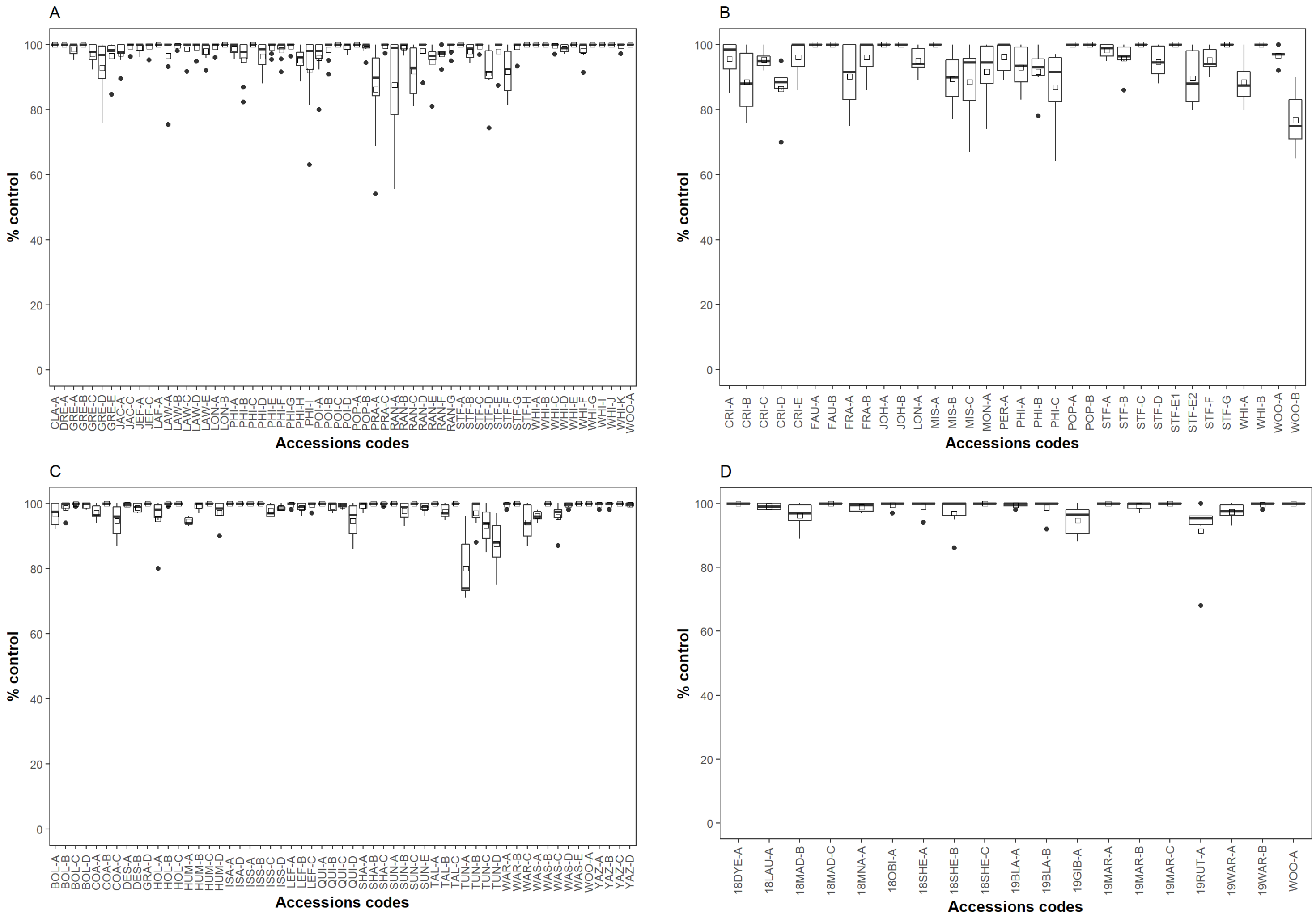

Figure 3. 2. Response of Palmer amaranth accessions to 1120 g ai ha^{-1} of *S*-metolachlor in the greenhouse, Milo J. Shult Agricultural Research & Extension Center, University of Arkansas, Fayetteville, USA. (A) Arkansas 2017 (B) Arkansas 2018, (C) Mississippi 2017 and (D) Tennessee 2018 and 2019.

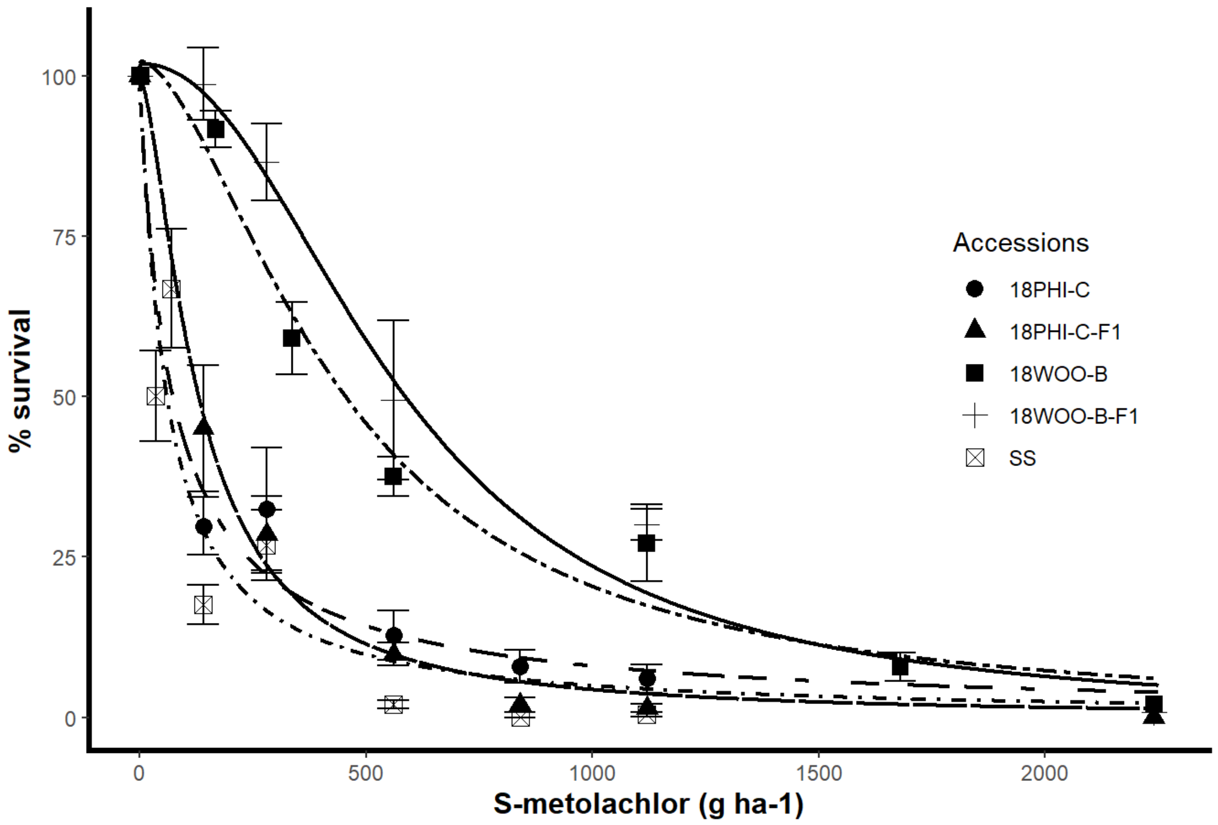

Figure 3. 3. Dose–response studies, of parental Palmer amaranth populations collected in Arkansas (in 2018) and first-generation populations obtained in greenhouse, conducted in the greenhouse at the Milo J. Shult Agricultural Research & Extension Center (University of Arkansas, Fayetteville, AR). Data were fit using a three-parameter log-logistic equation: $Y = d/1 + \exp[b(\log x - \log e)]$. Error bars represent standard errors.

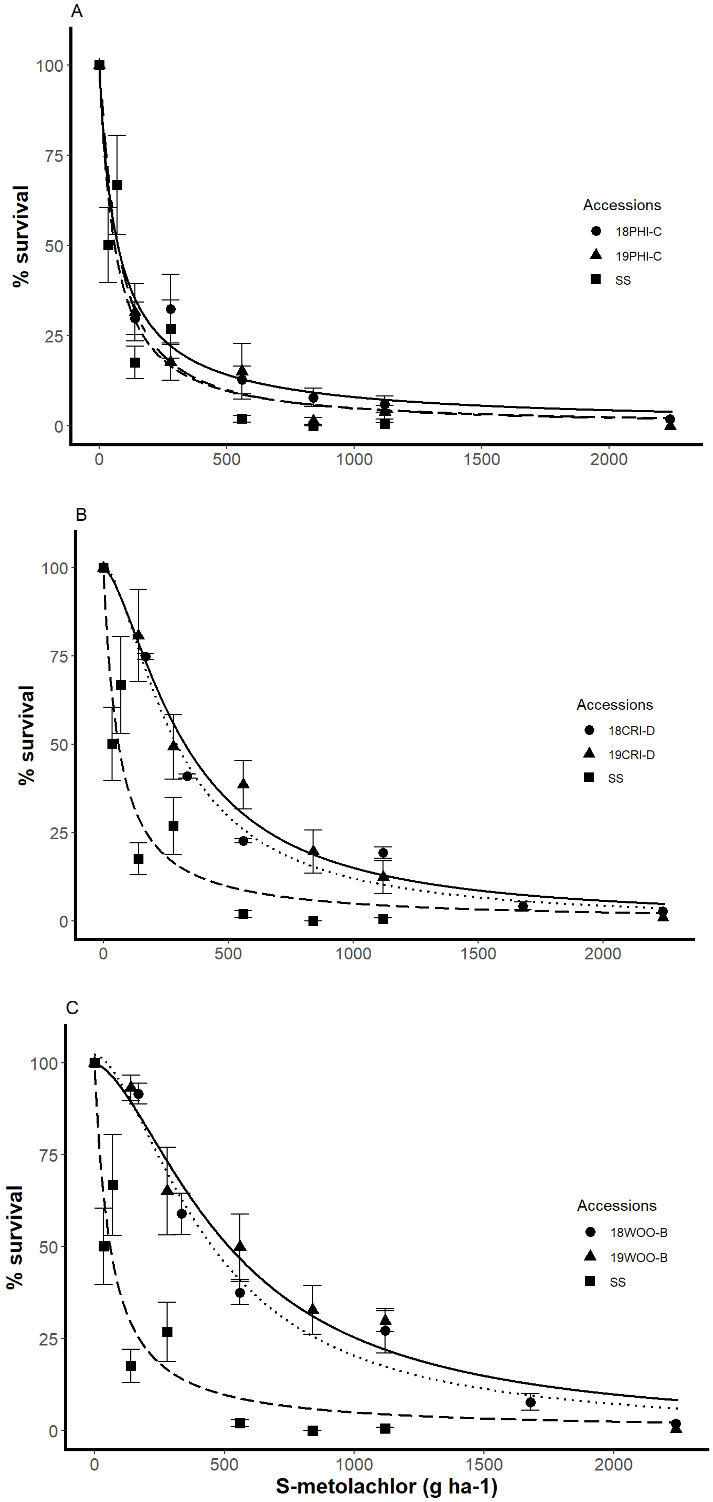

Figure 3. 4. *S*-metolachlor dose–response studies, of parental Palmer amaranth populations collected in Arkansas (in 2018) and first-generation populations collected in Arkansas (in 2019), conducted in the greenhouse at the Milo J. Shult Agricultural Research & Extension Center (University of Arkansas, Fayetteville, USA). Data were fit using a three-parameter log-logistic equation: $Y = d/1 + \exp[b(\log x - \log e)]$. Error bars represent standard errors.

Appendix

Table 3. 5. PROC GLIMMIX output for Palmer amaranth percent control 14 and 21 days after herbicide application

	14 DAT		24 DAT	
Effect	F Value	P > F	F Value	P > F
Greenhouse	0.08	0.8222	2.45	0.1260
Accession	1.63	0.1731	1.63	0.1728
Greenhouse*Accession	0.36	0.8383	0.85	0.4939
Herbicide	5.46	0.0005	7.91	<.0001
Greenhouse*Herbicide	0.21	0.9326	0.72	0.5772
Accession*Herbicide	0.83	0.6463	1.41	0.1522
Greenhouse*Accession*Herbicide	0.68	0.8045	0.86	0.6196

Table 3. 6. Palmer amaranth percent control as influenced by different soil applied herbicides 14 and 21 days after application[a]

Herbicide	%Control	
	14 DAT	21 DAT
Atrazine	93a	93a
Dimethenamid-P	92ab	93a
Flumioxazin	92abc	92a
Fomesafen	91bc	91b
Pyroxasulfone	90c	91b

[a] Means separation achieved using Tukey's HSD at a 0.05 significance level. Means with a common letter are significantly different.

[b] S-metolachlor-resistant accessions used are 18CRI-D, 18WOO-B, 17TUN-A and 17TUN-D

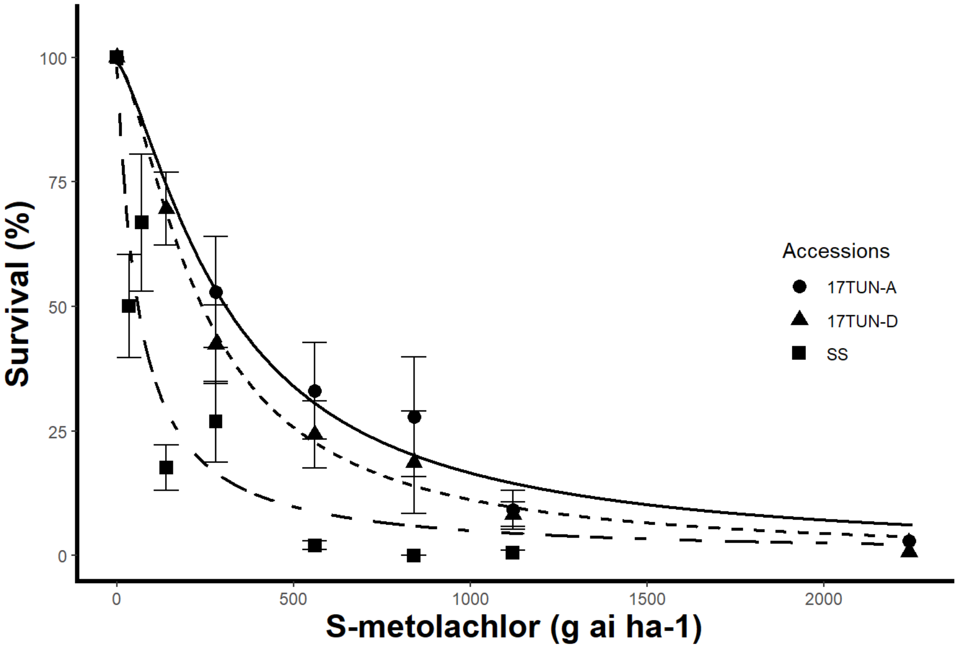

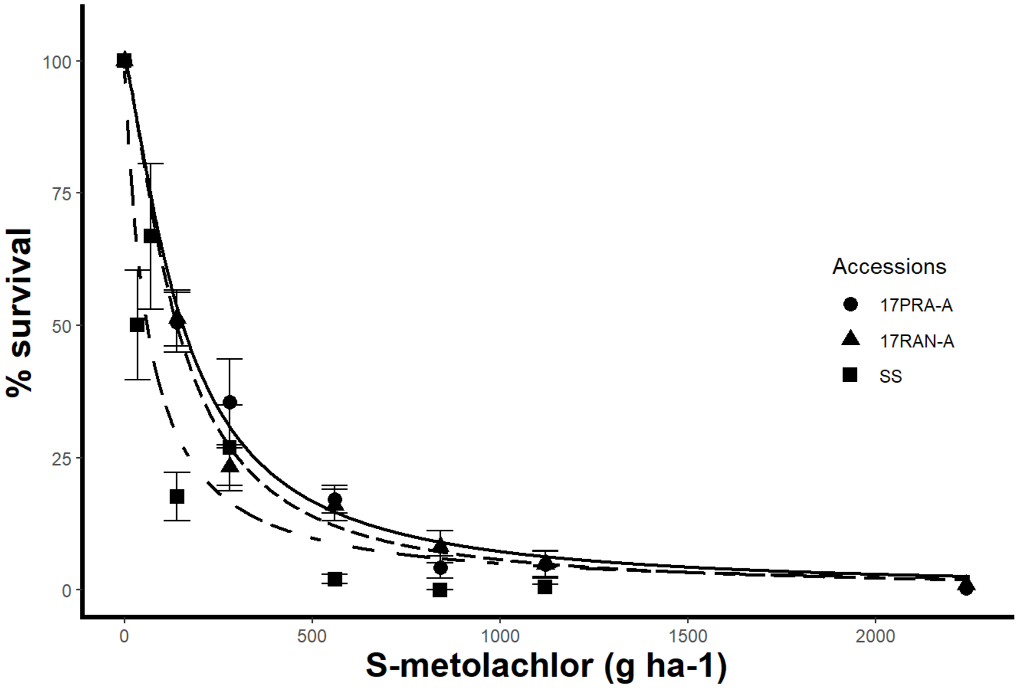

Figure 3. 5. *S*-metolachlor dose–response studies, of parental Palmer amaranth populations collected in 2017 in Mississippi and Arkansas, conducted in the greenhouse at the Milo J. Shult Agricultural Research & Extension Center (University of Arkansas, Fayetteville, USA). Data were fit using a three-parameter log-logistic equation: $Y = d/1 + \exp[b(\log x - \log e)]$. Error bars represent standard errors.

***S*-metolachlor persistence in soil as influenced by within-season and inter-annual herbicide use**

Abstract

The ability to predict fate of pesticides in the environment is crucial for sustainable management. This process starts with a proper characterization of the dissipation of a parent compound under different sets of conditions. *S*-metolachlor is a herbicide used commonly in many cropping systems. *S*-metolachlor dissipation in spiked soils was investigated in soil samples collected from paired, commercial fields from five Arkansas counties, where fields in each pair differed based on the number of herbicide applications within the past six years. Fields were categorized as low-use (0 to 2 years of application) or high-use (5 to 6 years of application). *S*-metolachlor dissipation was also investigated in spiked soils in an experiment determining the influence of single or repeated within-season herbicide applications to accelerate dissipation. *S*-metolachlor concentrations were extracted from soil during a 56-day incubation and *S*-metolachlor degradation was modeled using the single first order (SFO) equation. The half-life of *S*-metolachlor was greater for fields with high-use (5 to 6 years) compared to fields with low-use (0 to 2 years) of herbicide application history. Two within-season applications of *S*-metolachlor increased persistence in spiked soils; dissipation was faster in soils collected 1 and 24 days compared to 59 days after planting soybean [*Glycine max* (L.) Merr.]. Analysis of dissipation across a broad range of environments and cropping systems with concurrent investigation of the microbiome would provide understanding of the potential contribution of the factors and mechanisms controlling the dissipation of the herbicide.

Introduction

S-metolachlor is useful for weed management in general; it is frequently used on more than 70 crops (O'Connell et al., 1998) and has been used for more than 60 years (Busi, 2014). It is labelled for high-value, small-acreage crops including numerous vegetables and small fruits, as well as for major field crops such as cotton (*Gossypium hirsutum* L.), corn (*Zea mays* L.), and soybean [*Glycine max* (L.) Merr.] (O'Connell et al., 1998). It is effective on yellow nutsedge (*Cyperus esculentus* L.), annual grasses, and small-seeded broadleaf species (Barber et al., 2021). Its residual activity gives *S*-metolachlor an additional utility for management of weeds that are resistant to postemergence herbicides. Cotton, corn, and soybean acreages planted in the US in 2021 reached 4.7, 37.5 and 35.5 million hectares, respectively (USDA-NASS, 2021). In these cropping systems, major weeds have evolved resistance to herbicides of different mechanisms of action. Currently, *S*-metolachlor is applied, or can be applied, twice in the growing season: first, at planting in mixture with other herbicide mechanisms of action, then followed by an in-season application mixed with foliar herbicides. *S*-metolachlor is frequently applied in successive years. Therefore, understanding changes in fate resulting from multiple within-season and across-season applications of *S*-metolachlor has important agricultural as well as broader environmental implications. Pesticides in general can negatively impact biological processes and aquatic ecosystems in the proximity of agricultural areas (Neves et al., 2015) and metolachlor has been detected in lake water in Canada (Kurt-Karakus et al., 2011). In a study using lysimeters in Italy, it showed a potential to leach with concentrations above 0.25 $\mu g\ L^{-1}$ (Milan et al., 2015).

Herbicide degradation is affected by many factors, including use history (Abit et al., 2012; Krutz et al., 2008; Krutz et al., 2010a; Krutz et al., 2010b; Krutz et al., 2007; Zablotowicz et al., 2007). Previous research has investigated the effect of use history on *S*-metolachlor dissipation (Sanyal and Kulshrestha, 1999; Shaner and Henry, 2007). However, only the study by Sanyal and Kulshrestha (1999), conducted under field conditions, reported a significant effect of use history on *S*-metolachlor dissipation. A combination of field studies with laboratory experiments and improvement of sample processing may help capture the effect of prior exposure of soil on herbicide degradation. Laboratory experiments, conducted in a closed system can allow for control many external variables that may confound effects on biological and chemical processes responsible for herbicide degradation. Sanyal and Kulshrestha (1999) used air-dried soil samples from a field experiment and evaluated the dissipation of *S*-metolachlor after four applications of the herbicide to soil during an 8-month period. Because *S*-metolachlor is microbially degraded, air-drying and processing of soil affect microbial activity (Marti et al., 2012); thus, air-drying of soil may have adversely impacted the ability to accurately measure the dissipation from soil samples in the Sanyal and Kulshrestha (1999) study. Soil and weather conditions in fields also affect microbial degradation of herbicides (Jaikaew et al., 2015). Leaching, runoff, volatilization and photodegradation could all impact metolachlor dissipation in the field (Bedos et al., 2017; Coffinet et al., 2012; Dimou et al., 2005; Feigenbrugel et al., 2004; Gish et al., 2009; Kochany and Maguire, 1994; Marin-Benito et al., 2014; Prueger et al., 2005; Prueger et al., 1999; Sakkas et al., 2004).

In the field in an andisol soil, *S*-metolachlor has been reported to have a shorter half-life during the summer and longer half-life during the winter, in part due to environmental conditions that favor leaching into deeper soil layers through infiltration and percolation during the summer (Jaikaew et al., 2015). The examination of the dynamics of *S*-metolachlor dissipation in soil samples collected throughout a single growing season would provide valuable decision-making information to scientists and growers to inform management practices. To investigate the fate of

S-metolachlor, laboratory incubation experiments were conducted using soil from crop fields with a low-use (defined as 0 to 2 years of successive applications) and high-use (5 to 6 years of successive applications) history of *S*-metolachlor. Also, the dissipation rate of *S*-metolachlor was determined in soils collected throughout the season from nontreated plots and from plots differing in the frequency and timing of within-season *S*-metolachlor applications. We hypothesized that *S*-metolachlor dissipation would be faster when soil had previously received multiple inter-annual or within-season applications than when soil had low-use prior history.

Material and Methods

S-metolachlor dissipation rate in crop field soils with different herbicide use history

Soil collection

Soil samples were collected from ten agricultural fields with 5 to 6 years of known management history (Table 4. 1). Fields were located in five counties of Arkansas (Clay, Crawford, Drew, Lonoke and Monroe) (Fig. 4. 1). Selected paired-fields from the same soil series per county, all with a silt loam texture, represented low (0 to 2 years) and high (5 to 6 years) intensity of *S*-metolachlor use history. Farmers were contacted by the University of Arkansas System Division of Agriculture County Extension agents who obtained baseline information on the use history of *S*-metolachlor and the magnitude of the Palmer amaranth [*Amaranthus palmeri* (S.) Wats.] problem. Farmers gave permission for soil sample collection in their respective fields. Twenty soil samples were composited per field using a soil probe (2.2-cm diameter) from the 0 to 10.2-cm depth in March 2018 before herbicide application and crop planting in order to minimize residual metolachlor concentrations. Samples were collected along five 50-m transects of approximately 17-m spacing intervals between sampling points, perpendicular to row plantings (except in the pasture), and GPS coordinates were recorded. In fields with populations of Palmer amaranth exhibiting putative resistance to metolachlor, soil samples were collected from areas where plants had survived treatment with *S*-metolachlor. Soils were stored on ice in the field and for transport and stored at 4 ºC in the laboratory until analysis. A subsample of soil from each commercial field was sent to the Fayetteville Agricultural Diagnostic Laboratory of the Arkansas Agricultural Experiment Station in Fayetteville, AR for analysis. Soil pH and electrical conductivity (EC) were measured in a 1:2 soil:water mixture (Sikora and Kissel, 2014) and soil carbon and total nitrogen (N) were measured by thermal combustion analysis (Provin, 2014). Soil EC, carbon (C), and N contents are provided in Table 4.1.

S-metolachlor spiking, incubation, dissipation sub-sampling procedures

For soil samples collected from each field, triplicate sub-samples were weighed into labeled styrofoam cups poked with holes at the bottom, and 200 mL deionized water were added and allowed to drain overnight. Analytical grade *S*-metolachlor ($C_{15}H_{22}ClNO_2$); CAS 87392-12-9 607-432-00-4 (Lot # BCBZ6026) with a purity of 99.1% (Sigma-Aldrich, St. Louis, MO) was used for spiking. The moist sample of each triplicate soil sample (500 g), at field capacity, was spiked with equivalent of 0.9375 mg *S*-metolachlor kg^{-1} dry soil and mixed well. The spiked soil was transferred to a labeled mason jar wrapped with aluminum foil. The weight of each foil-wrapped jar with moist soil was recorded and jars were placed randomly into a growth chamber at 25 ºC and 75% RH and incubated for 56 days. Soil (5 g) was sub-sampled on day 0, 3, 7, 14, 28, and 56 from each jar. Jars were weighed at each sample collection date and weekly between sub-sampling times to determine how much water to add to maintain moisture content. Lids of jars were opened three times a week to aerate.

S-metolachlor extraction

S-metolachlor was extracted from soil by adding 5 mL Optima ultrapure water (Thermo Fisher Scientific, Waltham, MA) and 5 mL water-saturated toluene (Ricca Chemical Company, Arlington, TX) to 5 g soil. Soil matrix blank was obtained with 5 g soil, 5 mL Optima ultrapure water and 5 mL water-saturated toluene. The soil matrix high concentration spike was obtained with 5 g soil, 5 mL Optima ultrapure water, 5 mL water-saturated toluene and 27 µL of 100 mg L^{-1} *S*-metolachlor in 10% acetonitrile. Soil matrix low concentration spike contained 5 g soil, 5 mL Optima ultrapure water, 5 mL water-saturated toluene and 27 µL of 10 mg L^{-1} *S*-metolachlor. The solvent matrix blank was obtained from 5 mL Optima ultrapure water and 5 mL water-saturated toluene. Each subsample was shaken using a benchtop reciprocal shaker (E6010, Eberbach Corporation, Belleville, MI) at low speed for 2 h, centrifuged for 20 min at 5000 rpm on a benchtop centrifuge. The toluene layer (2 mL) was aspirated and filtered through a 0.2-µm PTFE filter. Moreover, 2 mL of *S*-metolachlor (1 mg L^{-1}) in toluene was retained and analyzed as "Storage Spike." Extracted *S*-metolachlor samples were stored in the freezer until subsequent analysis. *S*-metolachlor analysis was carried out using a Shimadzu GC instrument equipped with a mass spectrometer detector (TQ8040 GC-MS/MS, Shimadzu Corporation, Japan). Chromatographic separation was accomplished with an SH-Rxi-5Sil MS capillary GC column (30 m, 0.25 mm i.d., 0.25 µm). The GC oven temperature was programed as follows: 50 °C (1 min), 50 - 300 °C at 35 °C min^{-1} and finally held for 3 min. The carrier gas was helium at a constant flow rate of 1 mL min^{-1}. The injection was accomplished in a split mode with an injection volume of 1 μL and a temperature of 250 °C. The mass spectrometer detector was operated in scan mode and the temperature of the interface and ion source were 250 and 200 °C, respectively. *S*-metolachlor was monitored at the mass-to-charge ratio (m/z) of 162.15. The average retention time was 7.31 min. Five standard solutions (0.01, 0.05, 0.1, 0.5, 1 mg L^{-1}, R^2 between 0.9994 and 1) were injected to perform calibration.

Effect of frequency and timing of in-season applications on S-metolachlor dissipation in soil

A field experiment was conducted during the summer of 2019 at the Milo J. Shult Agricultural Research & Extension Center (University of Arkansas, Fayetteville, AR 36º05.970 N and 94º10.741W), to evaluate the effect of frequency and timing of in-season applications of *S*-metolachlor and the effect field sampling time has on dissipation of *S*-metolachlor. The taxonomic class of the soil is fine-silty, siliceous, active, mesic Typic Fragiudult, mapped as a Captina silt loam soil with slopes between 1 and 3% (USDA-SCS, 1969). The site had a summer fallow and a winter rye cover crop in 2018, which were preceded by a fallow and a soybean field in 2017 and 2016, respectively. The experimental site is classified as a low *S*-metolachlor-use history field, with the herbicide having been applied at 1.55 L ha^{-1} in 2013 and 2016. A composite subsample of soil from the entire plot, collected prior to soybean planting, was sent to the Fayetteville Agricultural Diagnostic Laboratory of the Arkansas Agricultural Experiment Station in Fayetteville, AR for analysis. Soil pH, EC, soil C and total N were measured as described previously. Additionally, soil nutrients were extracted using Mehlich-3 method (Zhang et al., 2014). Soil test results are provided in Table 4. 2.

The experimental design was a randomized complete block design with four replications. Four treatments were tested: a nontreated control, preemergence only (PRE), postemergence only (POST), and preemergence followed by postemergence (PRE *fb* POST). The experimental unit was composed of four 6-m length soybean rows with a row spacing of 91.5 cm. A soybean XTEND variety (Asgrow AG55X7, Roundup Ready2 Xtend) was planted at a seeding rate of 322,667 seeds ha^{-1}. Preemergence treatment of *S*-metolachlor (Dual II Magnum; Syngenta Crop Protection, LLC, Greensboro, NC, USA) was applied 2 days after planting soybean at a rate of 1345 g ai ha^{-1}. The POST application of *S*-metolachlor occurred 25 days after planting soybean, or 23 days after the PRE application. Additional weed management was achieved by a broadcast POST application of glyphosate (Roundup PowerMax; Bayer Crop Science, Research Triangle Park, NC) to all plots at the rate of 1120 g ae ha^{-1}, which was complemented with hand pulling of uncontrolled weeds.

Herbicide treatments were applied using a CO_2 pressurized backpack sprayer calibrated to deliver 187 L ha^{-1} at a pressure of 276 kPa. The boom had a nozzle spacing of 46 cm with Teejet XR8002 nozzles. *S*-metolachlor was activated within 24 h after application with 12.76 ± 0.19 mm of water using a sprinkler irrigation system installed in the experiment. One rain gauge was installed per replicate to quantify the amount of water applied to the experiment throughout the growing season. Daily precipitation and average air temperatures were acquired from the University of Arkansas Turfgrass Science Weather Station located less than 1 km away (Fig. 4. 2).

Soil samples were collected from all 16 experimental units during the experiment at three sampling dates. Sample collection occurred 1 day after planting soybean, 22 days after PRE herbicide application (24 days after planting soybean), and 34 days after POST herbicide application (57 days after PRE application or 59 days after planting soybean). Twenty samples were collected randomly per plot, within the 0 and 10.2 cm depth using a sterile probe (2.2-cm diameter), to form a composite sample per plot at each sampling date. Moist soil samples were sieved, the day of sampling, using an 8-mm sieve. Prior to planting soybean, a soil sample was collected from the field, 24 h after a rain event, oven dried at 105 ºC for 24 h to determine soil water content at field capacity. Then, a subsample of soil was collected the day before the field sampling date and , oven dried to determine soil water content.

S-metolachlor spiking, incubation and extraction

S-metolachlor spiking, incubation and sub-sampling procedures were similar to those described above with a few exceptions. For soil collected from each plot, the gravimetric soil moisture estimates from field conditions were used to bring moisture content back to field capacity by adding the estimated water volume to soil, mixing, and allowing to equilibrate. Soil (1 kg) was weighed and spiked with equivalent of 0.9375 mg *S*-metolachlor kg^{-1} dry soil on the day of soil collection and split into two jars containing 500 g soil. Incubation sub-samplings occurred at day 0, 1, 4, 7, 14, 28, and 56 from each jar.

Data analysis

Single first order (SFO) kinetics (equation 4. 1) was fitted to *S*-metolachlor concentrations, calculated as a percent of initial concentration, over time, using nonlinear least squares regression (nls) in R version 4.0.0 (R Core Team, 2020). The initial sub-sampling (day 0 after spiking) concentration represented 100% in equation 4. 1:

$$C = C_0 * e^{-kt} \tag{4. 1}$$

where C and C_0 are the percent of concentration of the herbicide in the soil at time t and t = 0, respectively, and k is the rate constant at which *S*-metolachlor dissipated in the soil. Differences between model parameters and zero were evaluated using a t-test (p-value ≤ 0.05). Fit of the data using SFO kinetics was assessed using root mean square error (RMSE, equation 4. 2),

$$RMSE = \sqrt{\frac{1}{N}\sum_{i=1}^{N}(Y_i - \hat{Y}_i)^2} \qquad (4.\ 2)$$

where Y_i is the measured value for situation i and $\hat{Y}_i$ is the corresponding value predicted by the model. N is the total number of observations. Mean absolute error (MAE measures the average difference between measured and predicted % *S*-metolachlor concentration in soil using equation 4. 3.

$$MAE = \frac{1}{N}\sum_{i=1}^{N} |Y_i - \hat{Y}_i\ | \qquad (4.\ 3)$$

Smaller RMSE and MAE values indicate a better model fit to the data because the predicted values are closer to the observed values. The RMSE and MAE indicate error in the units of the Y axis; they are valuable tools that aid in analysis of the results. Perfect fit is indicated by RMSE and MAE values of 0 (Moriasi et al., 2007; Wallach et al., 2006).

As a normalized statistic, the Nash-Sutcliffe efficiency (NSE) determines the relative magnitude of the residual variance compared to the measured data variance (Moriasi et al., 2007). NSE was calculated using equation 4. 4.

$$NSE = 1 - \frac{\sum_{i=1}^{N}(Y_i - \hat{Y}_i)^2}{\sum_{i=1}^{N}(Y_i - \bar{Y})^2} \qquad (4.\ 4)$$

Where $\bar{Y}$ is the mean observed value. The closer the values are to 1, the more accurate the predictions. A perfect model has NSE=1 because $Y_i = \hat{Y}_i$ (Wallach et al., 2006)

S-metolachlor half-lives were calculated using equation 4. 5.

$$t_{1/2} = \frac{\ln(2)}{k} \qquad (4.\ 5)$$

Calculated *S*-metolachlor half-lives were compared among treatments using ANOVA (PROC GLIMMIX) in SAS 9.4 (SAS Institute Inc., Cary, NC, USA). Treatment means were separated using Tukey's HSD method ($P \leq 0.05$). Calculated *S*-metolachlor half-lives for paired fields from the inter-annual study and for the effect of a preemergence application (22 days after PRE) were compared using a two-sample t-test.

Results and discussion

Model goodness of fit

The SFO equation (equation 4. 1) describes a log-linear decay of pesticide with time. Parameter estimates of initial herbicide concentration and for the *S*-metolachlor dissipation rate constant were different from zero ($P \leq 0.05$) for inter-annual (Table 4. 3) and within-season herbicide use histories (Tables 4. 4, 4. 5). The RMSE values ranged between 6.52 and 14.31 for the inter-annual (Table 4. 6) and between 7.75 and 10.52 for within-season herbicide use histories (Table 4. 7), respectively. The MAE values were between 5.34 and 12.45 and between 6.12 and 8.72 for the inter-annual and within season herbicide use history, respectively (Tables 4.6, 4. 7). Finally, the NSE values for the inter-annual herbicide use history study varied from 0.62 and 0.96, whereas the NSE values for the within-season herbicide use study ranged between 0.89 and 0.93.

Dissipation of *S*-metolachlor in this study was described satisfactorily by the SFO kinetic model. Sarmah and Rohan (2011) reported RMSE values between 0.41 and 26.08 while modeling the dissipation of 4-n-NP and BPA. Srinivasan et al. (2014) reported RMSE 0.6 to 23.9 in deriving dissipation endpoints of sulfamethoxazole using different models. As a normalized statistic that determines the relative magnitude of the residual variance compared to the measured data variance, NSE values > 0.59 were reported by Pullan et al. (2016) to indicate a good model performance for predictions of pesticide concentrations.

S-metolachlor dissipation rate in crop field soils differing in herbicide use history

The SFO dissipation constants (k) were smaller for high-use than low-use, except in Monroe county (Table 4. 3). Thus, in four of five counties sampled, *S*-metolachlor dissipation was faster in soil with low-use history (Fig. 4. 3); these results contradicted our hypothesis. A means comparison test revealed that *S*-metolachlor dissipation in spiked soils, collected from fields that received the herbicide continuously over a 5 to 6-year period, was slower than that in spiked soils collected from fields that received the herbicide a maximum of two times during the same 6-year period ($P \leq 0.05$). Therefore, enhanced dissipation was not observed for *S*-metolachlor in this study, which is in agreement with previous research (Bridges et al., 2008; Dowler et al., 1987; Harvey, 1987; Kotoula-Syka et al., 1997; Shaner and Henry, 2007).

The effect of use history was evaluated in 5 paired fields in the current study and the period of prior known management exposure was 5 to 6 years maximum. Investigating the impact of high-use after a longer period of exposure (10 years of continuous applications, for example) with a larger number of fields might provide additional information. Cultural practices that increase soil organic matter (SOM) can have a direct impact on metolachlor behavior (Teasdale et al., 2003). For example, metolachlor sorption to soil showed a 6-fold and 5-fold increase after addition of an organic waste to a sandy soil and to a soil with a higher clay content, leading to a reduction of leaching from 61 to 3.5%, and from 37 to < 1% in sandy and clayey soils, respectively (Canero et al., 2015).

Moreover, *S*-metolachlor dissipation in this study was variable across locations (Table 4.3), which aligned with previous research. The estimated half-lives ranged between 8 and 39 days. Dissipation half-lives obtained directly from field soil may vary as *S*-metolachlor in addition to degradation will also be subjected to losses via runoff, leaching and photodegradation. *S*-metolachlor half-lives reported in the literature have been variable. For example, *S*-metolachlor half-lives of 13.7 days were reported in Mississippi, Kentucky and Tennessee (Mueller et al., 1999). In a study conducted more than 10 years ago in Tennessee, Mueller and Steckel (2011) reported values between 8.8 and 27 days. Half-life values reported in northern Colorado ranged between 39 and 63 days (Westra et al., 2014), while in Eastern Colorado values ranged between 10.6 and 28.2 days (Shaner and Henry, 2007). In Georgia, averaged over a two-year period, *S*-metolachlor half-lives were 2 days and 4 days for bare soil and soil under low-density polyethylene mulch, respectively (Grey et al., 2007). Half-lives between 12 and 31 and 13 and 28 days were reported for five soils from five US states for metolachlor and *S*-metolachlor, respectively (Shaner et al., 2006). Longer half-lives were also reported with values of 112 days (sandy loam soil with 0.9% OM, pH 6 in Wisconsin), 97 days (loamy sand with 0.8% OM, pH 6.8 in California), and 124 days (silty clay loam with 3.3% OM, pH 6.8 in Iowa) (Senseman, 2007). The *S*-metolachlor half-life values obtained in the current study are within the low range of values (or relatively faster dissipation) reported in the literature.

Variability in *S*-metolachlor degradation under field conditions is due to various physical, chemical and microbial processes that drive its dissipation. Field dissipation of *S*-metolachlor occurs mainly by microbial decomposition, photodegradation and volatilization. Microbial degradation of metolachlor in the soil is accomplished by both aerobic and anaerobic microorganisms, with half-lives of 81 and 67 days in sandy soils reported for anaerobic and aerobic microbes, respectively (Senseman, 2007).

Microbial degradation of metolachlor is affected by several factors including soil depth, soil moisture, organic carbon, temperature and size and composition of microbial populations (Braverman et al., 1986; Rice et al., 2002). Rice et al. (2002) reported that metolachlor persisted longer in subsurface than in surface soils regardless of soil moisture and the initial concentration of herbicide. It had a shorter half-life at 40 °C than 30 °C and its adsorption was positively correlated with clay and organic carbon content (Braverman et al., 1986). Half-lives of 22 and 205 days were reported in summer and winter, respectively, near the surface in lake water for sunlight degradation of the herbicide (Kochany and Maguire, 1994). Volatilization of metolachlor is affected by both environmental conditions and cultural practices. Temperatures higher than 30 ºC increased metolachlor volatilization from water (Feigenbrugel et al., 2004; Lau et al., 1995). A correlation between soil surface temperatures and metolachlor volatilization has been established when soils are moist (Gish et al., 2009). Important factors such as residue cover, spatial concentration on soil surface, and rainfall timing all influence metolachlor volatilization (Bedos et al., 2017, Gish et al., 2009; Prueger et al., 1999; Prueger et al., 2017).

Effect of frequency and timing of in-season applications on S-metolachlor dissipation in soil

Dissipation rate constants (k) were greater for soil from nontreated compared to treated plots (Table 4. 4). Half-lives obtained from the nontreated control plots 22 days after preemergence application were 6 days while half-lives from the treated plots were 7 days (Fig. 4. 4; Table 4. 4). The half-life was not significantly different between the nontreated control and the PRE treatment ($P > 0.05$). Half-lives calculated 34 days after postemergence application (or 57 days after preemergence application) were 12, 14, 14, and 17 days, for the control, PRE, POST, and PRE *fb* POST treatments, respectively. Means revealed that *S*-metolachlor dissipation in spiked soils collected from plots that received a single application (either as a preemergence or as a postemergence treatment) was identical to that of soils collected from plots that did not receive any application of the herbicide in the field. In contrast, a sequential application of the herbicide (PRE *fb* POST) decreased *S*-metolachlor dissipation in comparison to the control ($P \leq 0.05$).

Based on these results, *S*-metolachlor degradation does not appear to be accelerated by multiple within-season applications. *S*-metolachlor may not serve as a growth substrate for microorganisms. Contrasting results are reported in the literature for metolachlor biodegradation. Metolachlor degradation by microbes was reported as partial and co-metabolic (Stamper and Tuovinen, 1998). More recently, others reported that metolachlor can be mineralized by soil organisms closely related to *Bacillus* spp. and *Acidobacteria* (Kanissery et al., 2018). Also, *Candida xestobii* has been reported to mineralize metolachlor and use it as a sole source of carbon for growth (Munoz et al., 2011).

Sanyal and Kulshrestha (1999) reported accelerated degradation after four applications of metolachlor in an 8-month period over two growing seasons. Fundamental differences exist between the current study and the study reported by Sanyal and Kulshrestha (1999). Sanyal and Kulshrestha (1999) studied the dissipation kinetics of the herbicide after field applications and reported enhanced degradation. In the current study, one or two applications of *S*-metolachlor to the same plot within a single growing season were followed by spiking soils with *S*-metolachlor in the laboratory, and dissipation was quantified in spiked soils. In the current study, *S*-metolachlor was incorporated into moist soil and the incubation experiment was started the same day soil was collected, while soil was air dried before processing by Sanyal and Kulshrestha (1999).

Influence of time of sample collection on S-metolachlor dissipation

The *S*-metolachlor dissipation half-lives from the nontreated plots were 6, 6, and 12 days for samples collected 1 day, 24, and 59 days after planting soybean, respectively (Table 4. 5). The *S*-metolachlor dissipation in spiked soils collected from nontreated plots in the field 59 days after planting soybean was slower than that in spiked soils collected from the same plots 1 day and 24 days after planting ($P \leq 0.05$) (Fig. 4. 5). Moisture and temperature in the field prior to sample collection (Fig. 4. 2) could be factors contributing to the differences observed in half-lives throughout the season. The last sampling 59 days after planting soybean occurred in mid-August, after a hot and dry period, which may have reduced microbial diversity and biomass and consequent activity in the spiked soils. In support of the altered degradation rates measured in the spiked soil in the laboratory in this current study, metolachlor dissipation under fields conditions is known to present seasonal variation in part related to environmental conditions (Jaikaew et al., 2015).

The faster dissipation of *S*-metolachlor in samples collected 1 day and 24 days after planting in this current study also might be related to changes in the microbial community throughout the season. A winter rye cover crop in 2018 had been preceded by two years of fallow (2017 and 2018). It was hypothesized that 2 years of fallow with cover crops increased carbon supply to microorganisms and resulted in greater microbial activity in the soil earlier in the growing season. Cover crop residues in the field might have increased the soil microbial community biomass, diversity, and/or activity resulting in greater activity in the spiked soil in the laboratory experiment. Teasdale et al. (2003) reported faster degradation of *S*-metolachlor in the presence of cover crop residues. Cover crops increase carbon availability to soil microbial communities (Lundquist et al., 1999). Mbuthia et al. (2015) reported a significant change in microbial community structure and activity by the use of cover crops. The state of decomposition of cover crop residues is known to influence metolachlor degradation with a half-life of 23 days on a bare soil but half-lives of 9, 15, 39 and 25 days for progressive levels of decomposition of cover crops (Cassigneul et al., 2015; Cassigneul et al., 2018, Aslam et al., 2013).

Conclusion

Successive applications of *S*-metolachlor over 5 to 6 years induced a decrease in the dissipation rate compared to commercial fields where *S*-metolachlor had been applied 0 to 2 years within the same six-year period. Within the same growing season, applying *S*-metolachlor twice as a sequential application program induced a significant increase in the persistence of the herbicide in spiked, incubated soil under laboratory conditions. Moreover, *S*-metolachlor dissipation was faster earlier in the season, 1 day and 24 days after planting compared to 59 days after planting, most likely due to the rye cover crop residue enhancing microbial diversity and activity. The longest half-life of *S*-metolachlor determined in this study was 39 days in soil collected from Lonoke County, AR from a commercial soybean-corn field that had been sprayed with *S*-metolachlor multiple times annually since 2013. Further investigation of the activity of *S*-metolachlor-degrading microbes and enzymes as affected by cover crop, multiple inter-annual exposure, frequency and timing of within-season applications of the herbicide will shed light on the long-term impact of management practices and ability to predict herbicide dissipation and persistence in soils.

Acknowledgements

This research has been funded by the Arkansas Soybean Promotion Board. Authors thank Ryan Grewe for his help in field and laboratory work.

References

Abit M, Rainbolt C, Krutz L, Shaner D, Hanson B (2012) Effects of long-term use on simazine dissipation in central California vineyards. Weed Science 60: 531-536.

Aslam S, Garnier P, Rumpel C, Parent SE, Benoit P (2013) Adsorption and desorption behavior of selected pesticides as influenced by decomposition of maize mulch. Chemosphere 91: 1447-1455.

Barber LT, Butts TR, Boyd JW, Cunningham K, Selden G, Norsworthy JK, Burgos N, Bertucci MB (2021) Recommended chemicals for weed and brush control (MP-44). Little Rock, AR: University of Arkansas cooperative Extension Service, Fayetteville, AR. Publication #MP44-12M-1-00RV

Braverman MP, Lavy TL, Barnes CJ (1986) The degradation and bioactivity of metolachlor in the soil. Weed Science 34: 479-484.

Bedos C, Alletto L, Durand B, Fanucci O, Brut A, Bourdat-Deschamps M, Giuliano S, Loubet B, Ceschia E, Benoit P (2017) Observed volatilization fluxes of *S*-metolachlor and benoxacor applied on soil with and without crop residues. Environmental Science and Pollution Research 24: 3985-3996.

Bexfield LM, Belitz K, Lindsey BD, Toccalino PL, Nowell LH (2021) Pesticides and pesticide degradates in groundwater used for public supply across the United States: occurrence and human-health context. Environmental Science & Technology 55: 362-372.

Bridges M, Henry WB, Shaner DL, Khosla R, Westra P, Reich R (2008) Spatial variability of atrazine and metolachlor dissipation on dryland no-tillage crop fields in Colorado. Journal of Environmental Quality 37: 2212-2220.

Busi R (2014) Resistance to herbicides inhibiting the biosynthesis of very-long-chain fatty acids. Pest Management Science 70: 1378-1384.

Canero AI, Cox L, Cabrera A, Cornejo J (2015) Different effects of a by-product from olive oil extraction on *S*-metolachlor and bentazone soil fate. Clean-Soil Air Water 43: 948-957.

Cassigneul A, Alletto L, Benoit P, Bergheaud V, Etievant V, Dumeny V, Le Gac A, Chuette D, Rumpel C, Justes E (2015) Nature and decomposition degree of cover crops influence pesticide sorption: Quantification and modelling. Chemosphere 119: 1007-1014.

Cassigneul A, Benoit P, Nobile C, Bergheaud V, Dumeny V, Etievant V, Maylin A, Justes E, Alletto L (2018) Behaviour of *S*-metolachlor and its oxanilic and ethanesulfonic acids metabolites under fresh vs. partially decomposed cover crop mulches: A laboratory study. Science of the Total Environment 631-632: 1515-1524.

Coffinet S, Rifai A, Genty C, Souissi Y, Bourcier S, Sablier M, Bouchonnet S (2012) Characterization of the photodegradation products of metolachlor: structural elucidation, potential toxicity and persistence. Journal of Mass Spectrometry 47: 1582-1593.

Dimou AD, Sakkas VA, Albanis TA (2005) Metolachlor photodegradation study in aqueous media under natural and simulated solar irradiation. Journal of Agricultural and Food Chemistry 53: 694-701.

Dowler CC, Marti LR, Kvien CS, Skipper HD, Gooden DT, Zublena JP (1987). Accelerated degradation potential of selected herbicides in the southeastern United States. Weed Technology 1: 350-358.

Dubus IG, Beulke S, Brown CD (2002) Calibration of pesticide leaching models: critical review and guidance for reporting. Pest Management Science 58: 745-758.

Feigenbrugel V, Le Calve S, Mirabel P (2004) Temperature dependence of Henry's law constants of metolachlor and diazinon. Chemosphere 57: 319-327.

Gish TJ, Prueger JH, Kustas WP, Daughtry CST, McKee LG, Russ A, Hatfield JL (2009) Soil moisture and metolachlor volatilization observations over three years. Journal of Environmental Quality 38: 1785-1795.

Grey T, Vencill W, Mantripagada N, Culpepper A (2007) Residual herbicide dissipation from soil covered with low-density polyethylene mulch or left bare. Weed Science 55: 638-643.

Harvey RG (1987) Herbicide dissipation from soils with different herbicide use histories. Weed Science 35: 583-589.

Jaikaew P, Boulange J, Thuyet DQ, Malhat F, Ishihara S, Watanabe H (2015) Potential impacts of seasonal variation on atrazine and metolachlor persistence in andisol soil. Environmental Monitoring and Assessment 187: 760.

Kanissery RG, Welsh A, Gomez A, Connor L, Sims GK (2018) Identification of metolachlor mineralizing bacteria in aerobic and anaerobic soils using DNA-stable isotope probing. Biodegradation 29: 117-128.

Kochany J, Maguire RJ (1994) Sunlight photodegradation of metolachlor in water. Journal of Agricultural and Food Chemistry 42: 406-412.

Kotoula-Syka E, Hatzios K, Berry D, Wilson H (1997) Degradation of acetanilide herbicides in history and non-history soils from eastern Virginia. Weed Technology 11: 403-409:

Krutz L, Shaner D, Accinelli C, Zablotowicz R, Henry W (2008) Atrazine dissipation in *S*-triazine-adapted and non-adapted soil from Colorado and Mississippi: Implications of enhanced degradation on atrazine fate and transport parameters. Journal of Environmental Quality 37: 848-857.

Krutz LJ, Shaner DL, Weaver MA, Webb RMT, Zablotowicz RM, Reddy KN, Huang YB, Thomson SJ (2010a) Agronomic and environmental implications of enhanced *S*-triazine degradation. Pest Management Science 66: 461-481.

Krutz L, Shaner D, Zablotowicz R (2010b) Enhanced degradation and soil depth effects on the fate of atrazine and major metabolites in Colorado and Mississippi soils. Journal of Environmental Quality 39: 1369-1377.

Krutz L, Zablotowicz R, Reddy K, Koger C, Weaver M (2007) Enhanced degradation of atrazine under field conditions correlates with a loss of weed control in the glasshouse. Pest Management Science 63: 23-31.

Kurt-Karakus PB, Teixeira C, Small J, Muir D, Bidleman TF (2011) Current-use pesticides in inland lake waters, precipitation, and air from Ontario, Canada. Environmental Toxicology and Chemistry 30: 1539-1548.

Lau YL, Liu DLS, Pacepavicius GJ, Maguire RJ (1995) Volatilization of metolachlor from water. Journal of Environmental Science and Health Part B-Pesticides Food Contaminants and Agricultural Wastes 30: 605-620.

Lundquist E, Scow K, Jackson L, Uesugi S, Johnson C (1999) Rapid response of soil microbial communities from conventional, low input, and organic farming systems to a wet/dry cycle. Soil Biology & Biochemistry 31: 1661-1675.

Marin-Benito JM, Pot V, Alletto L, Mamy L, Bedos C, Barriuso E, Benoit P (2014) Comparison of three pesticide fate models with respect to the leaching of two herbicides under field conditions in an irrigated maize cropping system. Science of the Total Environment 499: 533-545.

Marti E, Caliz J, Montserrat G, Garau MA, Cruanas R, Vila X, Sierra J (2012) Air-drying, cooling and freezing for soil sample storage affects the activity and the microbial communities from two Mediterranean soils. Geomicrobiology Journal 29: 151-160.

Mbuthia LW, Acosta-Martinez V, DeBruyn J, Schaeffer S, Tyler D, Odoi E, Mpheshea M, Walker F, Eash N (2015) Long term tillage, cover crop, and fertilization effects on microbial community structure, activity: Implications for soil quality. Soil Biology & Biochemistry 89: 24-34.

Milan M, Ferrero A, Fogliatto S, Piano S, Vidotto F (2015) Leaching of *S*-metolachlor, terbuthylazine, desethylterbuthylazine, mesotrione, flufenacet, isoxaflutole, and diketonitrile in field lysimeters as affected by the time elapsed between spraying and first leaching event. Journal of Environmental Science and Health Part B-Pesticides Food Contaminants and Agricultural Wastes 50: 851-861.

Moriasi DN, Arnold JG, Van Liew MW, Bingner RL, Harmel RD, Veith TL (2007) Model evaluation guidelines for systematic quantification of accuracy in watershed simulations. Transactions of the ASABE 50: 885-900.

Mueller T, Shaw D, Witt W (1999) Relative dissipation of acetochlor, alachlor, metolachlor, and SAN 582 from three surface soils. Weed Technology 13: 341-346.

Mueller T, Steckel L (2011) Efficacy and dissipation of pyroxasulfone and three chloroacetamides in a Tennessee field soil. Weed Science 59: 574-579.

Munoz A, Koskinen WC, Cox L, Sadowsky MJ (2011) Biodegradation and mineralization of metolachlor and alachlor by *Candida xestobii*. Journal of Agricultural and Food Chemistry 59: 619-627.

Neves M, Castro BB, Vidal T, Vieira R, Marques JC, Coutinho JAP, Goncalves F, Goncalves AMM (2015) Biochemical and populational responses of an aquatic bioindicator species, *Daphnia longispina*, to a commercial formulation of a herbicide (Primextra (R) Gold TZ) and its active ingredient (*S*-metolachlor). Ecological Indicators 53: 220-230.

O'Connell P, Harms C, Allen J (1998) Metolachlor, *S*-metolachlor and their role within sustainable weed-management. Crop Protection 17: 207-212.

Provin T (2014) Total carbon and nitrogen and organic carbon via thermal combustion analysis. *In*: Sikora FJ, Moore KP (Eds.), Soil test methods from the southeastern United States. Southern Coop. Ser. Bull. 419: 149-154.

Prueger JH, Alfieri J, Gish TJ, Kustas WP, Daughtry CST, Hatfield JL, McKee LG (2017) Multi-year measurements of field-scale metolachlor volatilization. Water Air and Soil Pollution 228: 11.

Prueger JH, Gish TJ, McConnell LL, McKee LG, Hatfield JL, Kustas WP (2005) Solar radiation, relative humidity, and soil water effects on metolachlor volatilization. Environmental Science & Technology 39: 5219-5226.

Prueger JH, Hatfield JL, Sauer TJ (1999) Field-scale metolachlor volatilization flux estimates from broadcast and banded application methods in central Iowa. Journal of Environmental Quality 28: 75-81.

Pullan SP, Whelan MJ, Rettino J, Filby K, Eyre S, Holman IP (2016) Development and application of a catchment scale pesticide fate and transport model for use in drinking water risk assessment. Science of the Total Environment 563: 434-447.

R Core Team R (2020) R: A language and environment for statistical computing. Vienna, Austria: R Core Team (2020).

Rice PJ, Anderson TA, Coats JR (2002) Degradation and persistence of metolachlor in soil: Effects of concentration, soil moisture, soil depth, and sterilization. Environmental Toxicology and Chemistry 21: 2640-2648. Sakkas VA, Arabatzis IM, Konstantinou IK, Dimou AD, Albanis TA, Falaras P (2004) Metolachlor photocatalytic degradation using TiO2 photocatalysts. Applied Catalysis B-Environmental 49: 195-205.

Sanyal D, Kulshrestha G (1999) Effects of repeated metolachlor applications on its persistence in field soil and degradation kinetics in mixed microbial cultures. Biology and Fertility of Soils 30: 124-131.

Sarmah AK, Rohan M (2011) Evaluation of four mathematical models to describe dissipation kinetics of 4-n-nonylphenol and bisphenol-A in groundwater-aquifer material slurry. Journal of Environmental Monitoring 13: 157-166.

Senseman S (2007) Herbicide handbook. 9th ed. Lawrence, KS: Weed Science Society of America. Pp. 458.

Shaner D, Brunk G, Belles D, Westra P, Nissen S (2006) Soil dissipation and biological activity of metolachlor and *S*-metolachlor in five soils. Pest Management Science 62: 617-623.

Shaner D, Henry W (2007) Field history and dissipation of atrazine and metolachlor in Colorado. Journal of Environmental Quality 36: 128-134.

Sikora FJ, Kissel DE (2014) Soil pH. *In*: Sikora FJ, Moore KP (Eds), Soil test methods from the southeastern United States. Southern Coop. Ser. Bull. 419. p.48-53.

Srinivasan P, Sarmah A, Rohan M (2014) Deriving sulfamethoxazole dissipation endpoints in pasture soils using first order and biphasic kinetic models. Science of the Total Environment 488: 146-156.

Stamper D, Tuovinen O (1998) Biodegradation of the acetanilide herbicides alachlor, metolachlor, and propachlor. Critical Reviews in Microbiology 24: 1-22.

Teasdale J, Shelton D, Sadeghi A, Isensee A (2003) Influence of hairy vetch residue on atrazine and metolachlor soil solution concentration and weed emergence. Weed Science 51: 628-634.

USDA-SCS (1969) Soil Survey of Washington County, Arkansas. U.S. Gov. Print. Office, Washington, DC.

USDA-NASS (2021) Acreage. (June 2021) 3 USDA. National Agricultural Statistics Service (NASS), Agricultural Statistics Board, United States Department of Agriculture (USDA).

Accessed on October 12, 2021. https://www.nass.usda.gov/Publications/Todays_Reports/reports/acrg0621.pdf

Wallach D (2006) Evaluating crop models. *In*: Wallach D, Makowski D, Jones J (Eds). Working with dynamic crop models: evaluation, analysis, parameterization, and applications. Pp. 11: 50.

Westra E, Shaner D, Westra P, Chapman P (2014) Dissipation and leaching of pyroxasulfone and *S*-metolachlor. Weed Technology 28: 72-81.

Zablotowicz RM, Robert M, Krutz LJ, Reddy KN, Weaver MA, Koger CH, Locke MA (2007) Rapid development of enhanced atrazine degradation in a dundee silt loam soil under continuous corn and in rotation with cotton. Journal of Agricultural and Food Chemistry 55: 852-859.

Zhang H, Hardy DH, Mylavarapu R, Wang J (2014) Mehlich-3. *In*: Sikora FJ, Moore KP (Eds). Soil test methods from the southeastern United States. Southern Coop. Ser. Bull. 419. p. 101-110.

Zhang GT, Cui P, Jin W, Zhang ZT, Wang H, Bazai NA, Li Y, Liu DZ, Alessandro P (2021) Changes in hydrological behaviours triggered by earthquake disturbance in a mountainous watershed. Science of the Total Environment 760: 1-16

Tables and Figures

Table 4. 1. Herbicide use, cropping systems, and select data for silt loam soil samples (n = 20) collected in 10 commercial row-crops fields from five Arkansas counties to study the impact of low use (0 to 2 years *S*-metolachlor application) and high use (5 to 6 years of *S*-metolachlor application) on dissipation of *S*-metolachlor in spiked soils (0.9375 mg kg^{-1} soil) during a 56-day laboratory incubation[a].

County	History	EC[b] (µmhos cm^{-1})	% N[c]	% C	Herbicide programs	Cropping systems	Area (ha)
Clay	Low	78	0.10	1.7	None	Pasture site	~10.0
	High	78	0.07	1.1	▪ Corn: metolachlor + atrazine in 2012, 2014 & 2016. ▪ Soybean: metolachlor + fomesafen in 2013 & 2015 ▪ Soybean: metolachlor + fomesafen followed by metolachlor + metribuzin in 2017	▪ Corn: 2012, 2014, & 2016 soybean: 2013, 2015 & 2017	~16.0
Crawford	Low	114	0.04	0.4	▪ No herbicide application from 2012 to 2018	▪ No crop from 2012 to 2018	0.2
	High	114	0.02	0.3	▪ 2012: 0.91 L ha^{-1} (Dual Magnum) ▪ 2013: 1.17 L ha^{-1} (Dual Magnum) ▪ 2014: 1.17 L ha^{-1} (Dual II Magnum) ▪ 2015: 0.78 L ha^{-1} (Dual II Magnum) ▪ 2016: 0.78 L ha^{-1} (Charger Max) ▪ 2017: 0.78 L ha^{-1} (Dual Magnum)	▪ 6 years of continuous spinach	0.4
Drew	Low	100	0.07	1.1	▪ Metolachlor application in 2017	▪ Continuous soybean system	3.0
	High	43	0.04	0.6	▪ Metolachlor applied every year	▪ Cotton planted in 2012 followed by 4 years of continuous soybean and a rotation to corn in 2017	57.0
Lonoke	Low	115	0.06	1.1	▪ Metolachlor applied only in 2017	▪ Rice: 2014 & 2016 ▪ Soybean: 2015 & 2017	23.0
	High	139	0.07	1.4	▪ Multiple applications of metolachlor every year	▪ Soybean: 2013, 2015 & 2017 ▪ Corn: 2014 & 2016.	65.0
Monroe	Low	119	0.05	0.6	▪ Metolachlor only in 2014	▪ Continuous soybean since 2013	32.0
	High	107	0.06	0.9	▪ Two applications of metolachlor each year at a rate of 1.2 L ha^{-1}	▪ Continuous soybean since 2013	~14.0

[a] All fields investigated had a silt loam texture

[b] Soil EC measured in a 1:2 soil: water mixture (Sikora and Kissel, 2014).

[c] Measured by thermal combustion analysis (Provin, 2014).

Table 4. 2. Soil chemical and physical data for the Captina silt loam soil (slopes between 1 and 3%) used for the field experiment conducted during summer 2019 at the Milo J. Shult Agricultural Research & Extension Center (University of Arkansas, Fayetteville) in order to evaluate the influence of the number and timing of in-season applications of *S*-metolachlor on its dissipation.

Soil pH[a]	**Soil EC[a]**	**Total N[b]**	**Total C**	**Mehlich-3 extractable soil nutrients[c]**											**Sand**	**Silt**	**Clay**
				P	**K**	**Ca**	**Mg**	**S**	**Na**	**Fe**	**Mn**	**Zn**	**Cu**	**B**			
	μmhos cm-^{1}	%	%		---------------------- (mg kg^{-1}) ----------------------------										%	%	%
6.4	69	0.05	0.63	71	124	554	30	5.7	5.6	152	146	6.8	0.8	0.8	28.4	65.3	6.3

[a] Soil pH and EC measured in a 1:2 soil: water mixture (Sikora and Kissel, 2014).
[b] Measured by thermal combustion analysis (Provin, 2014).
[c] Extracted using Mehlich-3 method (Zhang et al., 2014).

Table 4. 3. Single first-order (SFO) equation model parameters for initial concentration (C_0), rate constant (k), and half-life ($t_{1/2}$) of *S*-metolachlor added to soil in 10 silt-loam soils collected from commercial producer fields across five Arkansas counties with a known history of low (0 to 2 years) and high (5 to 6 years) of *S*-metolachlor-use history. Final spiked *S*-metolachlor concentration of 0.9375 mg kg^{-1} soil.

County	**History**	**Parameters**	**Estimate**	**Std. Err**	**t value**	**Pr(>|t|)**	**$t_{1/2}$**
Clay	Low	C_0	95.59	3.48	27.46	6.86E-15***	8
		k	0.09	0.01	11.22	5.43E-09***	
	High	C_0	76.88	5.91	13.01	6.31E-10***	35
		k	0.02	0.01	4.05	0.001***	
Crawford	Low	C_0	82.18	6.53	12.58	1.04e-09***	14
		k	0.05	0.01	4.68	0.000251 ***	
	High	C_0	86.33	6.13	14.09	1.94e-10***	18
		k	0.039	0.01	4.94	0.000147 ***	
Drew	Low	C_0	89.21	5.55	16.06	2.73E-11***	10
		k	0.07	0.01	6.28	1.10E-05***	
	High	C_0	92.54	3.97	23.29	9.07E-14***	35
		k	0.02	0.003	6.94	3.33E-06***	
Lonoke	Low	C_0	92.26	5.62	16.43	1.94E-11***	12
		k	0.06	0.01	6.30	1.05E-05***	
	High	C_0	83.14	4.20	19.77	1.14E-12***	39
		k	0.018	0.003	5.43	5.56E-05***	
Monroe	Low	C_0	84.60	5.11	16.57	1.70E-11***	14
		k	0.05	0.01	6.08	1.59E-05***	
	High	C_0	88.42	4.16	21.27	3.70E-13***	12
		k	0.06	0.01	7.98	5.68E-07***	

[1] Asterisks (***) next to p-value (labelled Pr(>|t|)) indicate parameter estimates significantly different from 0 ($\alpha = 0.01$)

Table 4. 4. Single first-order (SFO) equation model parameters for initial concentration (C_0), rate constant (k), and half-live ($t_{1/2}$) to evaluate the time of field soil collection from nontreated and *S*-metolachlor-treated plots on dissipation of the herbicide from spiked soil during a subsequent laboratory incubation. Final spiked *S*-metolachlor concentration of 0.9375 mg kg^{-1} dry weight soil

Sampling	**Treatment**	**Parameter**	**Estimate**	**Std. Err**	**t value**	**Pr(>|t|)**	**$t_{1/2}$**
24 days after planting soybean	Control	C_0	92.87	1.87	49.77	<2e-16***	6
		k	0.11	0.01	18.48	<2e-16***	
	PRE	C_0	94.50	1.75	54.07	<2e-16***	7
		k	0.10	0.005	19.81	<2e-16***	
59 days after planting soybean	Control	C_0	94.45	2.39	39.58	<2e-16***	12a
		k	0.06	0.004	13.19	<2e-16***	
	PRE	C_0	98.24	2.04	48.15	<2e-16***	14ab
		k	0.05	0.003	15.48	<2e-16***	
	POST	C_0	94.21	1.81	51.91	<2e-16***	14ab
		k	0.05	0.003	16.73	<2e-16***	
	PRE fb POST	C_0	96.41	2.32	41.56	<2e-16***	17b
		k	0.04	0.003	12.95	<2e-16***	

[1] Control is nontreated soil; PRE is soil collected 22 d after preemergence herbicide application (24 days after planting soybean; POST is soil collected 34 days after postemergence herbicide application (57 days after preemergence application or 59 days after planting soybean; and PRE fb POST is soil collected from a field receiving sequential PRE followed by POST applications Agricultural Research & Extension Center (University of Arkansas, Fayetteville, AR).
[2] Half life means lacking letters (24 days after planting soybean) are not significantly different
[3] Half life means with different letters for the same sampling date (59 days after planting soybean) are different according to the means separation test ($P \leq 0.05$) using the glimmix procedure in SAS 9.4 with a Tukey's HSD adjustment (SAS Institute Inc., Cary, NC, USA).

[4] Asterisks (***) next to p-value (labelled Pr(>|t|)) indicate parameter estimates significantly different from 0 ($\alpha = 0.01$)

Table 4. 5. Single first-order (SFO) equation model parameters for initial concentration (C_0), rate constant (k), and half-live ($t_{1/2}$) to evaluate the time of field soil collection from nontreated plots on *S*-metolachlor on dissipation in spiked soil (0.9375 mg kg^{-1} dry weight soil)[1] during a subsequent laboratory incubation.

Sampling	**Parameter**	**Estimate**	**Std. Err**	**t value**	**Pr(>|t|)**	**$t_{1/2}$**
1 day after planting soybean	C_0	93.49	2.53	36.97	<2e-16***	6a
	k	0.12	0.01	13.84	<2e-16***	
24 days after planting soybean	C_0	91.57	2.90	31.51	<2e-16***	6a
	k	0.11	0.01	11.84	<2e-16***	
59 days after planting soybean	C_0	94.45	2.39	39.58	<2e-16***	12b
	k	0.06	0.004	13.19	<2e-16***	

[1] Soil was collected from a field experiment conducted during summer 2019 at the Milo J. Shult Agricultural Research & Extension Center (University of Arkansas, Fayetteville, AR).

[2] Half life means with different letters are different according to the means separation test ($P \leq 0.05$). Means separation was carried out using the glimmix procedure in SAS 9.4 with a Tukey's HSD adjustment (SAS Institute Inc., Cary, NC, USA).

[3] Asterisks (***) next to p-value (labelled Pr(>|t|)) indicate parameter estimates significantly different from 0 ($\alpha = 0.01$)

Table 4. 6. Single first order (SFO) goodness of fit to *S*-metolachlor dissipation data obtained from of *S*-metolachlor added to soil in 10 silt-loam soils collected from commercial producer fields across five Arkansas counties with a known history of low (0 to 2 years) and high (5 to 6 years) of *S*-metolachlor-use history within the 6 preceding years. Final spiked *S*-metolachlor concentration of 0.9375 mg kg^{-1} soil.

County	**History**	**RMSE[1]**	**MAE**	**NSE**
Clay	Low	6.52	5.34	0.96
	High	14.31	11.88	0.62
Crawford	Low	13.63	10.61	0.75
	High	13.62	12.45	0.76
Drew	Low	10.95	9.18	0.87
	High	9.81	8.65	0.84
Lonoke	Low	11.31	9.74	0.86
	High	10.67	9.23	0.72
Monroe	Low	10.82	9.56	0.85
	High	8.58	7.85	0.91

[1] RMSE, MAE, and NSE are the root mean square error, mean absolute error, and Nash-Sutcliffe efficiency, respectively.

Table 4. 7. Single first order (SFO) goodness of fit to *S*-metolachlor dissipation data obtained to evaluate the time of field soil collection from nontreated and *S*-metolachlor-treated plots[1] on dissipation of the herbicide from spiked soil during a subsequent laboratory incubation. Final spiked *S*-metolachlor concentration of 0.9375 mg kg^{-1} dry weight soil.

Field sampling	**Treatments[2]**	**RMSE[3]**	**MAE**	**NSE**
24 days after planting soybean	Control	9.77	8.09	0.91
	PRE	9.28	7.44	0.92
59 days after planting soybean	Control	9.82	8.02	0.90
	PRE	8.68	6.41	0.92
	POST	7.75	6.12	0.93
	PREPOST	10.24	7.56	0.89
1 days after planting soybean	Control	9.00	7.80	0.92
24 days after planting soybean	Control	10.52	8.72	0.90
59 days after planting soybean	Control	9.82	8.02	0.90

[1] Soil was collected from a field experiment conducted during summer 2019 at the Milo J. Shult Agricultural Research & Extension Center (University of Arkansas, Fayetteville, AR)

[2] Control is nontreated soil; PRE is soil collected 22 d after preemergence herbicide application (24 days after planting soybean); POST is soil collected 34 days after postemergence herbicide application (57 days after preemergence application or 59 days after planting soybean); and PRE fb POST is soil collected from a field receiving sequential PRE followed by POST applications

[3] RMSE, MAE, and NSE are the root mean square error, mean absolute error, and Nash-Sutcliffe efficiency, respectively.

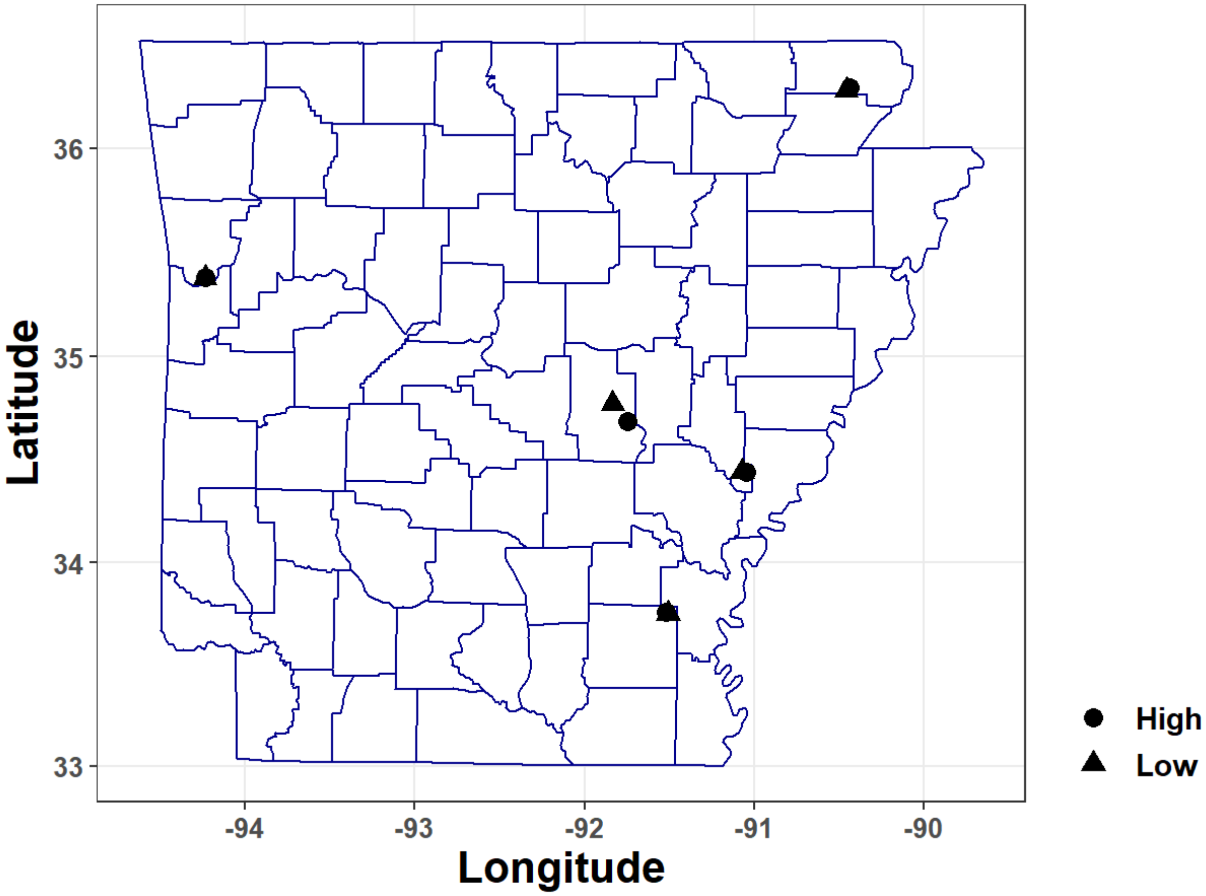

Figure 4. 1. Distribution of pairs of producer fields for soils collected from five Arkansas counties (USA) with low (0 to 2 years) and high (5 to 6 years) intensity of *S*-metolachlor use history within the preceding six years

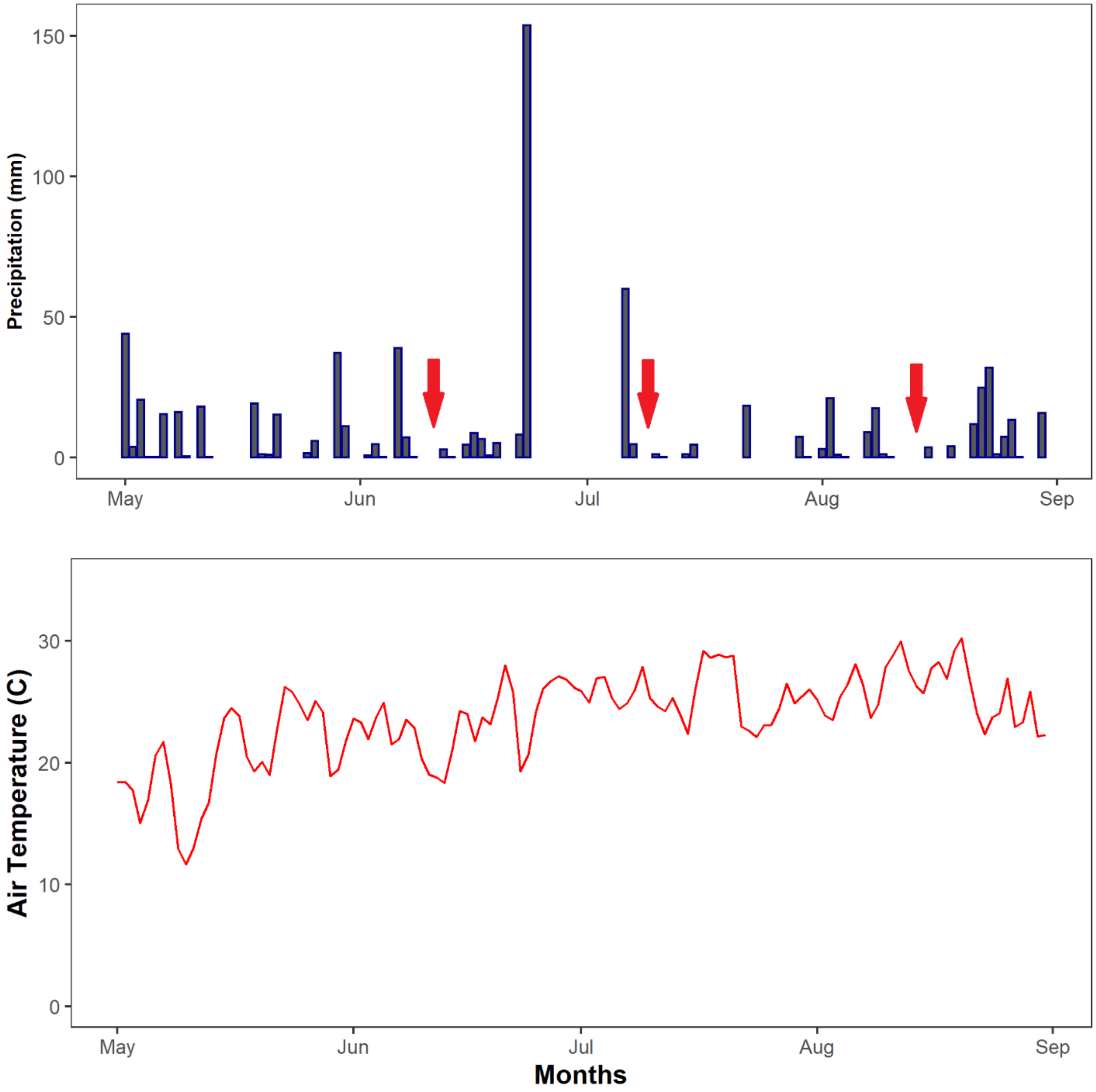

Figure 4. 2. Total daily precipitation (mm) (top panel) and average daily air temperature (˚C) (bottom panel) acquired from the nearest weather station to the experiment conducted at the Milo J. Shult Agricultural Research & Extension Center (University of Arkansas, Fayetteville) in 2019. Red arrows indicate soil samplings on June 13th, July 8th and August 11th.

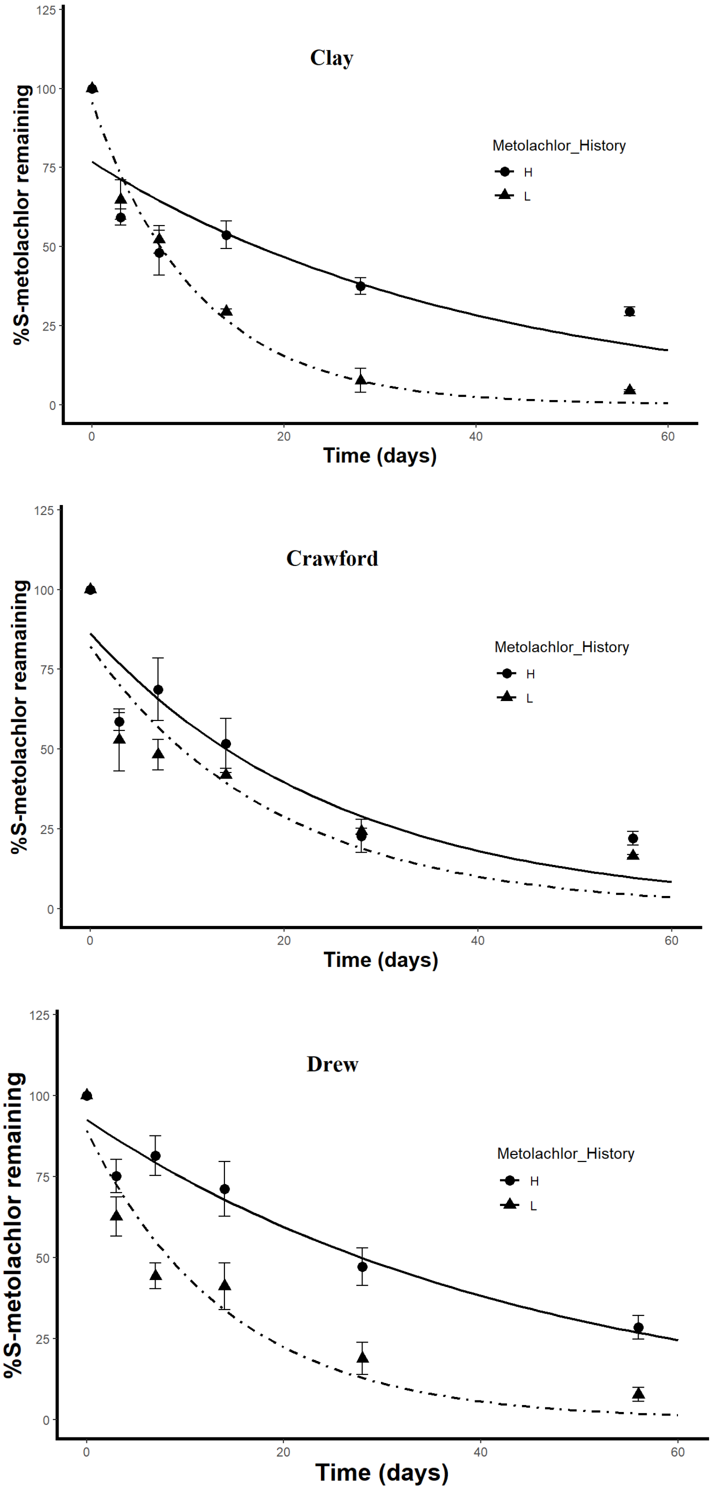

Figure 4. 3. Dissipation kinetics of *S*-metolachlor in soils (0.9375 mg kg^{-1} soil) from low (0 to 2 years) and high (5 to 6 years) intensity of *S*-metolachlor use history, within the preceding six years, collected from 5 counties in Arkansas (USA) and fitted to the single first order (SFO) model. Each panel is labeled according to the Arkansas county where commercial fields were located. Error bars indicate standard error.

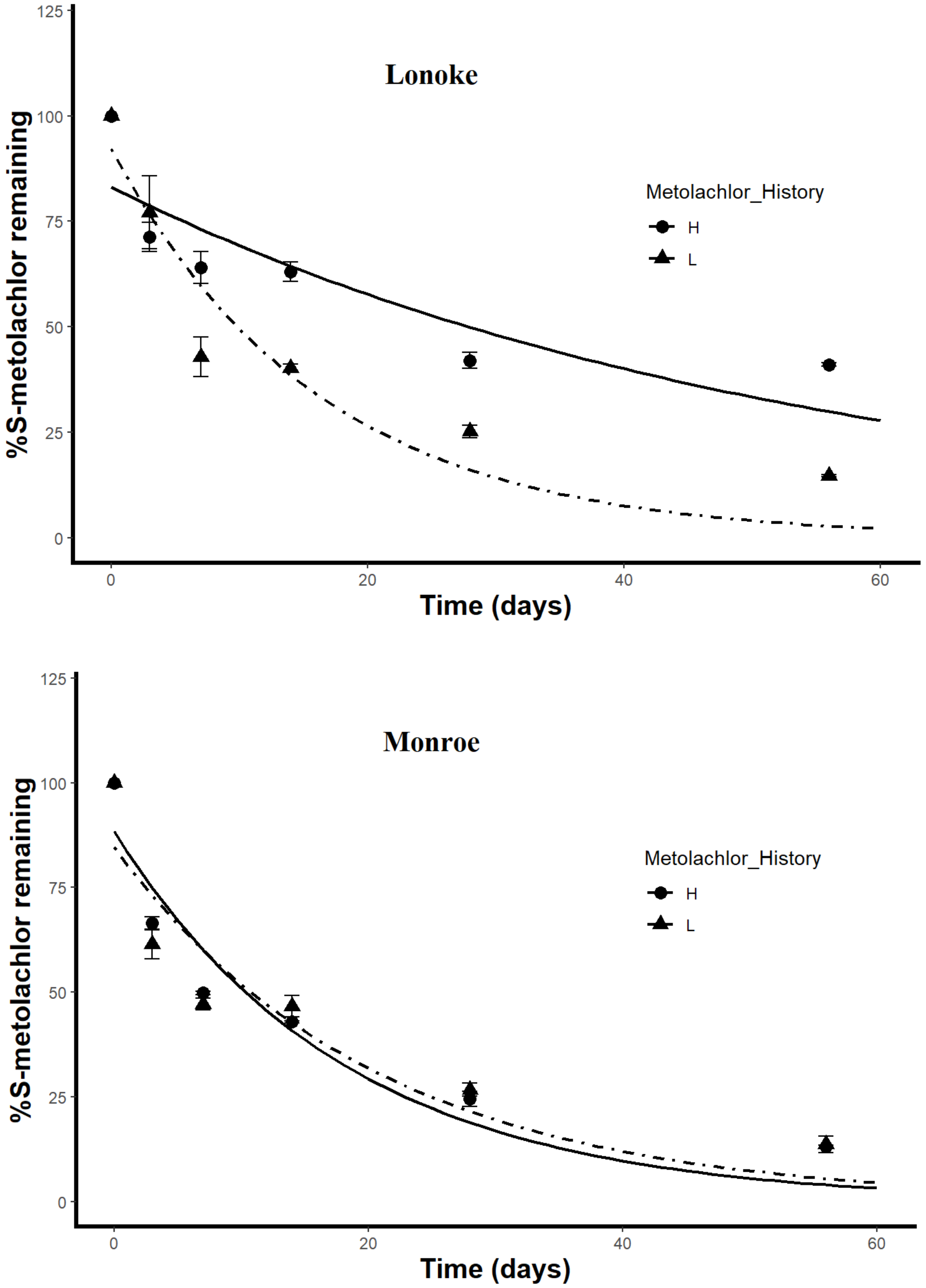

Figure 4. 3 (continued). Dissipation kinetics of *S*-metolachlor in soils (0.9375 mg kg^{-1} soil) from low (0 to 2 years) and high (5 to 6 years) intensity of *S*-metolachlor use history, within the preceding six years, collected from 5 counties in Arkansas (USA) and fitted to the single first order (SFO) model. Each panel is labeled according to the Arkansas county where commercial fields were located. Error bars indicate standard error.

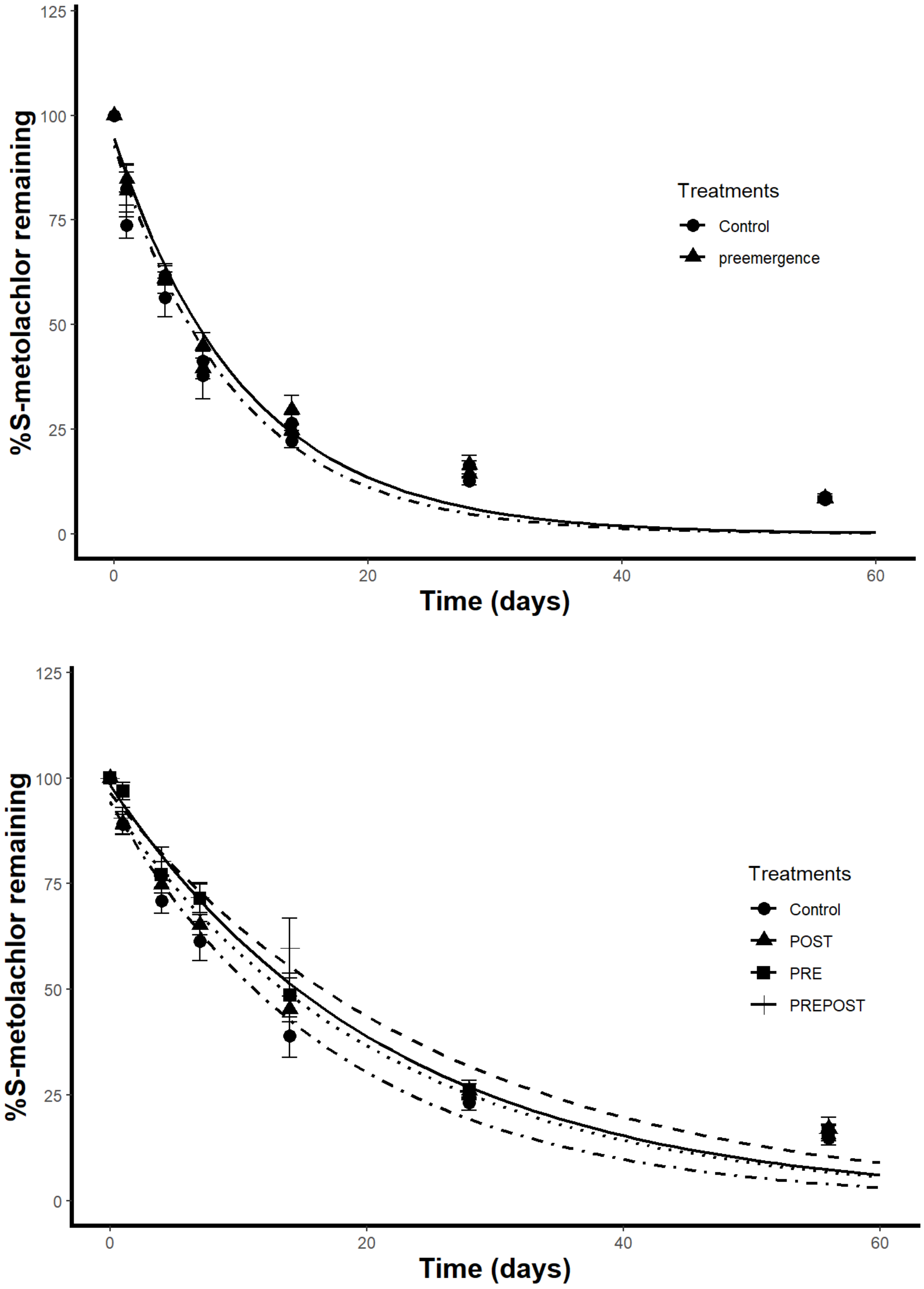

Figure 4. 4. Dissipation kinetics of *S*-metolachlor (spiked at 0.9375 mg kg^{-1} dry weight soil) in nontreated (control) soil and soil collected 22 days after preemergence herbicide application (24 days after planting soybean, PRE; top panel). Dissipation kinetics of *S*-metolachlor (spiked at 0.9375 mg kg^{-1} dry weight soil) in nontreated (control), PRE soil, soil collected 34 days after postemergence herbicide application (57 days after preemergence application or 59 days after planting soybean, POST; and soil collected from a field receiving sequential PRE followed by POST applications; PREPOST; bottom panel). Error bars indicate standard error.

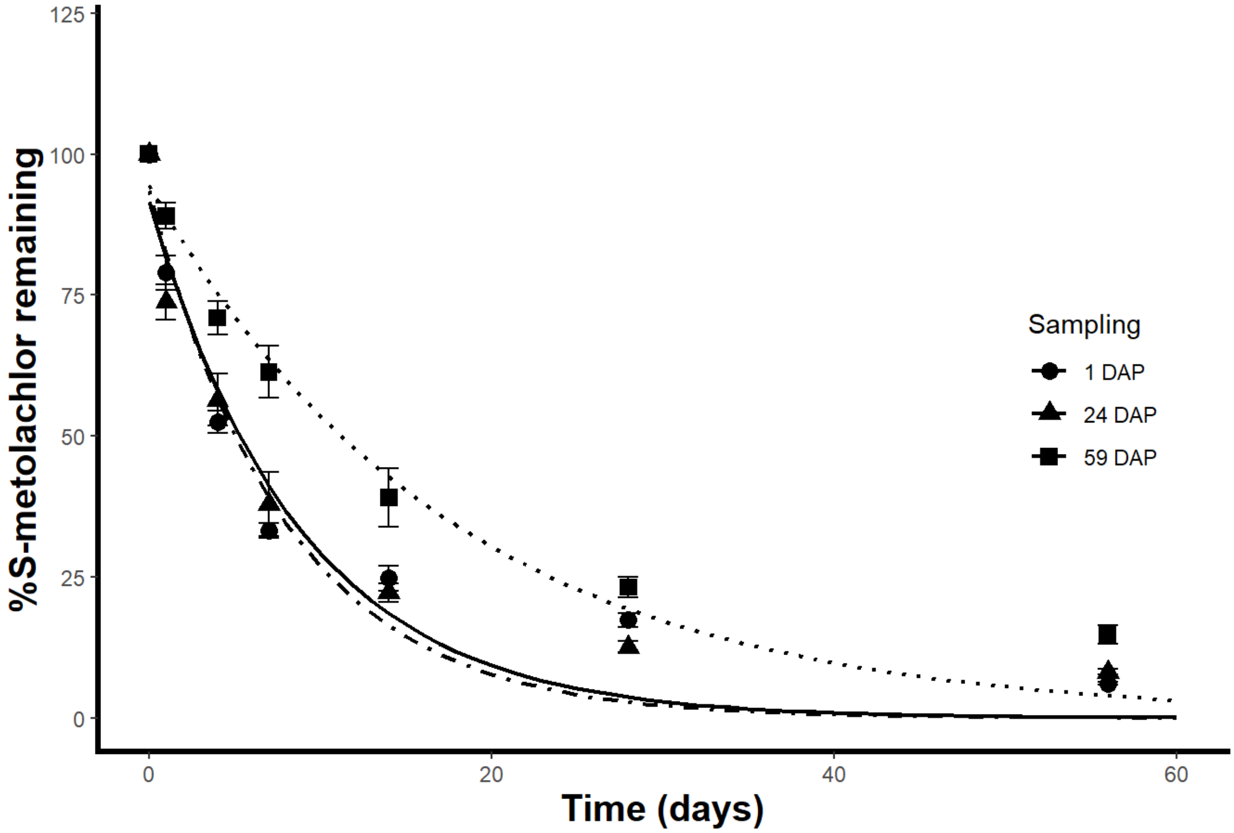

Figure 4. 5. Dissipation kinetics of *S*-metolachlor (0.9375 mg kg^{-1} dry weight soil) in soil collected from nontreated control plots at three different sampling times (1 day, 24 days and 59 days after planting (DAP) soybean) of a field experiment conducted at the Milo J. Shult Agricultural Research & Extension Center (University of Arkansas, Fayetteville) in 2019. Data were fitted to the single first order (SFO) model. Error bars indicate standard error.

Performance of five mathematical models for predicting the dissipation endpoints of *S*-metolachlor

Abstract

Understanding the fate of pesticides in the environment is crucial for sustainable weed management. Accurate predictions of herbicide dissipation endpoints are essential for predicting the potential duration of weed control and deciding crop replant options and rotation restrictions. The performance of five mathematical models (single first order kinetics (SFO), Gustafson and Holden (FOMC), quadratic or bi-exponential model (BEXP), first-order double-exponential decay (FODED), and first-order two-compartment (FOTC)) was evaluated to describe *S*-metolachlor dissipation kinetics in soil samples collected 1 day after planting (DAP) soybean [*Glycine max* (L.) Merr.] in a field experiment conducted in Fayetteville AR in 2019. Model performance to describe dissipation was first evaluated using the significance levels of optimized parameters. Results showed that the BEXP and FOTC models were not appropriate as their parameters were not all significantly different from 0 ($P > 0.05$). Statistical indices used to evaluate the remaining three models, included visual assessment of residuals, goodness of fit using model bias, root mean square error, mean absolute error, and Nash-Sutcliffe efficiency. Models were also selected using Akaike Information Criteria (AIC), and *S*-metolachlor dissipation endpoints were predicted for SFO, FOMC, and FODED models. Model selection and goodness of fit showed that the biphasic FOMC and FODED models better supported data compared to the SFO model. *S*-metolachlor dissipation endpoints predicted for 25 and 50% by SFO were greater than those predicted by FOMC and FODED. On the contrary, *S*-metolachlor dissipation endpoints predicted by SFO for 75 and 90% were lower than those predicted by

FOMC and FODED. The SFO under-predicted *S*-metolachlor concentrations in soil during the later stages of the dissipation process. The gap between *S*-metolachlor dissipation endpoints predicted by SFO and FOMC and FODED was larger at higher dissipation percentages. Therefore, caution might be required when making inference about 90% dissipation of pesticides in the soil using the SFO.

Keywords: dissipation, model selection, endpoints

Introduction

Pesticide fate impacts important agricultural and broader environmental management decision-making processes. Determination of how quickly herbicides dissipate in the soil is useful for predicting the potential duration of weed control and crop management such as replant options and rotation restrictions. Degradation is crucial for the assessment of the safety of a pesticide by regulatory agencies, and it is a fundamental input parameter for several pesticide transport models (Sarmah and Close, 2009). Persistence is one of the five basic properties of pesticides that can inform potential to be a pollutant with the other four properties being water solubility, volatility, sorption tendency and ionization potential (Wauchope et al., 1992). Persistence is generally determined using endpoints DT_{50} and DT_{90}, with endpoint defining the time required for the dissipation of 50 or 90% of the initial concentration of a given pesticide. Pesticide leaching and runoff models are sensitive to the degradation rate constant (k, day^{-1}) (Sarmah and Close, 2009). Accurate estimation of dissipation rate constant is essential to both ensure precise prediction with these models and validate utility as a fundamental input parameter for risk assessment models (Srinivasan et al., 2014).

Dissipation endpoints are estimated using empirical non-linear equations or mechanistic models (Sarmah and Close, 2009). The single first order model (SFO), the commonly used non-linear regression equation, is a two-parameter exponential decay model that assumes that pesticide degradation rate at any given time is directly proportional to the concentration remaining in the system (FOCUS, 2006). The SFO has been widely used for pesticide dissipation endpoints prediction (Kirksey et al., 1996; Mueller et al., 1990; Mueller et al., 2014; Mueller et al., 1999; Shaner, 2012; Shaner and Henry, 2007; Westra et al., 2014). Many factors can affect the degradation rate of pesticides; therefore, the dissipation rate has been hypothesized to be variable because soil is a heterogeneous medium (Gustafson and Holden, 1990). Thus, the SFO might not always be appropriate (Aldworth and Jackson, 2008; Srinivasan et al., 2014). Cases include when the degradation of the chemical in the soil is concentration- or time-dependent (Sarmah and Close, 2009). A systematic fitting of the SFO equation to all pesticide dissipation datasets can lead to under- or over-estimation of endpoints (Herman and Scherer, 2006; Srinivasan et al., 2014); thus, leading to poor agricultural and environmental decisions. Mojasevic et al. (1996) reported the frequent use of inaccurate SFO for describing dissipation as a major factor influencing dissipation endpoint predictions.

Alternative equations have been proposed to account for cases where the assumption of the SFO does not hold and that the SFO cannot explain dissipation. For example, in many cases a biphasic trend has been reported with an early fast decrease in pesticide concentrations followed by a slower reduction (Gustafson and Holden, 1990). Moreover, pesticide degradation has been hypothesized to occur in two or more compartments with different rate constants (Scherr et al., 2008). Reducing over- and under-estimation and improving accuracy of endpoint estimation requires the use of the most appropriate regression equations (Herman and Scherer, 2003; Herman and Scherer, 2006; Ma et al., 2004; Sarmah and Close, 2009; Sarmah and Rohan, 2011b; Srinivasan et al., 2014). The use of the Akaike information criteria (AIC) can help improve dissipation endpoint predictions by ranking models based on their approximation of the available data (Anderson, 2008; Burnham and Anderson, 2004; Burnham et al., 2011). It determines a measure of the strength of evidence for possible biological assumptions (mechanisms) associated with a given model in comparison to a set of other candidate models (Anderson, 2008).

Metolachlor, an important soil-applied herbicide for US agriculture, has been widely used globally in more than 70 crops (O'Connell et al., 1998) for many decades (Busi, 2014). Its optimal use ensures effective weed control and environmental protection. Therefore, understanding the performance of different mathematical models for predicting the dissipation endpoints of *S*-metolachlor will improve decision-making processes for growers and regulatory agencies. The objective of this research was to evaluate the performance of five mathematical models for predicting the dissipation endpoints of *S*-metolachlor.

Materials and methods

Data collection

A field experiment was conducted during the summer 2019 at the Milo J. Shult Agricultural Research & Extension Center (University of Arkansas, Fayetteville, AR 36º05.970 N and 94º10.741W) to evaluate the ability of different mathematical models to explain the dissipation of *S*-metolachlor. Soil samples were collected from 16 experimental units one day after planting (1 DAP) soybean. Twenty samples were collected randomly per plot, within the 0 and 10.2 cm depth using a sterile probe (2.2-cm diameter), to form a composite sample per plot. Moist soil samples were sieved the day of sampling using an 8-mm sieve.

The details of sample processing, spiking, incubation, extraction, and analysis are provided in chapter 4. Analytical grade *S*-metolachlor with a purity of 99.1% (Sigma-Aldrich, St. Louis, MO) was spiked and mixed into 1 kg moist soil at the equivalent of 0.9375 mg *S*-metolachlor kg^{-1} dry soil. Soil was split into two jars containing 500 g soil and incubated for 56 d. Sub-sampling were extracted for analysis of *S*-metolachlor on days 0, 1, 4, 7, 14, 28, and 56 from each jar.

S-metolachlor was analyzed using a Shimadzu GC instrument equipped with a mass spectrometer detector (TQ8040 GC-MS/MS, Shimadzu Corporation, Japan). Chromatographic separation was accomplished with an SH-Rxi-5Sil MS capillary GC column (30 m, 0.25 mm i.d., 0.25 µm). The GC oven temperature was programed as follows: 50 °C (1 min), 50 - 300 °C at 35 °C min^{-1} and finally held for 3 min. The carrier gas was helium at a constant flow rate of 1 mL min^{-1}. The injection was accomplished in a split mode with an injection volume of 1 µL and a temperature of 250 °C. The mass spectrometer detector was operated in scan mode and the temperature of the interface and ion source were 250 and 200 °C, respectively. *S*-metolachlor was monitored at the mass-to-charge ratio (m/z) of 162.15. The average retention time was 7.31 min. In total, thirty-two data points were obtained for each of the seven incubation sampling times (0, 1, 4, 7, 14, 28, and 56 days).

Modeling approach

The modeling approach used to test the performance of five mathematical models for predicting the dissipation endpoints of *S*-metolachlor followed several steps including formulation of the set of candidate models, fitting individual models to data, evaluating the significance of model parameters, model selection and ranking, goodness of fit, and prediction of dissipation endpoints.

Formulation of the set of candidate dissipation models

Data were fit to five candidate models, chosen based on their relative simplicity (2, 3, or 4 parameters) and frequent use in the scientific community (Sarmah and Close, 2009; Sarmah and Rohan, 2011b; Srinivasan et al., 2014; Zimdahl et al., 1994). The five models used to formulate the set of candidate models were the single first order kinetic (SFO) and four biphasic kinetic models (the Gustafson and Holden (GH) also called First-Order Multi-Compartment (FOMC) model (FOCUS, 2006; Gustafson and Holden, 1990), the quadratic or bi-exponential model (BEXP) (Sarmah and Close, 2009; Sarmah and Rohan, 2011a; Zimdahl et al., 1994), the first-order, double-exponential decay model (FODED) (Ma et al., 2004; Sarmah and Close, 2009; Sarmah and Rohan, 2011b; Srinivasan et al., 2014) and the first-order two-compartment (FOTC) (Hill and Schaalje, 1985; Ma et al., 2004; Sarmah and Close, 2009; Sarmah and Rohan, 2011a; Srinivasan et al., 2014).

Model 1. Single first-order kinetic

The equation of this model is a simple first-order differential equation (equation 5. 1):

$$\frac{dC}{C} = -kdt \qquad (5.\ 1)$$

According to this equation, the rate of change of the pesticide at any given time is directly proportional to the concentration. It is integrated as equation 5. 2:

$$C = C_0 * e^{-kt} \qquad (5.\ 2)$$

where C is the concentration of the herbicide in the soil at time t, C_0 is the concentration of the herbicide in the soil at time t = 0, and k is the first-order reaction rate constant (day^{-1}). Application of a logarithmic transformation to the equation provides a linear relationship. Because pesticide dissipation is fit on an empirical basis and dissipation often is not linear when plotted after a logarithmic transformation, biphasic or “two-compartment” models have been suggested, corresponding to dissipation occurring in two different soil compartments at different rate constants (Hill and Schaalje, 1985). Two-compartment models may provide a better fit to data.

Model 2. Quadratic or bi-exponential model (BEXP)

For the quadratic or bi-exponential model (Reyes and Zimdahl, 1989; Zimdahl et al., 1994), the relationship between pesticide concentration and time is described by the sum of first and second-order differential rate equations (Sarmah and Rohan, 2011a; Sarmah and Rohan, 2011b):

$$\frac{dC}{dt} = -(k_1C + k_2C^2) \tag{5. 3}$$

Integration and simplification of the equation gives equation 5. 4

$$C = \frac{k_1 * C_0}{(k_1 + k_2 * C_0) * exp(k_1 * t) - k_2 * C_0} \tag{5. 4}$$

where k_1 is the first-order rate constant (day^{-1}), k_2 is the second-order rate constant (day^{-1}), t is the time, C is the concentration at time t, and C_0 is the concentration at $t = 0$. When $k_2 = 0$ equation 5.3 reduces to equation 5. 1.

Model 3. First-order, double-exponential decay (FODED)

The first-order, double-exponential decay equation (equation 5. 5) models pesticide dissipation occurring in two separate compartments.

$$C = C_s * exp(-k_1 * t) + C_b * exp(-k_2 * t) \tag{5. 5}$$

where C_s and C_b are constants representing herbicide concentrations initially distributed between two pools (e.g. solution phase and sorbed phase) with dissipation rate constants of k_1 and k_2, respectively. This model assumes the solution phase to be accessible to microorganisms and showing a faster degradation while the second phase, sorbed to soil particles, showed a slower degradation (usually $k_1 > k_2$) (Sarmah and Rohan, 2011a). The sum of C_s and C_b gives the total amount of applied pesticide. The model has been used by several researchers in the past (Sarmah and Close, 2009; Sarmah and Rohan, 2011a; Srinivasan et al., 2014).

Model 4. First-order, two-compartment (FOTC)

Used initially for description of deltamethrin dissipation in soil (Hill and Schaalje, 1985), the FOTC is a two-compartment model that describes the fast and slow dissipation of pesticides. It assumes that dissipation occurs in two compartments as “fast” surface loss in deposited residue and “slow” dissipation in a retained residue compartment. The two-loss processes and the transfer between compartments are assumed to be first-order (Sarmah and Close, 2009; Sarmah and Rohan, 2011a; Srinivasan et al., 2014). Equations are written as equations 5. 6 and 5. 7:

$$\frac{dC}{dt} = -(k_1 + k_R)C_1 \tag{5. 6}$$

$$\frac{dC}{dt} = k_R C_1 - k_2 C_2 \tag{5. 7}$$

$$C = C_1 + C_2 \tag{5. 8}$$

where C_1 and C_2 are the concentrations of the pesticide in the fast and slow compartments, respectively, and C is the total concentration of the pesticide. Integration and transformation of the equation gives equation 5. 9

$$C = C_0 * exp\{-(k_1 + k_R) * t\} + C_0 \frac{k_R}{k_1 + k_R - k_2}\{exp(-k_2 * t) - exp[-(k_1 + k_R) * t]\} \tag{5. 9}$$

where C_0 is the concentration at t = 0, k_R (usually >0) is the retention rate constant of pesticide transfer between the fast and slow dissipation compartments, k_1 is the rate constant of the “fast” dissipation compartment, and k_2 is the rate constant of the “slow” compartment.

Model 5. Gustafson and Holden

Gustafson and Holden (1990) considered the spatial variability observed in soil and introduced an infinite-compartment model that could be representative of spatial variability of dissipation in the soil. Assuming a continuum of spatially segregated compartments with each one showing a simple first-order dissipation with a rate k, authors derived a three-parameter equation which was applicable to both field and laboratory studies (Gustafson and Holden, 1990). The initial equation was equation 5. 10

$$C = C_0(1 + \beta t)^{-\alpha} \tag{5. 10}$$

where C_0 is the concentration at $t = 0$, α is dimensionless, is β has the units of the rate constant (day^{-1}). An alternative form of the equation was proposed by FOCUS (2006) as equation 5. 11:

$$C = \frac{C_0}{(\frac{t}{\theta}+1)^{\alpha}} \tag{5. 11}$$

where θ is simply the reciprocal of β in equation 5. 10 (FOCUS, 2006). The equation, also called the first-order, multiple-compartment (FOMC), was used by previous researchers for studying dissipation of several pesticides (Carpio et al., 2021; Chen et al., 2019; Etzerodt et al., 2008; Gluhar et al., 2019; Mantzos et al., 2016; Vargas-Perez et al., 2019).

Model fitting, selection and ranking

The formulated set of candidate models were fitted separately, using the nonlinear least squares regression (nls) of R version 4.0.0 (R Core Team, 2020), to *S*-metolachlor concentrations over time, calculated as a percent of initial concentration, with the initial sub-sampling (day 0 after spiking) representing 100%. According to FOCUS (2006), model parameters not significantly different from zero are either very uncertain or the model is not adequate for the data. For that reason, model parameters for each model in the set of candidate models were evaluated for significant difference compared to zero. Only models with parameters all significantly different from zero were retained for model ranking, goodness of fit evaluation and dissipation endpoints predictions. Model selection and rankings were made using information-theoretic criterion (AIC) (Anderson, 2008; Burnham and Anderson, 2001; Burnham and Anderson, 2004) with the AICcmodavg package (Mazerolle, 2019). Second-order bias corrected Akaike's Information Criterion (AICc) (equation 5. 12), AICc differences (Δ_i) (equation 5. 13), weight of evidence in favor of each model or model probability (w_i) (equation 5. 14) and cumulative weight of evidence (Cum. w_i) were generated using the aictab function in the AICcmodavg package in R. The model with the smallest AICc and the largest w_i is the model that provides the most support to the dataset within the set of candidate models (Anderson, 2008; Burnham and Anderson, 2001; Burnham and Anderson, 2004; Burnham et al., 2011).

$$AICc = -2\log\left(L\left(\hat{\theta}\right)\right) + 2K(\frac{n}{n-K-1}) \tag{5. 12}$$

$$\Delta_i = AICc_i - AICc_{min} \tag{5. 13}$$

$$w_i = \frac{\exp(-\Delta_i/2)}{\sum_{r=1}^{R} exp(-\Delta_r/2)}) \tag{5. 14}$$

$$\sum_i^R w_i = 1 \tag{5. 15}$$

where K is the number of estimated parameters, n is the sample size and $L\left(\hat{\theta}\right)$ is the maximum likelihood estimate for the model (Anderson, 2008; Burnham and Anderson, 2001).

Model goodness of fit.

The difference between each parameter of a given model and zero was evaluated using a t-test within R software (p-value ≤ 0.05). The models' performance at describing data was also assessed using statistical indices including model bias, root mean square error (RMSE), mean absolute error (MAE), and Nash-Sutcliffe efficiency (NSE). Measures of the average difference between measured and predicted % of *S*-metolachlor concentration remaining in soil were calculated using equations 16-19.

Bias (equation 5. 16) is a measure of the average difference between measured and predicted values. The model is considered to under-predict when the bias is positive and over-predict on average when the bias is negative (Wallach et al., 2006).

$$Bias = \frac{1}{N}\sum_{i=1}^{N}(Y_i - \hat{Y}_i) \qquad (5.\ 16)$$

where Y_i is the measured value for situation i and $\hat{Y}_i$ is the corresponding value predicted by the model. N is the total number of observations.

Root mean square error (RMSE) and mean absolute error (MAE) of each model were calculated using equation 5. 17 and 5. 18, respectively.

$$RMSE = \sqrt{\frac{1}{N}\sum_{i=1}^{N}(Y_i - \hat{Y}_i)^2} \qquad (5.\ 17)$$

$$MAE = \frac{1}{N}\sum_{i=1}^{N}|Y_i - \hat{Y}_i| \qquad (5.\ 18)$$

Smaller RMSE and MAE values indicate a better model fit to the data because the predicted values are closer to the observed values.

As a normalized statistic, the Nash-Sutcliffe efficiency (NSE) determines the relative magnitude of the residual variance compared to the measured data variance (Moriasi et al., 2007). NSE was calculated using equation 5. 19.

$$NSE = 1 - \frac{\sum_{i=1}^{N}(Y_i - \hat{Y}_i)^2}{\sum_{i=1}^{N}(Y_i - \bar{Y})^2} \qquad (5.\ 19)$$

where $\bar{Y}$ is the mean observed value. The closer the values are to 1, the more accurate the predictions. A perfect model has NSE = 1 as $Y_i = \hat{Y}_i$ (Wallach et al., 2006)

Calculation of dissipation endpoints

Dissipation endpoints derived from the SFO model were calculated using equation 5. 20.

$$DT_x = \frac{\ln(\frac{100}{100-x})}{k} \tag{5. 20}$$

where X is the is the percent dissipation, DT_x is the time required for X% dissipation of the herbicide and k the rate constant. Prediction of the time necessary for a pesticide to decline by 50% using the SFO is a constant. In other words, using the SFO model, the time required for a pesticide to decline from 100% to 50% is the same as the time required to decline from 50% to 25%. Despite fit of data to the equation, the biphasic nature of dissipation observed in some studies might suggest the use of other equations.

Dissipation endpoints derived from the FOMC model were calculated using equation 5.21.

$$DT_x = \theta * \left((\frac{100}{100-x})^{(\frac{1}{\alpha})} - 1 \right) \tag{5. 21}$$

where X, θ, and α were previously defined.

FODED

No analytical equation exists for the endpoints of the FODED (FOCUS, 2006). The time required for X% dissipation of *S*-metolachlor (DT_X, t_X) was predicted by plugging the optimized values of C_s, C_b, k_1 and k_2 (obtained from fitting each model) into equation 5. 5 and solving equation 5. 22 for t_X by using the uniroot() function in R within a 0 - 56 days interval of dissipation.

$$X + C_s * exp(-k_1 * t_X) + C_b * exp(-k_2 * t_X) - C_{est} = 0 \qquad (5.\ 22)$$

where X is the same as defined earlier, C_{est} is the predicted value of % *S*-metolachlor initial concentration for each replicate.

Dissipation endpoints comparisons

S-metolachlor dissipation endpoints for 25, 50, 75, and 90% dissipation were compared among models using the glimmix procedure in SAS 9.4 (SAS Institute Inc., Cary, NC, USA). Treatments means were separated at $P \leq 0.05$ using the Fisher's protected LSD.

Results and Discussion

Significance of optimized parameters

S-metolachlor dissipation data were fit to all five non-linear regression models (Fig. 5. 1). The SFO optimized parameters C_0 (initial concentration) and k (rate constant) were different from zero ($P \leq 0.05$) (Table 5. 1). Similarly, the FODED optimized parameters C_s (herbicide concentration initially distributed in the solution phase) and C_b (herbicide concentration initially distributed in the sorbed phase), k_1 and k_2 (herbicide dissipation rate constants) were all different from zero ($P \leq 0.05$). Likewise, the FOMC model's optimized parameters C_0 (initial concentration), the dimensionless α and the parameter θ (reciprocal of initial β that has units of the rate constant) were all different from 0 ($P \leq 0.05$).

On the contrary, optimized parameters of the BEXP model were not all different from zero. The first-order-rate constant (k_1) was not different from zero ($P = 0.098592$). Likewise, optimized parameters for the FOTC model were not all different from 0. Parameters C_0 (initial concentration) and k_2 (rate constant of the "slow" compartment) were different from 0 in both cases ($P < 0.05$). However, the retention rate constant of pesticide transfer between the fast and slow dissipation compartments (k_R), and the rate constant of the "fast" dissipation compartment (k_1) were not significantly different from zero ($P > 0.05$). According to FOCUS (2006), models with non-significant parameters are either uncertain or inappropriate for dissipation data. As recommended by the FOrum for the Co-ordination of pesticide fate models and their Use (FOCUS), only models with significant parameters SFO, FODED, and FOMC were selected in this study as candidate models for making inferences about *S*-metolachlor dissipation endpoints.

The BEXP model, dividing the dissipation pattern into two parallel compartments, fast and slow, was not used for *S*-metolachlor dissipation endpoints prediction. The BEXP was previously reported to be unlikely to converge when data are well described with the SFO model (Herman and Scherer, 2006; Scherr et al., 2008; Srinivasan et al., 2014). In their study deriving sulfamethoxazole dissipation endpoints in pasture soils using first order and biphasic kinetic models, Srinivasan et al. (2014) reported inconsistency in data fitting with the BEXP in comparison to the two other 4-parameter models FODED and FOTC.

Model diagnostic

Residual plots depict the deviation of data from zero for each of the three models (SFO, FODED, and FOMC) (Fig. 5. 1). The SFO deviated from the horizontal zero line compared to other models. The curvature displayed by SFO revealed that the SFO was the least appropriate to describe *S*-metolachlor dissipation in the set of three candidate models.

Model ranking and selection

Model selection and ranking revealed that the FODED and FOMC provided the most support to data within the set of candidate models (Table 5. 2). The FODED model was ranked top model with the lowest AICc (1586) and the largest model probability weight of 0.99 among the set of three candidate models. The FODED model was followed by the FOMC model with an AICc (1596) and a probability of 0.01. The second-order bias corrected Akaike's Information Criterion (AICc), estimator of the Kullback-Leibler information, ranks models based on their approximation of the biological process (Anderson, 2008; Burnham and Anderson, 2001). Greater model support is associated with a smaller AICc value.

Model goodness of fit

According to Wallach et al. (2006), the bias, as a measure of the average difference between measured and predicted values, is considered to under-predict when the bias is positive and over-predict when the bias is negative. Model biases for the three candidate models varied between -0.04 and 3.08. The RMSE values ranged between 8.42 and 11.43, MAE were between 5.08 and 9.16, and the NSE values varied between 0.88 and 0.93 (Table 5. 3). The SFO bias is positive with a value of 3.08. These positive bias values of the SFO model revealed that this model under-predicted *S*-metolachlor dissipation in the present study. Figure 5. 2 reveals that the SFO model under-predicted *S*-metolachlor dissipation later during the experiment with larger errors compared to the other two biphasic models (Figs. 5. 2, 5. 3). The SFO displayed the largest RMSE (11.43), MAE (9.16), and smallest NSE (0.88) values within the set of three candidate models (Table 5. 3) and this result is in agreement with the Akaike's Information Criterion (AICc) selection that showed that the FOMC and FODED models were superior to the SFO model. The NSE values calculated for both biphasic models are identical (Table 5. 3). Their bias values are near zero, which may be the consequence of very small model errors for the two biphasic models. The FODED, ranked top model by the AIC model selection approach, also showed the smallest RMSE and MAE.

Dissipation of *S*-metolachlor in the present study was described satisfactorily by the three candidate models (Tables 5. 1). However, results showed that the two biphasic models provided the most support to data compared to the SFO (Tables 5. 2, 5. 3; Figs. 5. 1, 5. 2). Other authors also reported that biphasic models provided greater support to dissipation datasets than the SFO (Srinivasan et al., 2014). Sarmah and Rohan (2011) reported RMSE values between 0.41 and 26.08 while modeling the dissipation of 4-n-nonylphenol and bisphenol-A. Srinivasan et al. (2014) reported RMSE 0.6 to 23.9 in deriving dissipation endpoints of sulfamethoxazole using different models. As a normalized statistic that determines the relative magnitude of the residual variance compared to the measured data variance, NSE values > 0.59 were reported by Pullan et al. (2016) to indicate a good model performance for predictions of pesticide concentrations.

The FODED model assumes that only the solid-water phase, accessible to microorganisms, shows a faster degradation while the phase sorbed to soil particles is slowly degraded (Sarmah and Rohan, 2011a). The FOMC model has some mechanistic background

(Gustafson and Holden, 1990; Srinivasan et al., 2014) as its accounts accounted for soil heterogeneity by dividing it into a large number of sub-compartments each with a different first-order degradation rate constant (Gustafson and Holden, 1990). In previous studies the FOMC better explained the behavior of propoxycarbazone in soil and water than did the SFO model (Vargas-Perez et al., 2019).

The good fit provided to dissipation data by biphasic models might be due to the decrease, with time, of the fraction of pesticide available for degradation, which can induce a decrease in the rate of the herbicide diffusion to organisms for degradation at the later stage of the dissipation process (Scow, 1993). The activity of degrading soil microorganisms may also decrease with time due to a limited availability of nutrient and carbon sources under laboratory conditions (Lucas and Jones, 2006; Scherr et al., 2008). Seasonal changes in temperature and/or moisture can also change degradation patterns for dissipation studies under field conditions (FOCUS, 2006).

Comparisons of dissipation endpoints

Mean comparison revealed significant differences between *S*-metolachlor dissipation endpoints predicted by SFO, FOMC and FODED at 25, 50, 75, and 90% dissipation ($P \leq 0.05$). In all four cases (25, 50, 75 and 90%) endpoints predicted by the SFO were different from those predicted by the FOMC and FODED ($P \leq 0.05$). However, there was no difference between dissipation endpoints predicted by FOMC and FODED ($P > 0.05$). At 25 and 50% *S*-metolachlor dissipation SFO showed greater endpoint values of 2.5 and 6.1 days, respectively, but the endpoints predicted by the FOMC and FODED were 1.4 and 1.6 days, and 4.3 and 4.3 days for 25 and 50% dissipation, respectively (Fig. 5. 3). On the contrary, dissipation endpoints predicted by the SFO were smaller than those predicted by the two other models at 75 and 90% dissipation. The SFO predicted 12.2 and 20.2 days for 75 and 90% dissipation, respectively, while FOMC and FODED predicted 14.6 and 15 days for 75% dissipation and 53.3 and 53.3 days for 90% dissipation, respectively.

The gap between SFO and the FOMC and FODED predictions increased with increasing time of dissipation (Fig. 5. 3). This trend supported results obtained in bias calculations that reported under-prediction of the dissipation by the SFO (Table 5. 3, Fig. 5. 2). Similar results had previously been reported in the literature. Herman and Scherer (2006) reported large systematic deviations from experimental data especially apparent at low residues around the DT_{90} values. Likewise, Zimdahl et al. (1994) reported that the SFO predicted a faster dissipation later in the degradation process and ignored small residues remaining late in the dissipation process. According to Gustafson and Holden (1990), the assumption of linearity of the SFO is generally violated to a wide degree by the time 90% of the material has dissipated. The FOMC, as a simple non-linear first-order kinetic model, accounts for soil heterogeneity or spatial variability, provides an excellent fit to both laboratory and field dissipation data (Gustafson and Holden, 1990).

Conclusion

Five dissipation kinetics models were tested for their performance to predict *S*-metolachlor dissipation in soil samples collected from the field, spiked and incubated in a growth chamber. Results from this study showed that the BEXP and FOTC models were not acceptable for data analysis because their parameters were not all different from zero. The three models SFO, FOMC and FODED had all optimized parameters different from zero and were used for making inference *S*-metolachlor dissipation endpoints. In comparison to the two biphasic models, the SFO provided the least support to data and predominantly under-predicted *S*-metolachlor residues during the later stages of the dissipation process. The SFO predicted larger dissipation endpoints, or slower degradation, for 25 and 50% dissipation compared to FOMC and FODED. On contrary, it predicted smaller dissipation endpoints, or faster degradation, than the two biphasic models at 75 and 90% dissipation. Biphasic models were superior and predicted more accurate dissipation endpoints. However, because the SFO is a simple model with only two parameters to be estimated from data, it can still be an acceptable model for the prediction of half-lives when data points are limited. The gap between half-lives predicted by the SFO and biphasic models was smaller than that between endpoints for greater *S*-metolachlor dissipation such as 75% and 90%. Caution might be required when making inference about 90% dissipation of pesticides in the soil using the SFO. For datasets with a greater number of data points the use of biphasic models FOMC (3 parameters) and the FODED model (4 parameters) might provide more accurate predictions of pesticide dissipation in the soil.

References

Aldworth J, Jackson S (2008) Statistical tools for determining appropriate selection of regression models for analysis of environmental fate datasets. Pest Management Science 64: 536-543.

Anderson DR (2008) Model Based Inference in the Life Sciences: A Primer on evidence.

Burnham K, Anderson D (2001) Kullback-Leibler information as a basis for strong inference in ecological studies. Wildlife Research 28: 111-119.

Burnham K, Anderson D (2004) Multimodel inference - understanding AIC and BIC in model selection. Sociological Methods & Research 33: 261-304.

Burnham K, Anderson D, Huyvaert K (2011) AIC model selection and multimodel inference in behavioral ecology: some background, observations, and comparisons. Behavioral Ecology and Sociobiology 65: 23-35.

Busi R (2014) Resistance to herbicides inhibiting the biosynthesis of very-long-chain fatty acids. Pest Management Science 70: 1378-1384.

Carpio MJ, Marin-Benito JM, Sanchez-Martin MJ, Rodriguez-Cruz MS (2021) Accelerated dissipation of two herbicides after repeated application in field experiments with organically-amended soil. Agronomy-BASEL 11.

Chen JF, Jiang XS, Tong TL, Miao S, Huang J, Xie SG (2019) Sulfadiazine degradation in soils: Dynamics, functional gene, antibiotic resistance genes and microbial community. Science of the Total Environment 691: 1072-1081.

Etzerodt T, Mortensen AG, Fomsgaard IS (2008) Transformation kinetics of 6-methoxybenzoxazolin-2-one in soil. Journal of Environmental Science and Health Part B-Pesticides Food Contaminants and Agricultural Wastes 43: 1-7.

Focus (2006) Guidance document on estimating persistence and degradation kinetics from environmental fate studies on pesticides in EU registration. Pages 434 in E.D.R.S. Report of the FOCUS Work Group on Degradation Kinetics, ed.

Gluhar S, Kaurin A, Grubar T, Prosen H, Lestan D (2019) Dissipation of mecoprop-P, isoproturon, bentazon and *S*-metolachlor in heavy metal contaminated acidic and calcareous soil before and after EDTA-based remediation. Chemosphere 237: 9.

Gustafson D, Holden L (1990) Nonlinear pesticide dissipation in soil: A new model based on spatial variability. Environmental Science & Technology 24: 1032-1038.

Herman RA, Scherer PN (2003) Comparison of linear and nonlinear regression for modeling the first-order degradation of pest-control substances in soil. Journal of Agricultural and Food Chemistry 51: 4722-4726.

Herman RA, Scherer PN (2006) Fit of four curve-linear models to decay profiles for pest control substances in soil. Journal of Agricultural and Food Chemistry 54: 4343-4349.

Hill B, Schaalje G (1985) A 2-compartment model for the dissipation of deltamethrin in soil. Journal of Agricultural and Food Chemistry 33: 1001-1006.

Kirksey K, Hayes R, Krueger W, Mullins C, Mueller T (1996) Clomazone dissipation in two Tennessee soils. Weed Science 44: 959-963.

Lucas SD, Jones DL (2006) Biodegradation of estrone and 17 beta-estradiol in grassland soils amended with animal wastes. Soil Biology & Biochemistry 38: 2803-2815.

Ma Q, Rahman A, Holland P, James T, McNaughton D (2004) Field dissipation of acetochlor in two New Zealand soils at two application rates. Journal of Environmental Quality 33: 930-938.

Mojasevic M, Helling CS, Gish TJ, Doherty MA (1996) Persistence of seven pesticides as influenced by soil moisture. J. Environ Sci Health B31:469–476.

Mantzos N, Karakitsou A, Nikolaki S, Leneti E, Konstantinou I (2016) Dissipation and transport of quizalofop-p-ethyl herbicide in sunflower cultivation under field conditions. Environmental Science and Pollution Research 23: 3481-3490.

Mazerolle M (2019) AICcmodavg: Model selection and multimodel inference based on (Q)AIC(c).

Moriasi DN, Arnold, JG, Van Liew MW, Bingner RL, Harmel RD, Veith TL (2007) Model evaluation guidelines for systematic quantification of accuracy in watershed simulations. Transactions of the ASABE 50: 885-900.

Mueller T, Banks P, Bridges D (1990) Dissipation of flurtamone in 3 Georgia soils. Weed Science 38: 411-415.

Mueller T, Boswell B, Mueller S, Steckel L (2014) Dissipation of fomesafen, saflufenacil, sulfentrazone, and flumioxazin from a Tennessee soil under field conditions. Weed Science 62: 664-671.

Mueller T, Shaw D, Witt W (1999) Relative dissipation of acetochlor, alachlor, metolachlor, and SAN 582 from three surface soils. Weed Technology 13: 341-346.

O'Connell P, Harms C, Allen J (1998) Metolachlor, *S*-metolachlor and their role within sustainable weed-management. Crop Protection 17: 207-212.

R Core Team R (2020) R: A language and environment for statistical computing. Vienna, Austria: R Core Team (2020).

Reyes CC, Zimdahl RL (1989) Mathematical-description of trifluralin degradation in soil. Weed Science 37: 604-608.

Scow KM (1993) Effect of sorption-desorption and diffusion processes on the kinetics of biodegradation of organic chemicals in soil. SSSA Special Publication No. 32: 73-114.

Sarmah A, Close M (2009) Modelling the dissipation kinetics of six commonly used pesticides in two contrasting soils of New Zealand. Journal of Environmental Science and Health Part B-Pesticides Food Contaminants and Agricultural Wastes 44: 507-517.

Sarmah AK, Rohan M (2011a) Evaluation of four mathematical models to describe dissipation kinetics of 4-n-nonylphenol and bisphenol-A in groundwater-aquifer material slurry. Journal of Environmental Monitoring 13: 157-166.

Sarmah AK, Rohan M (2011b) Evaluation of four mathematical models to describe dissipation kinetics of 4-n-nonylphenol and bisphenol-A in groundwater-aquifer material slurry. Journal of Environmental Monitoring 13: 157-166.

Scherr FF, Sarmah AK, Di HJ, Cameron KC (2008) Modeling degradation and metabolite formation kinetics of estrone-3-sulfate in agricultural soils. Environmental Science & Technology 42: 8388-8394.

Shaner D (2012) Field dissipation of sulfentrazone and pendimethalin in Colorado. Weed Technology 26: 633-637.

Shaner D, Henry W (2007) Field history and dissipation of atrazine and metolachlor in Colorado. Journal of Environmental Quality 36: 128-134.

Srinivasan P, Sarmah A, Rohan M (2014) Deriving sulfamethoxazole dissipation endpoints in pasture soils using first order and biphasic kinetic models. Science of the Total Environment 488: 146-156.

Vargas-Perez M, Gonzalez FJE, Frenich AG (2019) Evaluation of the behaviour of propoxycarbazone herbicide in soils and water under different conditions. Post-targeted study. Ecotoxicology and Environmental Safety 183.

Wallach D, Makowski D, Jones J (2006) Working with dynamic crop models: evaluation, analysis, parameterization, and applications: ELSEVIER. Pp. 447.

Wauchope RD, Buttler TM, Hornsby AG, Augustijnbeckers PWM, Burt JP (1992) The SCS ARS CES pesticide properties database for environmental decision-making. Reviews of Environmental Contamination and Toxicology 123: 1-155.

Westra E, Shaner D, Westra P, Chapman P (2014) Dissipation and leaching of pyroxasulfone and *S*-metolachlor. Weed Technology 28: 72-81.

Zimdahl R, Cranmer B, Stroup W (1994) Use of empirical equations to describe dissipation of metribuzin and pendimethalin. Weed Science 42: 241-248.

Tables and Figures

Table 5. 1**.** Five candidate models parameters' optimized values, standard errors, t values and significance levels from a field experiment conducted during the summer 2019 at the Milo J. Shult Agricultural Research & Extension Center (University of Arkansas, Fayetteville, AR 36º05.970 N and 94º10.741W) to evaluate the performance of five mathematical models for predicting the dissipation endpoints of *S*-metolachlor. Soil samples collected in the field were spiked and incubated in the laboratory. Final spiked concentration of 0.9375 mg kg^{-1} dry weight soil

Model[1]	Parameters	Estimate	Std. Error[2]	t value	P(>|t|)[3]
SFO	C_0	94.649	1.558	60.76	<2e-16***
	k	0.113	0.005	22.60	<2e-16***
FOMC	C_0	100.796	1.433	70.35	<2e-16***
	θ	3.733	0.631	5.915	1.27E-08***
	α	0.869	0.080	10.85	<2e-16***
BEXP	C_0	100.687	1.383	72.79	<2e-16***
	k_1	-0.011	0.007	-1.66	0.0986
	k_2	0.002	0.0002	13.88	<2e-16***
FODED	C_s	67.640	4.114	16.44	<2e-16***
	C_b	32.396	4.183	7.75	3.55e-13 ***
	k_1	0.262	0.028	9.44	<2e-16***
	k_2	0.022	0.004	4.99	1.20e-06 ***
FOTC	C_0	68.175	4.124	16.53	< 2e-16 ***
	k_1	3.002	12.152	0.25	0.805
	k_2	0.022	0.004	5.05	9.24e-07 ***
	k_R	2.735	12.128	0.23	0.822

[1] SFO: single first-order kinetic, FOMC: Gustafson and Holden or First-order, multi-compartment (FOMC), BEXP: quadratic or bi-exponential model, FODED: first-order, double-exponential decay, and FOTC: first-order two components.

[2] Std. Error: standard error

[3] Asterisks (***) next to p-value (labelled Pr(>|t|)) indicate parameter estimates significantly different from 0 ($\alpha = 0.05$).

Table 5. 2. Model ranking using AICc, Δ_i and w_i for *S*-metolachlor concentration evolution with time (in spiked soils) in soils collected from a field experiment conducted during the summer 2019 at the Milo J. Shult Agricultural Research & Extension Center (University of Arkansas, Fayetteville, AR 36º05.970 N and 94º10.741W).

Model[1]	AICc[2]	Δi[3]	w_i[4]	Cum.Wi[5]	LL[6]
FODED	1586.54	0	0.99	0.99	-788.13
FOMC	1595.61	9.07	0.01	1	-793.71
SFO	1717.94	131.40	0	1	-855.92

[1] SFO: single first-order kinetic, FOMC: Gustafson and Holden or First-order, multi-compartment (FOMC) and FODED: first-order, double-exponential decay. Models are ordered from lowest to highest AICc with the lowest AICc being the model with the most support to *S*-metolachlor dissipation data and considered the best model,

[2] AICc, is the second-order bias corrected Akaike's Information Criterion

[3] Δi is a measure of the distance between each model in the set of candidate models and the top model

[4] w_i is the probability of each model in the set of candidate models

[5] Cum.Wi is the cumulative weight

[6] LL, is the log-likelihood of the model parameters

Table 5. 3. SFO, FOMC, and FODED goodness of fit to *S*-metolachlor dissipation data obtained from of *S*-metolachlor added to soils collected from a field experiment conducted during the summer 2019 at the Milo J. Shult Agricultural Research & Extension Center (University of Arkansas, Fayetteville, AR 36º05.970 N and 94º10.741W).

Model[1]	**Bias**	**RMSE**[2]	**MAE**	**NSE**
FODED	-0.04	8.42	5.08	0.93
FOMC	0.05	8.64	5.41	0.93
SFO	3.08	11.43	9.16	0.88

[1] SFO: single first-order kinetic, FOMC: Gustafson and Holden or First-order, multi-compartment (FOMC), and FODED: first-order, double-exponential decay.

[2] RMSE, MAE, and NSE are the root mean square error, mean absolute error, and Nash-Sutcliffe efficiency, respectively.

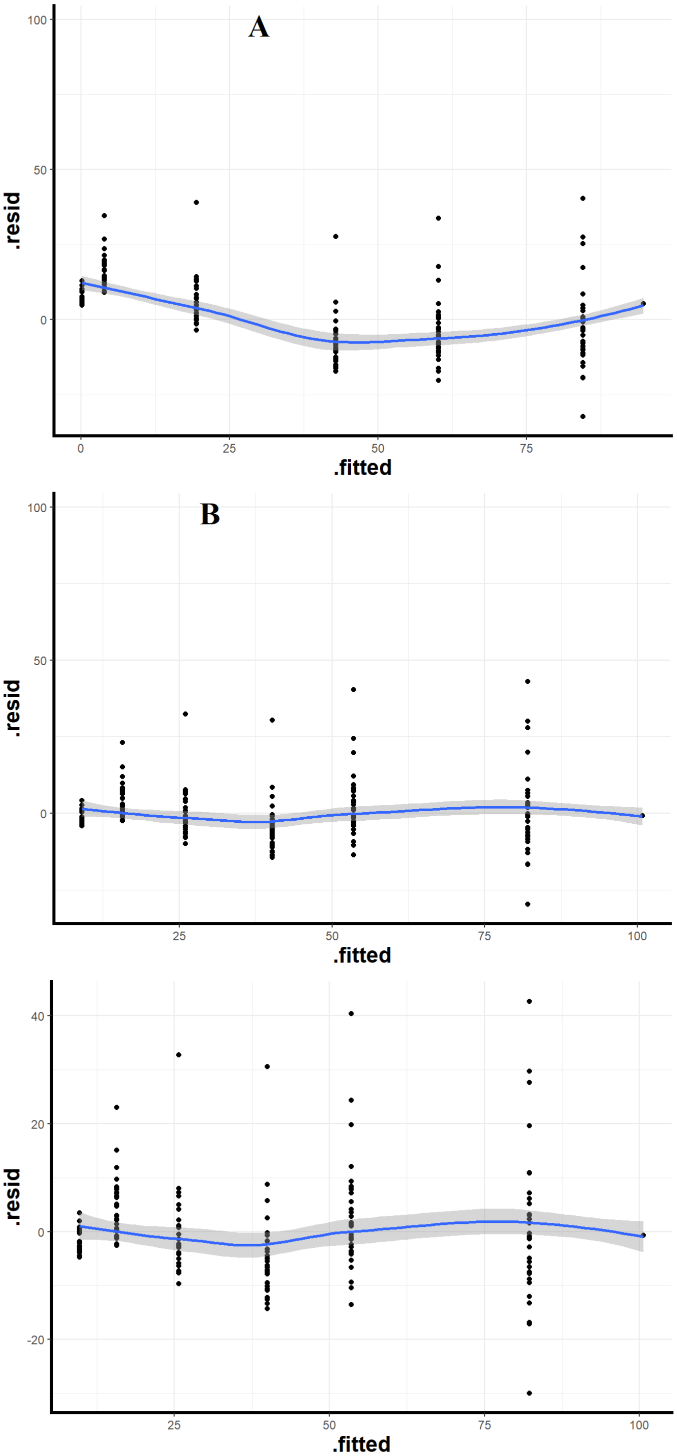

Figure 5. 1. Residual plots for *S*-metolachlor dissipation kinetics (spiked at 0.9375 mg kg^{-1} dry weight soil) from soils samples collected at 1 DAP from a field experiment conducted during the summer 2019 at the Milo J. Shult Agricultural Research & Extension Center (University of Arkansas, Fayetteville, AR 36º05.970 N and 94º10.741W). A: SFO: single first-order kinetic, B: FOMC: Gustafson and Holden or First-order, multi-compartment (FOMC), C: FODED: first-order, double-exponential decay.

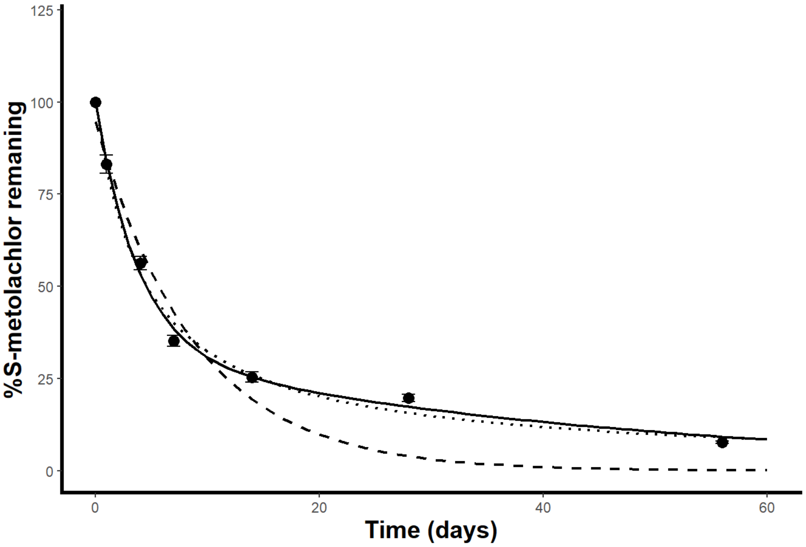

Figure 5. 2. Dissipation kinetics of *S*-metolachlor in soils (0.9375 mg kg^{-1} dry weight soil) collected from a field experiment conducted during the summer 2019 at the Milo J. Shult Agricultural Research & Extension Center (University of Arkansas, Fayetteville, AR 36º05.970 N and 94º10.741W), to evaluate the performance of five mathematical models for predicting the dissipation endpoints of *S*-metolachlor. Error bars indicate standard error. Single first-order kinetic (dashed line), First-order, multi-compartment (dotted line) and first-order, double-exponential decay (solid line). Error bars indicate standard error.

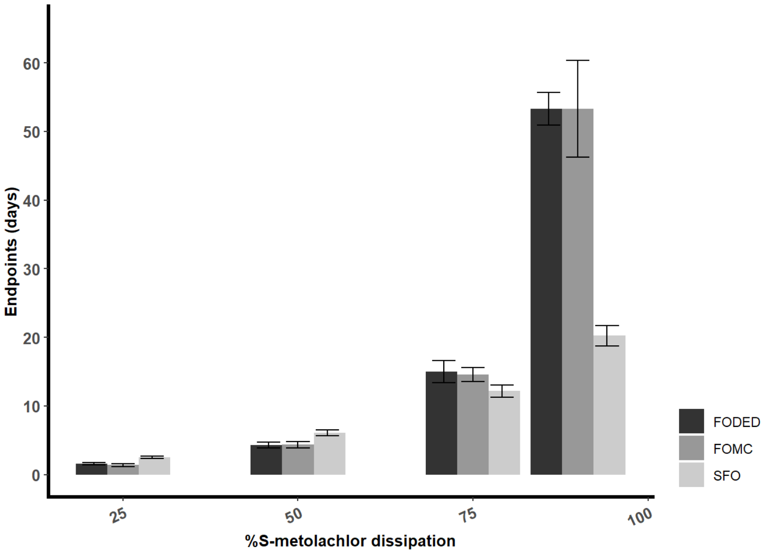

Figure 5. 3. *S*-metolachlor dissipation endpoints prediction in soils (0.9375 mg kg^{-1} dry weight soil) collected from a field experiment conducted during the summer 2019 at the Milo J. Shult Agricultural Research & Extension Center (University of Arkansas, Fayetteville, AR 36º05.970 N and 94º10.741W). Error bars indicate standard error. SFO: Single first-order kinetic, FOMC: First-order, multi-compartment, FODED: First-order, double-exponential decay.

Transpiration responses of herbicide-resistant and susceptible Palmer amaranth [*Amaranthus palmeri* (S.) Wats.] to progressively drying soil

Abstract

Drought events are predicted to become more prevalent in the future. Evaluating the performance of herbicide-resistant and susceptible weed ecotypes to progressive drought can provide insights into whether the resistance trait(s) increased or reduced the fitness of the resistant population. Two separate greenhouse experiments were conducted between January and May 2021 to evaluate the drought tolerance differences between *S*-metolachlor-resistant and susceptible Palmer amaranth accessions and between glyphosate-resistant and susceptible plants differing by the number of 5-enolpyruvylshikimate-3-phosphate synthase (*EPSPS*) gene copy number. The accessions used were: *S*-metolachlor-resistant (17TUN-A), a susceptible standard (09CRW-A), and glyphosate-resistant (21.5 to 164.7 gene *EPSPS* copies) and glyphosate-susceptible (2.7 to 10 *EPSPS* copies) plants from accession 16CRW-D. Daily transpiration of each plant was measured. The daily transpiration rate of drought-stressed plants was converted to normalized transpiration ratio (NTR) using a double-normalization procedure. The daily soil water content was expressed as a fraction of transpirable soil water (FTSW). The threshold FTSW (FTSW_{cr}), after which NTR decreases linearly, was estimated using a two-segment linear regression analysis. The data showed differences between *S*-metolachlor- resistant and -susceptible accessions ($P \leq 0.05$), while no differences ($P > 0.05$) were detected between glyphosate-resistant and glyphosate-susceptible plants. The FTSW remaining in the soil at the breakpoint for the *S*-metolachlor-susceptible accession (09CRW-A) was 0.17±0.007. The FTSW remaining in the soil at the breakpoint for the *S*-metolachlor-resistant accession (17TUN-A) was 0.23±0.004. The glyphosate-resistant plants with an increase in *EPSPS* gene copy number were not more

drought-tolerant than the glyphosate-susceptible without an increase in *EPSPS* gene copy. But, the *S*-metolachlor-resistant accession showed a greater drought tolerance than the susceptible accession (09CRW-A). However, tolerance to drought may not only be due to *S*-metolachlor resistance.

Introduction

Drought can negatively affect physiological and biochemical processes and provoke yield reduction (Khan et al., 2018). As the world's largest exporter of major grain and oilseed crops, the United States accounted for 49% and 46% of total global exports of corn (*Zea mays* L.) and soybean [*Glycine max* (L.) Merr.], respectively, between 2008 and 2010 (Boyer et al., 2013). However, the occurrence of the 'flash drought' event in the US in 2012 disrupted the production of major crops and affected international grain markets (Boyer et al., 2013). This most detrimental drought of the past century in the US Midwest had a greater impact on agricultural systems (crop and grassland) than on forests (Jin et al., 2019). Unfortunately, drought frequency and severity are likely to increase in the future (Jin et al., 2019; Liu and Basso, 2020; Lobell et al., 2020). Consequently, yields of crops such as corn and soybean are predicted to decline by 8-21% (Bowling et al., 2020). Under rainfed conditions, seasonal water supply and soil water holding capacity are major determinants of crop productivity (Kropff and van Laar, 1993). The largest corn and soybean production area, the US Corn Belt, is 92% rainfed; thus, vulnerable to climate variability and droughts (Kimm et al., 2020). Also, under irrigated conditions, irrigation does not always fully supply crop water demand during drought (Grassini et al., 2015).

Evapotranspiration (ET), a combination of water used by plants via transpiration and direct soil water loss via evaporation, provides valuable information about soil moisture availability (Yang et al., 2021). Plant transpiration is a key component of soil water consumption that needs to be understood; it is a crucial physiological process and is closely related to biomass production (Li et al., 2020). Under drought conditions, plants can sense water stress around the roots and respond by sending chemical signals such as abscisic acid (ABA) to close stomata (Saradadevi et al., 2017). The determination of the threshold value for the initiation of stomatal closure is critical for understanding plant physiological responses to drought (Sinclair, 2012). However, a major challenge in studying plant responses to soil drying is the ability to characterize soil water content in a way that is relevant to biological processes (Cathey et al., 2013). The simple method of volumetric measure of soil water content was reported to be a good predictor of physiological response in plants [Sinclair and Ludlow, 1985; Ray et al., 2002; Ray and Sinclair (1997, 1998)].

The fraction of transpirable soil water (FTSW) is defined as the amount of water available to plants at any given time in the drying cycle relative to the total amount of water available for transpiration at the pot-holding capacity. Plant transpiration in response to a drying soil has been well characterized by previous research and reported to display two phases (the initial plateau where transpiration is optimal and a linear decline in response to a drying soil) that are connected by a breakpoint also known as threshold value for the initiation of stomatal closure [Sinclair and Ludlow, 1985; Ray et al., 2002; Ray and Sinclair (1997, 1998)]. The threshold value ($FTSW_{cr}$) is a crucial parameter for comparing accessions and genotypes. Differences in threshold values at which transpiration begins to decline can provide valuable information about plants water use pattern and stomatal closure during a drying cycle (Ray et al., 2002; Ray et al., 1997; Ray and Sinclair, 1997). Palmer amaranth [*Amaranthus palmeri* (S.) Wats.] has the ability to adapt to various stress conditions (Bravo et al., 2018). It uses osmoregulation to keep stomates open during drought to continue carbon fixation (Ehleringer 1983).

Previous research documented the association of herbicide resistance traits with fitness cost and competitive disadvantages in the absence of herbicide selection (Butts et al., 2018; Tardif et al., 2006). Additionally, gene families (P450s and GSTs) involved in non-target site resistance play a critical role in plant protection against and survival to adverse climatic conditions (Montellano, 2005). In Arkansas, Palmer has evolved a target-site resistance to glyphosate due to *EPSPS* gene amplification (Singh et al., 2018) and a non-target-site resistance to *S*-metolachlor due GSTs (Brabham et al., 2019; Rangani et al., 2021). Understanding the impact of *EPSPS* gene amplification and *S*-metolachlor-resistance on Palmer amaranth transpiration during a drying cycle can improve our understanding of weed resistance evolutionary ecology. The objective of this research was to quantify the transpiration changes that occur in herbicide-resistant and susceptible Palmer amaranth accessions when they are submitted to a progressive drying cycle.

Materials and Methods

Two separate greenhouse experiments were conducted from January to May 2021 at the Milo J. Shult Agricultural Research & Extension Center (University of Arkansas, Fayetteville) and repeated in time to evaluate drought tolerance differences both between *S*-metolachlor-, resistant and susceptible populations and between glyphosate- resistant and susceptible plants of the same accession differing by the number of *EPSPS* gene copy number.

Impact of EPSPS gene copy number on Palmer amaranth transpiration

Plant material preparation

Palmer amaranth accession 16CRW-D is resistant to glyphosate due to an increase in 5-enolpyruvylshikimate-3-phosphate synthase (*EPSPS*) gene copy number (Singh et al., 2018) and was used for this study. Seeds of 16CRW-D were collected in Crawford County (Arkansas) in 2016. One hundred seeds were planted in 50-cell trays filled with Sunshine ® Premix #1 (Sun Gro Horticulture, Bellevue, WA). When seedlings reached 8 cm in height, they were transplanted to 13 cm x 11 cm (diameter-by-depth) pots using the same soil. Plants were fertilized weekly using a water-soluble, all-purpose plant food (Scotts Miracle-Gro Products, Marysville, OH) containing 24% N, 8% P, and 16% K.

Plant tissue was collected to determine the relative *EPSPS* gene copy number using the method described by Singh et al. (2018). Briefly, genomic DNA was extracted from approximately 100 mg of leaf tissue using a modified CTAB protocol and quantified using a NanoDrop spectrophotometer (Thermo Scientific, Wilmington, DE). The *EPSPS* gene copy number was determined by quantitative real-time polymerase chain reaction (qPCR) relative to the A36 gene (Singh et al., 2018). The A36 primers were designed using Biolign and Primer 3 software from sequences of the *Amaranthus* genus: A36_F244 (5′TTGGAACTGTC AGAGCAACC3′) and A36_R363 (5′GAACCCACTT CCA CCAAAAC3′). To amplify the *EPSPS* gene, the primer sets EPSPS1CNF (5′ATGTTGGACGCT CTCAGAACTCTTGGT3′) and EPSPS1CNR (5′TGAATTTCCTCCAGCAACGGCAA3′) were used. Two technical replicates of genomic DNA template (20 ng) were amplified in a 10-µL reaction volume using Sybr-Green master mix (Bio-Rad, Hercules, CA). For the qPCR, the 10-µL reactions were prepared using a Master-mix composed of 5 µL SYBR-itaq (Bio-Rad, Hercules, CA), 0.5 µL of 5 µM forward primer, 0.5 µL of 5 µM reverse primer, 3 µL water and 1 µL gDNA. The thermo-profile used was 95°C for 15 min, then 30 cycles of 95°C for 30 s and 60°C for 1 min. Real-time fluorescence data were captured during the amplification cycles. Melt-curve analysis was conducted by holding the samples at 95°C for 5 min, then reducing the temperature to 55°C for 5 min, followed by increasing the temperature by 0.5°C every 10 s to 95°C.

Selected plants of similar size (25 cm height) were used for the experiment and transplanted into pots, 19 cm x 17 cm pots (diameter-by-depth), at the same depth of 11 cm. Two and half kilograms of a mixed soil, 1:1 mixture ratio of field soil and Sunshine ® Premix #1 (Sun Gro Horticulture, Bellevue, WA) and field soil were weighed for all pots. The field soil, a Roxana silt loam soil (USDA-SCS, 1979) characterized by pH 7.3, 112 µmhos/cm EC, 0.04% total N and 0.4% total C, was collected at the Vegetable Research Station of the University of Arkansas near Kibler (AR).

Differences in drought tolerance between S-metolachlor-susceptible and resistant accessions

Plant material preparation

The resistant and susceptible accessions referred to as 17TUN-A and 09CRW-A, respectively, were used for the experiment. Accession 17TUN-A showed resistance to *S*-metolachlor and resistant plants required up to 5 times more *S*-metolachlor to reduce seedling emergence 50%. Seeds of accessions 09CRW-A and 17TUN-A were collected in Crawford County (Arkansas) in 2009 and Tunica County (Mississippi) in 2017, respectively. One hundred seeds of each accession, 09CRW-A and 17TUN-A, were grown in 50-cell tray using commercial soil as described experiment 1. Seedling 8 cm in height were transplanted to 13 cm x 11 cm (diameter-by-depth) pots filled with commercial soil. Plants were fertilized weekly using a water-soluble, all-purpose plant food. Selected plants of similar size were used for the experiment and transferred into pots, 19 cm x 17 cm pots (diameter-by-depth), at a constant depth of 11 cm when they reached 25 cm height. Two and half kilograms of a mixed soil, 1:1 mixture ratio of field soil and Sunshine ® Premix #1 and field soil were weighted for all pots.

Dry-down treatment

The experiment was conducted as a completely randomized design with six replications (Figure 6. 1) and pots were moved around during the experiment. The drought factor had two levels (well-watered and water-deficit). The method used was adapted from previous research (King and Purcell, 2017). The plants were watered daily and weekly fertilized with a water-soluble, all-purpose plant food (Scotts Miracle-Gro Products, Marysville, OH) until dry down imposition. The evening before starting dry down, pots were saturated and allowed to drain overnight. The pots were enclosed in black plastic bags (Ray and Sinclair, 1997; Schmidt et al., 2011) and each bag opening was sealed around the plant stem with twist ties to minimize evaporation. A 6-mL syringe barrel was inserted between the base of the plant and the plastic bag for water replenishment. Newly bagged pots were weighed to obtain an estimate of gravimetric water content at water holding capacity. The pots were weighed daily at 4 pm and in the same order for the duration of the experiment. Daily transpiration was calculated as the difference in mass of each pot on successive days. To maintain well-watered conditions but prevent anaerobic conditions in the control pots (Ray and Sinclair, 1998), the plants were maintained at 80% of well-watered pot-capacity weight. For the water stress treatments, the six plants of each accession were watered to a target level of 50 mL below the amount of water lost via transpiration in the past 24 h, starting at the beginning of drought stress treatment. Five pots with water-saturated soil in the greenhouse, without plants, were used to estimate daily evaporation rate.

Daily transpiration and normalized transpiration ratio

The transpiration data were analyzed using a double normalization procedure (Ray and Sinclair, 1998; Sinclair and Ludlow, 1986). A first normalization minimized the influence of daily fluctuations in transpiration on the transpiration rate (TR) of stressed plants across days (Ray and Sinclair, 1997; Sinclair and Ludlow, 1986), by normalizing daily transpiration rates for the stressed plants divided by the average for non-stressed plants for the same day (Ray and Sinclair, 1998) using equation 6. 1:

$$Transpiration\ rate\ (TR)\ of\ stressed\ plant = \frac{Transpiration\ of\ stressed\ plant}{Average\ transpiration\ of\ control\ plant} \qquad [6.\ 1]$$

The second normalization, normalized transpiration ratio (NTR), allowed the normalized transpiration rate of each plant to be centered on a value of 1. A mean TR was calculated for each plant for the first 3 d of the experiment when the soil water content in each pot was high (Ray and Sinclair, 1997; Sinclair and Ludlow, 1986). The daily TR for each stressed plant was divided by the mean TR of the same plant during the well-watered stage to give a daily normalized transpiration ratio (NTR) (Ray and Sinclair, 1997; Ray and Sinclair, 1998) as shown in equation 6. 2.

$$Normalized\ tranpiration\ ratio\ (NTR) = \frac{Daily\ TR}{Average\ TR\ of\ the\ first\ 3\ d} \qquad [6.\ 2]$$

The treatments were maintained for each resistant or susceptible accession or plant until NTR value dropped below 0.1, defined as the endpoint of the drying cycle (Ray and Sinclair, 1997; Sinclair and Ludlow, 1986).

Drought stress level in the root zone

The FTSW was defined as the amount of gravimetric water available for plant transpiration at any given time during the drying cycle relative to the total amount of water available for transpiration at the pot-holding capacity. Determination of the FTSW was accomplished using equation 6. 3:

$$daily\ FTSW = \frac{Daily\ pot\ weight - Final\ pot\ weight}{Initial\ pot\ weight - Final\ pot\ weight} \qquad [6.\ 3]$$

Calculations of FTSW were achieved with the average of the beginning and ending interval pot weights of each day (King and Purcell, 2017; King et al., 2009).

Data analysis

The relationship between NTR and FTSW were quantified using a two-segment linear regression analysis (Ray et al., 2002; Ray and Sinclair, 1997; Ray and Sinclair, 1998). The NTR calculated for each pot on each day was plotted for each accession versus the corresponding FTSW. The two-segment linear regression analysis was accomplished, for the six drying pots studied for the *S*-metolachlor- resistant and susceptible accessions and the glyphosate- resistant and susceptible plants, using nonlinear least squares regression (nls) of R version 4.0.0 (R Core Team, 2020). The intersection of the two linear regressions is the FTSW at the breakpoint in the soil drying cycle. The resulting R^2 for the regression analysis and breakpoint values for the NTR for each accession were determined and differences between breakpoints were compared using confidence intervals ($\alpha = 0.05$) (Cathey et al., 2013; King et al., 2009; Sinclair et al., 2015; Sinclair et al., 2018).

Results and Discussion

Differential response of S-metolachlor-resistant and suceptible accessions to daily tranpiration

The two-segmented linear regression analysis (Devi and Reddy, 2020) was used to relate NTR to FTSW for plants submitted to progressive drying treatment (Figure 6. 1). The breakpoints at which each accession initiates stomatal closure were compared using their respective confidence intervals. The NTR response of *A. palmeri* to progressive drying soil followed the two-segmented linear regression with R^2 values ranging between 0.85 and 0.93 (Table 6.1; 6. 2). The

FTSWcr of the two accessions differed ($P \leq 0.05$) (Table 6. 1), but no differences existed between breakpoints for the same accession across runs ($P > 0.05$); therefore, data were pooled across runs for each accession. The *S*-metolachlor-resistant accession 17TUN-A had a greater FTSWcr than the *S*-metolachlor-susceptible accession 09CRW-A, indicating that the *S*-metolachlor-resistant accession started reducing its transpiration at higher threshold levels of 0.23 ±0.004 with an R^2 value of 0.93. The *S*-metolachlor-susceptible accession 09CRW-A started reducing its transpiration at a lower FTSWcr of 0.17±0.007 with an R^2 value of 0.85. Advantages of early and late breakpoints are interpreted diversely by authors and depend on drought scenarios (Fuentealba et al., 2016; Miller, 2000). With smaller FTSWcr in this study, the *S*-metolachlor-susceptible accession is likely to sustain its normal transpiration and prevent growth reduction during short-term water stress (Fuentealba et al., 2016). On the contrary, the *S*-metolachlor-resistant accession with greater FTSWcr has a greater advantage under long-term water stress and drier conditions (Sinclair et al., 2015). Because the *S*-metolachlor-resistant accession closed its stomates early, it has the ability to conserve water and may increase its probability of survival under long-term drought conditions by delaying severe stress (Cathey et al., 2013; Devi et al., 2009; Ray and Sinclair, 1997; Sinclair, 2012).

S-metolachlor resistance reported in Arkansas is attributed to an increase in the metabolism of the herbicide in the plants catalyzed by glutathione *S*-transferases (GSTs) (Brabham et al. 2019; Rangani et al. 2021). As multifunctional enzymes encoded by large gene families, GSTs are known to have a protection role against different biotic and abiotic stresses including xenobiotics and oxidative stress (Lee et al., 2011; Montellano, 2005). An overexpression of GST genes might have improved drought tolerance in the resistant accession.

GSTs have been used to confer drought tolerance to transgenic tobacco (George et al., 2010; Ji et al., 2010; Liu et al., 2013) and transgenic *Arabidopsis* plants (Xu et al., 2018; Yang et al., 2019).

Conclusions drawn from experiment are constrained by the different genetic backgrounds of each of the accessions (Giacomini et al., 2014; Butts et al., 2019) and the fact that the accessions (17TUN-A and 09CRW-A) were not fully screened for other herbicide resistances. However, these results provided initial evidence that the evolution of metabolic resistance to *S*-metolachlor, as discussed above, can increase drought tolerance.

No impact of EPSPS gene amplification on threshold value for stomatal closure

The relative *EPSPS* gene copy number detected in 16CRW-D was variable and ranged between 2.7 and 226.5. Twelve plants with increased copy number between 21.5 and 164.7 and twelve plants without increase in gene copy number [copy number < 10 (Singh et al. (2018)] were selected for each run. Results showed no differences in the FTSWcr between plants with an increase *EPSPS* gene copy number and plants with no increase in gene copy number ($P > 0.05$).

The presence of an increase in *EPSPS* gene copy number in accession 16CRW-D did not induce any difference for the breakpoint ($P > 0.05$) (Figure 6. 3; Table 6. 2). This result is consistent with other studies that also reported a lack of fitness of cost associated with increased *EPSPS* gene copy in glyphosate-resistant kochia (Osipitan and Dille, 2019), or in glyphosate-resistant Palmer amaranth (Vila-Aiub et al., 2014; Giacomini et al., 2014). According to Vila-Aiub et al. (2019) glyphosate resistance associated with target-site *EPSPS* mutations are more likely to reduce *EPSPS* catalytic activity, thus, endowing a substantial plant fitness cost than *EPSPS* gene amplification and overexpression.

Conclusion

The *S*-metolaclor-resistant accession was more drought tolerant compared to the suceptible accession. The metabolic resistance to *S*-metolachlor is likely one of the factors that contributed to increased drought tolerance. Other contributing factors to investigate include differences in genetic background between resistant and susceptible accessions and other NTSR mechanisms harbored by the resistant plants. In contrast, *EPSPS* gene amplification did not impact threshold values for the initiation of stomatal closure. These results demonstrated that Palmer amaranth accessions with different resistance profile might present different strategies to conserve soil water that could lead to increasing their competitive abilities for soil water in water-limited environments. The *S*-metolachlor-resistant accessions, with a high FTSW threshold value, exhibited water conservation by limiting its transpiration early in the drought cycle. Early stomatal closure suggested a high water-use efficiency by continuing carbon assimilation and utilizing the water efficiently. Further research is needed to fully characterize the influence of metabolic herbicide resistance evolution on weeds tolerance to abiotic stress.

References

Asada K (1999) The water-water cycle in chloroplasts: Scavenging of active oxygens and dissipation of excess photons. Annual Review of Plant Physiology and Plant Molecular Biology 50: 601-639.

Bowling LC, Cherkauer KA, Lee CI, Beckerman JL, Brouder S, Buzan JR, Doering OC, Dukes JS, Ebner PD, Frankenberger JR, Gramig BM, Kladivko EJ, Volenec JJ (2020) Agricultural impacts of climate change in Indiana and potential adaptations. Climatic Change 163: 2005-2027.

Boyer JS, Byrne P, Cassman KG, Cooper M, Delmer D, Greene T, Gruis F, Habben J, Hausmann N, Kenny N, Lafitte R, Paszkiewicz S, Porter D, Schlegel A, Schussler J, Setter T, Shanahan J, Sharp RE, Vyn TJ, Warner D, Gaffney J (2013) The US drought of 2012 in perspective: A call to action. Global Food Security-Agriculture Policy Economics and Environment 2: 139-143.

Brabham C, Norsworthy JK, Houston M, Varanasi V, Barber T (2019) Confirmation of *S*-metolachlor resistance in Palmer amaranth (*Amaranthus palmeri*). Weed Technology 33: 720-726.

Bravo W, Leon R, Ferrell J, Mulvaney M, Wood C (2018) Evolutionary adaptations of Palmer amaranth (*Amaranthus palmeri*) to nitrogen fertilization and crop rotation history affect morphology and nutrient-use efficiency. Weed Science 66: 180-189.

Butts TR, Vieira BC, Latorre DO, Werle R, Kruger GR (2018) Competitiveness of herbicide-resistant waterhemp (*Amaranthus tuberculatus*) with Soybean. Weed Science 66: 729-737.

Cathey SE, Kruse JK, Sinclair TR, Dukes MD (2013) Transpiration and visual appearance of warm season turfgrasses during soil drying. Environmental and Experimental Botany 89: 36-43.

Devi MJ, Reddy V (2020) Cotton Genotypic Variability for Transpiration Decrease with Progressive Soil Drying. Agronomy-Basel 10.

Devi MJ, Sinclair TR, Vadez V, Krishnamurthy L (2009) Peanut genotypic variation in transpiration efficiency and decreased transpiration during progressive soil drying. Field Crops Research 114: 280-285.

Egan L, Hofmann R, Nichols S, Hadipurnomo J, Hoyos-Villegas V (2021) Transpiration Rate of White Clover (Trifolium repens L.) Cultivars in Drying Soil. Frontiers in Plant Science 12.

Ehleringer J (1983) Ecophysiology of *Amaranthus palmeri*: A Sonoran desert summer annual. Oecologia 57: 107-112.

Fuentealba MP, Zhang J, Kenworthy K, Erickson J, Kruse J, Trenholm L (2016) Transpiration responses of warm-season turfgrass in relation to progressive soil drying. Scientia Horticulturae 198: 249-253.

George S, Venkataraman G, Parida A (2010) A chloroplast-localized and auxin-induced glutathione *S*-transferase from Phreatophyte *Prosopis juliflora* confer drought tolerance on tobacco. Journal of Plant Physiology 167: 311-318.

Giacomini D, Westra P, Ward S (M) 2014. Impact of genetic background in fitness cost studies: An example from glyphosate-resistant Palmer amaranth. Weed Science 62: 29-37.

Grassini P, Torrion JA, Yang HS, Rees J, Andersen D, Cassman KG, Specht JE (2015) Soybean yield gaps and water productivity in the western US Corn Belt. Field Crops Research 179: 150-163.

Ji W, Zhu YM, Li Y, Yang LA, Zhao XW, Cai H, Bai X (2010) Over-expression of a glutathione *S*-transferase gene, GsGST, from wild soybean (*Glycine soja*) enhances drought and salt tolerance in transgenic tobacco. Biotechnology Letters 32: 1173-1179.

Jin C, Luo X, Xiao XM, Dong JW, Li XM, Yang J, Zhao DY (2019) The 2012 Flash drought threatened US Midwest agroecosystems. Chinese Geographical Science 29: 768-783.

Khan A, Pan XD, Najeeb U, Tan DKY, Fahad S, Zahoor R, Luo HH (2018) Coping with drought: stress and adaptive mechanisms, and management through cultural and molecular alternatives in cotton as vital constituents for plant stress resilience and fitness. Biological Research 51.

Kimm H, Guan KY, Gentine P, Wu J, Bernacchi CJ, Sulman BN, Griffis TJ, Lin CJ (2020) Redefining droughts for the US Corn Belt: The dominant role of atmospheric vapor pressure deficit over soil moisture in regulating stomatal behavior of Maize and Soybean. Agricultural and Forest Meteorology 287.

King C, Purcell L (2017) Evaluation of methods for estimating transpiration response to soil drying for container-grown plants. Crop Science 57: 2143-2148.

King C, Purcell L, Brye K (2009) Differential wilting among soybean genotypes in response to water deficit. Crop Science 49: 290-298.

Kropff M, van Laar H (1993) Modelling crop-weeds interactions: CAB International.

Lee J, Jo H, Kong K (2011) A plant-specific Tau class glutathione *S*-transferase from *Oryza sativa* having significant detoxification activity towards chloroacetanilide herbicides. Bulletin of the Korean Chemical Society 32: 3756-3759.

Li LJ, Song XY, Xia L, Fu N, Feng D, Li HY, Li YL (2020) Modelling the effects of climate change on transpiration and evaporation in natural and constructed grasslands in the semi-arid Loess Plateau, China. Agriculture Ecosystems & Environment 302.

Liu L, Basso B (2020) Impacts of climate variability and adaptation strategies on crop yields and soil organic carbon in the US Midwest. Plos One 15.

Liu D, Liu Y, Rao J, Wang G, Li H, Ge F, Chen C (2013) Overexpression of the glutathione *S*-transferase gene from *Pyrus pyrifolia* fruit improves tolerance to abiotic stress in transgenic tobacco plants. Molecular Biology 47: 515-523.

Lobell DB, Deines JM, Di Tommaso S (2020) Changes in the drought sensitivity of US maize yields. Nature Food 1: 729-735.

Miller GL (2000) Physiological response of bermudagrass grown in soil amendments during drought stress. Hortscience 35: 213-216.

Montellano P (2005) Cytochrome P450: Structure, mechanism, and biochemistryNew York: Kluwer Academic/Plenum Publishers.

Osipitan OA, Dille JA (2019) No Impact of Increased *EPSPS* Gene Copy Number on Growth and Fecundity of Glyphosate-Resistant Kochia (Bassia scoparia). Weed Science 67: 22-28.

R Core Team R (2020) R: A language and environment for statistical computing. Vienna, Austria: R Core Team (2020).

Rangani G, Noguera M, Salas-Perez R, Benedetti L, Roma-Burgos N (2021) Mechanism of resistance to *S*-metolachlor in Palmer amaranth. Frontiers in Plant Science 12: 13.

Ray J, Gesch R, Sinclair T, Allen L (2002) The effect of vapor pressure deficit on maize transpiration response to a drying soil. Plant and Soil 239: 113-121.

Ray J, Samson B, Sinclair T (1997) Vegetative growth and soil water extraction of two maize hybrids during water deficits. Field Crops Research 52: 135-142.

Ray J, Sinclair T (1997) Stomatal closure of maize hybrids in response to drying soil. Crop Science 37: 803-807.

Ray J, Sinclair T (1998) The effect of pot size on growth and transpiration of maize and soybean during water deficit stress. Journal of Experimental Botany 49: 1381-1386.

Saradadevi R, Palta JA, Siddique KH (2017) ABA-mediated stomatal response in regulating water use during the development of terminal drought in wheat. Front. Plant Sci. 8, 1251. https://doi.org/10.3389/fpls.2017.01251.

Schmidt J, Blankenship E, Lindquist J (2011) Corn and velvetleaf (*Abutilon theophrasti*) transpiration in response to drying soil. Weed Science 59: 50-54.

Sinclair T, Ludlow M (1986) Influence of soil-water supply on the plant water-balance of 4 tropical grain legumes. Australian Journal of Plant Physiology 13: 329-341.

Sinclair TR (2005) Theoretical analysis of soil and plant traits influencing daily plant water flux on drying soils. Agronomy Journal 97: 1148-1152.

Sinclair TR (2012) Is transpiration efficiency a viable plant trait in breeding for crop improvement? Functional Plant Biology 39: 359-365.

Sinclair TR, Manandhar A, Belko N, Riar M, Vadez V, Roberts PA (2015) Variation among cowpea genotypes in sensitivity of transpiration rate and symbiotic nitrogen fixation to soil drying. Crop Science 55: 2270-2275.

Sinclair TR, Shekoofa A, Isleib TG, Balota M, Zhang H (2018) Identification of Virginia-type peanut genotypes for water-deficit conditions based on early decrease in transpiration rate with soil drying. Crop Science 58: 2607-2612.

Singh S, Singh V, Lawton-Rauh A, Bagavathiannan M, Roma-Burgos N (2018) *EPSPS* Gene Amplification Primarily Confers Glyphosate Resistance among Arkansas Palmer amaranth (*Amaranthus palmeri*) Populations. Weed Science 66: 293-300.

Tardif FJ, Rajcan I, Costea M (2006) A mutation in the herbicide target site acetohydroxyacid synthase produces morphological and structural alterations and reduces fitness in *Amaranthus powellii*. New Phytologist 169: 251-264.

USDA-SCS (1979) Soil Survey of Crawford County, Arkansas. U.S. Gov. Print. Office, Washington, DC.

Vila-Aiub MM, Goh SS, Gaines TA, Han HP, Busi R, Yu Q, Powles SB (2014) No fitness cost of glyphosate resistance endowed by massive *EPSPS* gene amplification in *Amaranthus palmeri*. Planta 239: 793-801.

Vila-Aiub MM, Yu Q, Powles SB (2019) Do plants pay a fitness cost to be resistant to glyphosate? New Phytologist 223: 532-547.

Xu J, Zheng AQ, Xing XJ, Chen L, Fu XY, Peng RH, Tian YS, Yao QH (2018) Transgenic *Arabidopsis* plants expressing grape glutathione *S*-transferase gene (VvGSTF13) show enhanced tolerance to abiotic stress. Biochemistry-Moscow 83: 755-765.

Yang Y, Anderson MC, Gao F, Johnson DM, Yang Y, Sun L, Dulaney W, Hain CR, Otkin JA, Prueger J, Meyers TP, Bernacchi CJ, Moore CE (2021) Phenological corrections to a field-scale, ET-based crop stress indicator: An application to yield forecasting across the US Corn Belt. Remote Sensing of Environment 257.

Yang Q, Liu YJ, Zeng QY (2019) Overexpression of three orthologous glutathione S-transferases from Populus increased salt and drought resistance in Arabidopsis. Biochemical Systematics and Ecology 83: 57-61.

Tables and Figures

Table 6. 1. Breakpoint (threshold value for the initiation of stomatal closure), standard error (SE), R^2, and confidence intervals for the plateau regression analysis used to evaluate differences in drought tolerance between *S*-metolachlor- susceptible and -resistant Palmer amaranth accessions submitted to a progressive drought; greenhouse experiment conducted at the Milo J. Shult Agricultural Research & Extension Center (University of Arkansas, Fayetteville) in 2021.

Accessions	Breakpoint[a]	SE	R^2	Confidence intervals[b]	
09CRW-A	0.17a	0.007	0.85	0.15	0.19
17TUN-A	0.23b	0.004	0.93	0.22	0.25

[a] Means within a column, followed by different letters are different ($P \leq 0.05$).
[b] 95% confidence intervals of breakpoints

Table 6. 2. Breakpoint (threshold value for the initiation of stomatal closure), standard error (SE), R^2, and confidence intervals for the plateau regression analysis used to evaluate differences in drought tolerance between glyphosate- susceptible and -resistant Palmer amaranth accessions, differing by *EPSPS* gene copy number, submitted to a progressive drought; greenhouse experiment conducted at the Milo J. Shult Agricultural Research & Extension Center (University of Arkansas, Fayetteville) in 2021.

Gene copy number	Breakpoint[a]	SE	R^2	Confidence intervals[b]	
Increase	0.25a	0.007	0.90	0.23	0.26
No increase	0.25a	0.008	0.91	0.23	0.25

[a] Means within a column, followed by the same letter are not significant different ($P > 0.05$).
[b] 95% confidence intervals of breakpoints

Figure 6. 1. Experimental setup for evaluating the transpiration responses of herbicide-resistant and susceptible Palmer amaranth (*Amaranthus palmeri* (S.) Wats.) accessions to progressive drying soil; greenhouse experiment conducted at the Milo J. Shult Agricultural Research & Extension Center (University of Arkansas, Fayetteville) in 2021.

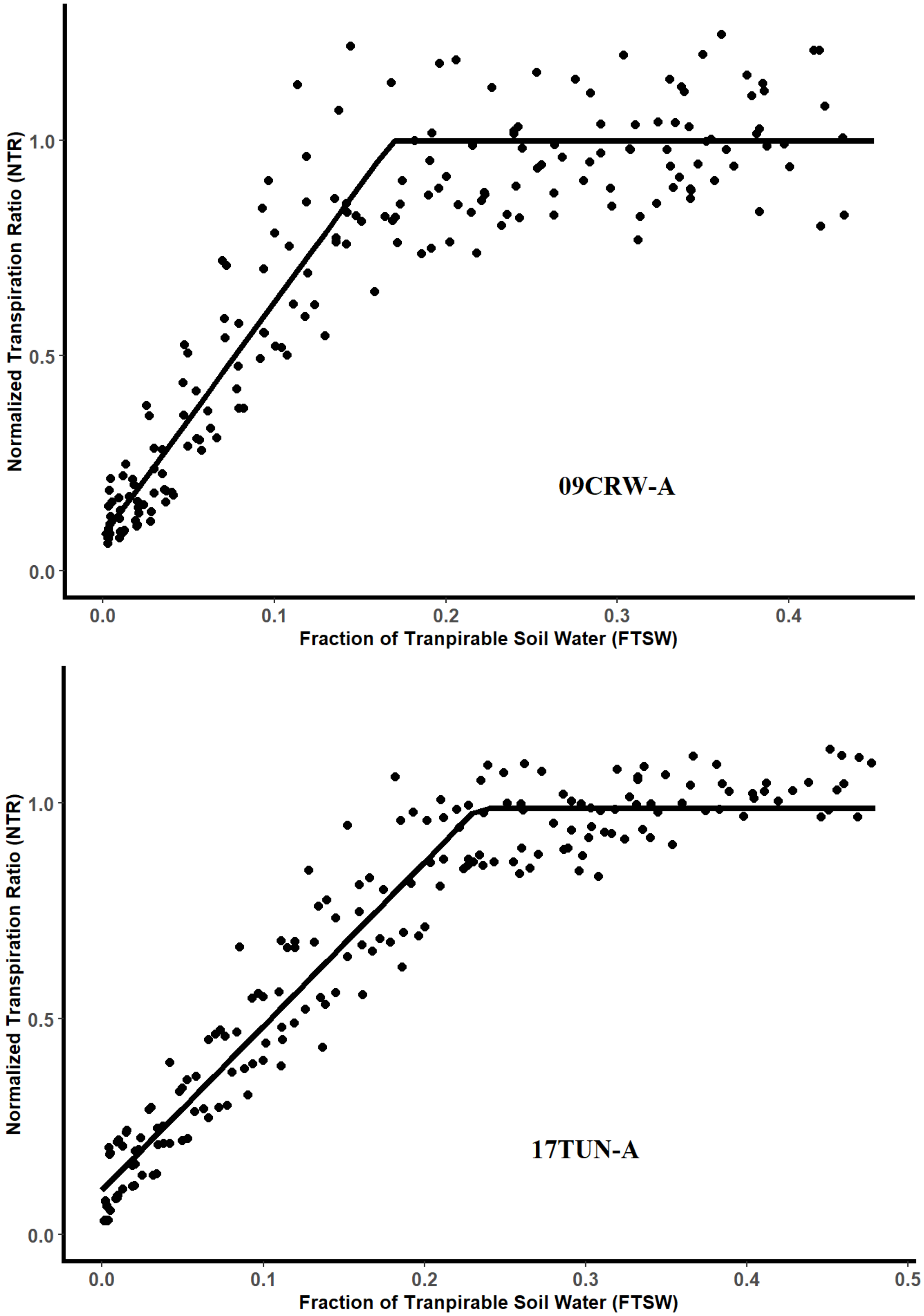

Figure 6. 2. Relationship between normalized transpiration ratio (NTR) and fraction of transpirable soil water (FTSW) during soil drying cycle for *S*-metolachlor- susceptible (09CRW-A) and resistant (17TUN-A) accessions of Palmer amaranth; greenhouse experiment conducted at the Milo J. Shult Agricultural Research & Extension Center (University of Arkansas, Fayetteville) in 2021.

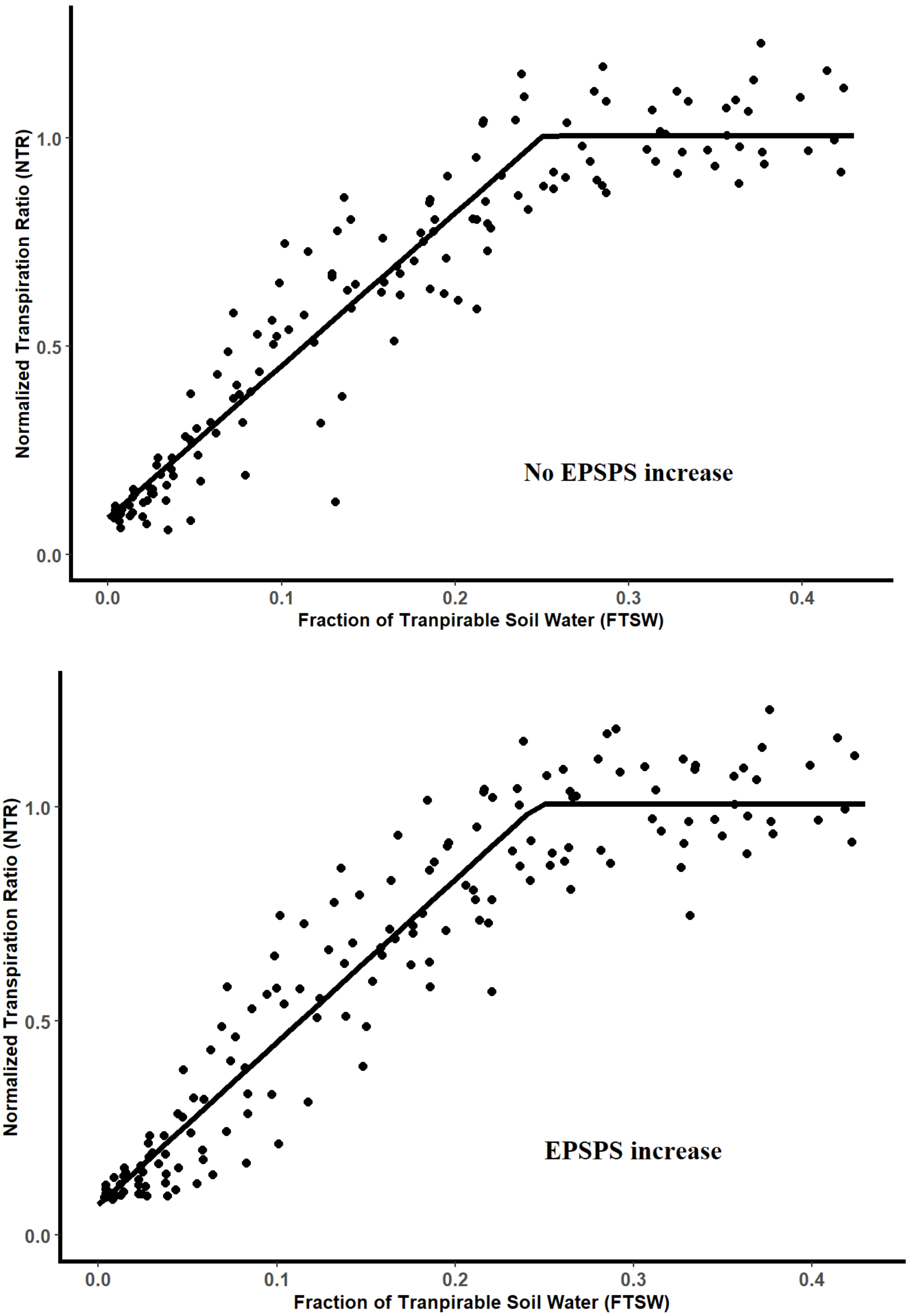

Figure 6. 3. Relationship between normalized transpiration ratio (NTR) and fraction of transpirable soil water (FTSW) during soil drying cycle for glyphosate- resistant and susceptible Palmer amaranth accessions differing by the number of *EPSPS* gene copy number; greenhouse experiment conducted at the Milo J. Shult Agricultural Research & Extension Center (University of Arkansas, Fayetteville) in 2021.

General conclusion

In Arkansas, Palmer amaranth is resistant to herbicides of seven sites-of-action, which are 5-enolpyruvylshikimate-3-phosphate synthase (*EPSPS*) inhibitor, acetolactate synthase (ALS) inhibitors, microtubule inhibitors, protoporphyrinogen oxidase (PPO) inhibitors, very long chain fatty acid (VLCFA) inhibitors, glutamine synthetase inhibitors, and hydroxyphenylpyruvate dioxygenase (HPPD) inhibitors. Resistance evolution results from persistent selection pressure and S-metolachlor has been labelled for more than 70 crops and used for more than 60 years. The occurrence of Palmer amaranth resistance to *S*-metolachlor as a result of long-term use of the herbicide led us to characterize the current status of resistance in the Mid-southern United States and evaluate alternative control methods for proactive control of this weed. Also, given the fact that long-term use (high-use) of some soil-applied herbicides lose efficacy quickly due to enrichment of some microbial populations that degrade the herbicide, we also investigated whether resistance to S-metolachlor could be related to increased dissipation rate of the herbicide. Finally, the importance of this non target site resistance on the drought tolerance of resistant accessions was investigated using threshold values for the initiation of stomatal closure of herbicide- susceptible and resistant accessions. Palmer amaranth resistance to *S*-metolachlor was documented in four Arkansas counties and one county of Mississippi. Parent populations and F_1 lines required up to 7- and 9.2-times more *S*-metolachlor, respectively, to reduce seedling emergence 50%. The half-life of *S*-metolachlor was longer for fields with high-use (5 to 6 yr) compared to fields with low-use (0 to 2 yr) history. A sequential application of *S*-metolachlor significantly slowed *S*-metolachlor dissipation compared to the nontreated control. *S*-metolachlor dissipation was faster earlier compared to later during the growing season. Model selection and goodness of fit showed that the biphasic Gustafson and Holden and first-order double-exponential decay models better supported data compared to the single first order (SFO) model. The SFO under-predicted *S*-metolachlor residues during the later stages of the dissipation process. The *S*-metolaclor-resistant accession was more drought tolerant compared to the suceptible accession. The metabolic resistance to *S*-metolachlor is likely one of the factors that contributed to increased drought tolerance. Other contributing factors to investigate include differences in genetic background between resistant and susceptible accessions and other NTSR mechanisms harbored by the resistant plants. In contrast, *EPSPS* gene amplification did not impact threshold values for the initiation of stomatal closure. These results demonstrated that Palmer amaranth accessions with different resistance profile might present different strategies to conserve soil water that could lead to increasing their competitive abilities for soil water in water-limited environments. The *S*-metolachlor-resistant accessions, with a high FTSW threshold value, exhibited water conservation by limiting its transpiration early in the drought cycle. Early stomatal closure suggested a high water-use efficiency by continuing carbon assimilation and utilizing the water efficiently. Further research is needed to fully characterize the influence of metabolic herbicide resistance evolution on weeds tolerance to abiotic stress. Dissipation is not increased from use, but resistance is occurring and resistance in plant has consequences for plant function under stress conditions. Continued research into plant mechanisms and consequences of increasing resistance needs investigation.